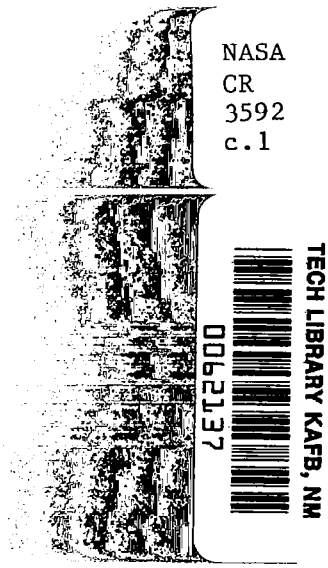

NASA Contractor Report 3592

Tensile Stress-Strain Behavior of Graphite/Epoxy Laminates

D. P. Garber

CONTRACT NAS1-16000
AUGUST 1982

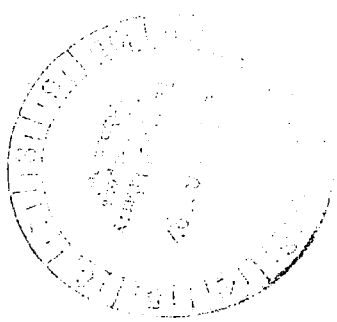

NASA

SUMMARY

The tensile stress-strain behavior of a variety of graphite/epoxy laminates was examined. Longitudinal and transverse specimens from eleven different layups were monotonically loaded in tension to failure. Ultimate strength, ultimate strain, and stress-strain curves were obtained from four replicate tests in each case. Polynominal equations were fitted by the method of least squares to the stress-strain data to determine average curves. Values of Young's modulus and Poisson's ratio, derived from polynomial coefficients, were compared with laminate analysis results.

While the polynomials appeared to accurately fit the stress-strain data in most cases, the use of polynomial coefficients to calculate elastic moduli appeared to be of questionable value in cases involving sharp changes in the slope of the stress-strain data or extensive scatter.

TABLE OF CONTENTS

INTRODUCTION

The study of the tensile fracture of continuous fiber laminated composites can be roughly divided into two categories: unnotched fracture and notched fracture. In unnotched composites, failure appears to be controlled in part by the complicated stress states occurring at the free edges. The edge stresses are determined not only by the presence of different ply orientations, but by the order of the ply orientations or stacking sequence. Failure models which are used to predict unnotched failure require some information about the behavior of the constituent laminae. Simple models need only elastic constants while more sophisticated models might use the nonlinear response of the individual laminae. In the fracture of notched composites, notch geometry plays a predominant role. In this category stacking sequence is of considerably less importance than flaw shape in determining failure (ref. 1). Notched composite failure models generally require the laminate unnotched strength and elastic constants.

The primary objective of this study was to provide elastic constants and unnotched strengths for analysis of the notched strengths of a wide variety of graphite/epoxy laminates. In order to achieve this objective, longitudinal and transverse specimens of each layup were monotonically loaded in tension to failure. The use of polynomial equations to model the stress-strain curves which were generated was also explored. Elastic constants were obtained from the polynomial coefficients and compared with laminate analysis results to evaluate the effectiveness of this approach.

SYMBOLS

a_{ixx}	i^{th} coefficient of the longitudinal strain polynomial, $(GPa)^{-i}$
a_{ixy}	i^{th} coefficient of the transverse strain polynomial, $(GPa)^{-i}$
E_x	Young's modulus, GPa
$(E_{tan})_x$	tangent modulus, GPa
E_1	lamina Young's modulus, fiber direction, GPa
E_2	lamina Young's modulus, perpendicular to fibers, GPa
F_{tu}	ultimate tensile strength, MPa
G_{12}	lamina shear modulus, GPa
R^2_{xx}	adjusted R^2 statistic of the longitudinal strain polynomial
R^2_{xy}	adjusted R^2 statistic of the transverse strain polynomial
V_f	fiber volume fraction
ε_x	longitudinal strain
ε_y	transverse strain
ε_{tu}	ultimate tensile strain
ν_{xy}	Poisson's ratio
$(\nu_{tan})_{xy}$	tangent Poisson's ratio
ν_{12}	lamina Poisson's ratio
σ_x	longitudinal stress, MPa

EXPERIMENTAL PROCEDURES

Material and Specimens

The material used in this investigation consisted of T300 fibers embedded in a matrix of 5208 epoxy. Four sheets of each of eleven different laminates (table I) were fabricated. Laminate stacking sequences were chosen to provide a large number of permutations of both ply orientation and percentage composition of plies. Ply orientations of 0°, 90°, and ±45° only were used. Thirty-one specimens were cut from each composite sheet and numbered according to the specimen code as shown in figure 1. The dimensions of each specimen type are listed in the table below.

Specimen type	Specimen direction	Specimen dimensions		Specimens per sheet
		Length (mm)	Width (mm)	
A	Longitudinal	914	305	3
B	Longitudinal	419	102	10
C	Longitudinal	305	50.8	6
D	Longitudinal	254	25.4	6
E	Transverse	254	25.4	6

For the purposes of this study, only specimens of types D and E were used. Some specimens, as noted in the data tables, were tested with fiberglass end-tabs 63.5 mm long, 25.4 mm wide, and 2.6 mm thick with a 12° taper.

The manufacturer supplied C-scans, matrix mass fraction, void content, and laminate thickness for each sheet. The C-scans indicated that the sheets were free of objectionable flaws. Void content for the various laminates ranged as high as 1.27 percent but averaged 0.18 percent. Fiber volume fraction for each sheet was calculated with assumed fiber density of 1.740 gm/cm^3 and matrix density of 1.263 gm/cm^3. Thickness, fiber volume fraction, and moisture mass fraction values for each sheet appear in table II. Because of the considerable period of time between manufacture and testing of the specimens, it can be safely assumed that the moisture mass fraction values typify steady state moisture content.

Test Procedure and Equipment

Specimens were tested in a single channel, closed loop, servo controlled, hydraulically activated testing machine equipped with hydraulic grips. Cellulose acetate shims 1.5 mm thick were placed between the specimen and grip faces, and gripping pressure was adjusted to prevent damage to the ends of the specimens. The controller was set to operate with feedback from the load cell and the command signal was provided by an external function generator set on ramp mode. The ramp rate was chosen so as to strain the specimens at approximately 10^{-4} mm/mm/second.

Strains were measured by bonded foil strain gages with 3.2 mm gage length. One longitudinal and one transverse gage were mounted on each side of the specimen. The longitudinal gages were wired in series and connected so as to constitute one arm of a Wheatstone bridge. The transverse gages were similarly connected to a separate bridge.

Data for each test were sampled and recorded by a digital data acquisition system (ref. 2). Analogue voltage signals from the load cell conditioner, strain gage circuits, and a peak meter connected to the load cell conditioner were sequentially sampled at fixed intervals by a scanner. An integrating digital voltmeter converted the analogue inputs, and the data were recorded on an incremental magnetic tape recorder and a digital paper tape printer.

DATA ANALYSIS

Data Reduction

Information recorded on magnetic tape by the data acquisition system was copied onto a computer file and processed by a data reduction program. Because the analogue signals varied with time but were sampled sequentially rather than instantaneously, data within a scan were interpolated to coincide in time. The linear interpolation was considered to be sufficiently accurate due to the linear nature of the command signal supplied to the testing machine controller. All data recorded prior to loading and after specimen failure were automatically eliminated by the data reduction program. Load was converted to stress using a

cross-sectional area based on an assumed ply thickness of 0.14 mm and the measured specimen width. The ultimate tensile strength was determined from the maximum value recorded on the peak meter channel.

Curve Fitting

The stress and strain data were fit to polynomial equations of the form:

$$\varepsilon_x = a_{0xx} + a_{1xx}\sigma_x + a_{2xx}\sigma_x^2 + \ldots + a_{nxx}\sigma_x^n$$

$$\varepsilon_y = a_{0xy} + a_{1xy}\sigma_x + a_{2xy}\sigma_x^2 + \ldots + a_{nxy}\sigma_x^n$$

by Gauss' least-squared-error method. The x and y subscripts refer, respectively, to the directions parallel with and perpendicular to the applied load. To satisfy the requirement that the stress-strain curves have inflection points at zero load, the coefficients a_{2xx} and a_{2xy} were set to zero prior to initiating the least squares procedure. The adjusted R^2 statistic (ref. 3) was calculated for polynomials of various orders to provide a quantitative measure for deciding which order to use. It was decided that a fourth order polynomial gave the best fit with the fewest parameters. The stress-strain parameters and the associated adjusted R^2 statistics for each specimen appear in table III.

Figure 2 shows the stress-strain curve for specimen 2A2E with the data plotted as symbols and the polynomials drawn as solid lines to give an example of the accuracy of the method. The rest of the specimens are plotted in groups according to stacking sequence (fig. 3-27). Data for each specimen are distinguished by the use of different symbols, and the polynomial curves in each case were determined by averaging the coefficients of the polynomials fit to each specimen (see table III).

Figure 28 shows the tangent modulus and tangent Poisson's ratio plotted against longitudinal strain for specimen 2A2E. The polynomial derivative curves:

$$(E_{tan})_x = \left(\frac{d\varepsilon_x}{d\sigma_x}\right)^{-1} \quad \text{and} \quad (\nu_{tan})_{xy} = -\left(\frac{d\varepsilon_y}{d\sigma_x}\right)\Big/\left(\frac{d\varepsilon_x}{d\sigma_x}\right)$$

are drawn as solid lines while the data, calculated using a first-order backward difference method, are plotted as symbols. The rest of the specimens are plotted in groups according to stacking sequence (fig. 29-53). Data for each specimen are distinguished by the use of different symbols as before and the polynomial derivative curves in each case are again determined by averaging the coefficients of the individual derivatives.

Laminate tensile elastic constants were determined from the polynomial equations which were fit to the digital data. Young's modulus was derived from the longitudinal strain polynomial:

$$E_x = \left(\frac{d\varepsilon_x}{d\sigma_x}\right)^{-1}\Bigg|_{\sigma_x = 0} = a_{1xx}^{-1}$$

and Poisson's ratio was derived from the longitudinal and transverse strain polynomials:

$$\nu_{xy} = \left\{-\left(\frac{d\varepsilon_y}{d\sigma_x}\right)\Big/\left(\frac{d\varepsilon_x}{d\sigma_x}\right)\right\}\Bigg|_{\sigma_x = 0} = -\,a_{1xy}/a_{1xx}$$

These constants along with the unnotched tensile strength and ultimate strain for each specimen appear in table IV.

Lamina elastic constants required for a laminate analysis (ref. 4) were calculated using laminate elastic values (from table III) for $[0]_8$, $[90]_8$, and $[\pm 45]_{2S}$ laminates. The lamina shear modulus was determined using Rosen's method (ref. 5). The constants used in the laminate analysis appear in the table below.

E_1	129.4 GPa
E_2	10.85 GPa
G_{12}	5.65 GPa
ν_{12}	.3118

Experimental and theoretical values of Young's modulus and Poisson's ratio appear in table V for comparison purposes. Cordell plots (ref. 6) have been drawn for the experimental values of Young's modulus (fig. 54), Poisson's ratio (fig. 55), and the unnotched tensile strength (fig. 56). A fourth order polynomial surface has been determined for each plot using Gauss' least-squares method to provide an aid for visualizing the material behavior. Data are plotted as symbols and the polynomials are plotted as lines of constant ply percentage.

DISCUSSION OF RESULTS

Stress-Strain Curves

Polynomials determined by the least squares method are used to represent the stress-strain data for several reasons. The primary reason is that the entire curve can be modeled with only a few parameters. Polynomials from several specimens of the same layup can be averaged quite simply by averaging coefficients, thereby also simplifying the determination of average elastic moduli. The calculation of the parameters involves no user bias beyond the selection of the highest order, and statistics (such as the adjusted R^2) are available as indicators of the accuracy of fit to guide in selecting the highest order. Derivatives are easy to calculate and the entire procedure can be automated on a digital computer. Residual plots are desirable for determining whether differences between data and the polynomial fit are systematic or random. It was decided, however, that the nature of the stress-strain behavior would yield systematic differences regardless of polynomial order so the adjusted R^2 statistic alone was used. Fourth order curves were considered to best meet the criterion of maximizing the adjusted R^2 while minimizing the number of parameters. Figure 2 shows just one example of polynomial fits to longitudinal and transverse stress-strain data.

Data and curves for $[0]_8$ specimens are shown in figure 3 for tests performed on un-tabbed specimens and in figure 4 for tests performed on end-tabbed specimens. The low failure strains observed in tests performed without tabs indicated that the gripping method might have contributed to early failure. Tests run on specimens with tapered tabs showed no significant differences in ultimate stress or strain or in polynomial coefficients. One study (ref. 7) has shown that tapered

tabs can debond and contribute to early failure. In the case of the $[0]_8$ laminate, the tabs debonded from the specimen but did not appear to affect the failure mode.

Figure 5 shows the results for tests of the $[90]_8$ laminate. Each specimen failed neatly at a grip edge. While the curves appear to fit the data very well, examination of the adjusted R^2 statistics in table III reveals that transverse strain data is not fit well. This is due to a very poor signal-to-noise ratio resulting from the extremely small strain levels. The data may also be biased because the effect of transverse sensitivity was not taken into account. The transverse sensitivity factor was not recorded when the gages were applied. Curves for the $[\pm 45]_{2S}$ laminate shown in figures 6 and 7 are extremely nonlinear but seem to be well fit by the polynomials.

The results of tests on so-called quasi-isotropic laminates, $[45/0/-45/90]_S$ and $[45/90/-45/0]_S$, are shown in figures 8 and 9. The laminate with 90° plies in the center exhibits significantly lower failure stresses and strains than the laminate with 0° plies in the center, and shows distinctly nonlinear behavior prior to failure. Examination of failed specimens revealed extensive delamination of the -45/90 interfaces for specimens with 90° plies at the center while specimens with 0° plies in the center showed only minor delamination at one 45/90 interface. Approximate interlaminar stresses were calculated using the method of Pipes and Pagano (ref. 8). Calculations for the $[45/0/-45/90]_S$ laminate show very high tensile stresses normal to the interface between the -45° and 90° plies. Calculations for the $[45/90/-45/0]_S$ laminate show compressive stresses at every interface except for the 45/90, which has a very slight tensile stress. The nonlinear behavior evident in figure 8 is due to extensive delamination growth which contributed to the low failure stress. In order to obtain more accurate elastic constants, polynomials were fit only to stress-strain data recorded prior to the onset of delamination for the $[45/0/-45/90]_S$ laminate.

Figures 10-13 show the stress-strain behavior of $[90/0]_{2S}$, $[0/90]_{2S}$, $[0_2/90/0]_S$, and $[90_2/0/90]_S$ laminates. The transverse strain is small in each case bacause of the presence of 90° plies and absence of ±45° plies. Only one laminate, $[90_2/0/90]_S$, figure 13, shows distinct nonlinearity in the longitudinal strain. All of the specimens of these layups broke in the test section in a nearly straight line. Specimens of the $[0_2/90/0]_S$ layup had very small delaminated areas at the break.

Stress-strain curves for $[90/45/90/-45]_S$, $[45/90/-45/90]_S$, and $[45/90/-45/90]_{2S}$ laminates shown in figures 14, 15, and 16 exhibit nearly identical behavior. Failure surfaces for all three laminates appear the same with straight breaks in 90° plies and pull out in 45° plies.

Figures 17-20 show the behavior of $[0/45/0/-45]_S$, $[45/0/-45/0]_S$, and $[45/0/-45/0]_{2S}$ laminates and the $[45/0/-45/0]_{2S}$ laminate with tapered end tabs. While all four sets of curves appear to have identical slopes, each laminate failed at a different strain. Interlaminar normal stresses appear to be the distinguishing factor. The Pipes and Pagano approximation (ref. 8) indicates that the interlaminar normal stresses in the laminate with the highest failure strain, $[0/45/0/-45]_S$, are compressive. The same method indicates that normal stresses in the laminate with the lowest failure strain, $[45/0/-45/0]_S$, are tensile. The interlaminar stresses in the $[45/0/-45/0]_{2S}$ laminate are intermediate in size, but postmortem examination of the end-tabbed specimens revealed that the end-tabs, instead of debonding, pulled the outer plies completely free in the region at the edge of the tab. All failures of the end-tabbed specimens occurred very near the tabs. Postmortem examinations revealed that delaminations were present, to some extent, in the failed region of every specimen in this group. There is no clear evidence, however, to indicate whether the delaminations contributed to or were caused by failure of the specimens.

Figures 21 and 22 show the behavior of the $[\pm45/0/\pm45/\overline{0}]_S$, $[\pm45/0/\mp45/0/\pm45/0/\pm45]_T$, $[\pm45/90/\pm45/\overline{90}]_S$, and $[\pm45/90/\mp45/90/\pm45/90/\pm45]_T$ laminates. Although layup errors occurred for this group of laminates (see table I), there appear to be no significant differences in behavior between the correctly and incorrectly stacked laminates. Specimen 5D2E failed at a very low stress and strain, but no conclusions may be drawn from a single test. The failure surface shape did not appear to depend on the stacking error.

Stress-strain behavior of the $[0_2/45/0_2/-45/0_2]_S$ laminate is shown in figure 23. All four specimens failed in the grip. Figure 24 shows the behavior of the same laminate tested with end tabs. In this case end tabs solved the gripping problem; none of the specimens failed in the grips and there was substantial improvement in the failure stress and strain. The behavior of the

$[90_2/45/90_2/-45/90_2]_S$ laminate is shown in figure 25. Although there is little difference between the failure stresses of the specimens, the range of failure strains is quite large. Since significant differences between specimens appear only above a strain of 0.004, approximately the ultimate strain of the $[90]_8$ laminate, it would seem that damage to the 90° plies is responsible.

Stress-strain curves for $[(90/0)_2/45/0/-45/0]_S$ and $[(0/90)_2/45/90/-45/90]_S$ laminates appear in figures 26 and 27. There is very little variation in ultimate stress, ultimate strain, or the appearance of the stress-strain curve between replicate tests for either laminate configuration.

Stiffness and Poisson's Ratio Curves

In order to display the manner in which stiffness and Poisson's ratio change with increasing strain, derivatives of the least squares polynomials are plotted. Figure 28 shows the results for specimen 2A2E. The symbols in that figure and subsequent figures represent slopes between successive pairs of scans determined by a first-order backward difference scheme. They show both the degree of agreement between data and polynomial derivatives, and the extent to which slight scatter in the raw data can be magnified by a simple finite difference procedure. The least squares method, it should be noted, does not involve fitting derivatives. Polynomial coefficients are determined only by minimizing discrepancies between data and the curve. The polynomial derivative curves should, therefore, be considered with this limitation in mind.

Tangent modulus and Poisson's ratio curves for the unidirectional laminates appear in figures 29-31. The $[0]_8$ laminate stiffness increases significantly with increasing strain while Poisson's ratio drops correspondingly. It appears from the data in figures 29 and 30 that even though the stiffness of the $[0]_8$ laminate has non-zero slope at zero strain, the polynomial adequately models the stiffness of the $[0]_8$ laminate. The results for the $[90]_8$ laminate (fig. 31) indicate a constant stiffness over nearly the entire strain range, but the lack of transverse strain sensitivity correction makes the plot of Poisson's ratio suspect. Plots of the $[\pm45]_{2S}$ laminate behavior in figures 32 and 33 show stiffness decreasing with increasing strain, while Poisson's ratio increases to nearly 1. The Poisson's ratio plots of the $[\pm45]_{2S}$ laminate show the value of using polynomials to

ameliorate the problem of data scatter caused by digital data acquisition. Although the curve-fitting method used is not perfect, it appears to work well for the $[0]_8$, $[90]_8$, and $[\pm 45]_{2S}$ laminate stress-strain data from which the lamina elastic properties are derived.

The disparity between the responses of the two different quasi-isotropic laminates mentioned previously is apparent in the plots of figures 34 and 35. The $[45/0/-45/90]_S$ laminate exhibits an abrupt stiffness drop at 0.004 strain. At that strain level scatter increases substantially. The ultimate strain of the $[90]_8$ laminate (table V) is about 0.0036. This suggests that splitting in the 90° plies may be responsible for the decrease of the laminate stiffness and the scatter in the data. An edge replicate obtained from one specimen indicates that cracks were present in the 90° plies at a strain as low as 0.0038. Also, an edge replicate indicated that delaminations were present at a strain as low as 0.0045. Although a report by O'Brien, et.al. (ref. 9) suggests that matrix cracking in off-axis plies contributes relatively little to laminate stiffness loss, it should be noted that small laminate stiffness changes are more pronounced when the tangent to the stress-strain curve, rather than the secant, is plotted. The relationship between tangent modulus and secant modulus is:

$$E_{tan} = E_{sec} + \varepsilon \frac{d}{d\varepsilon}\left(E_{sec}\right)$$

while changes in the tangent modulus are related to changes in the secant modulus by:

$$\frac{d}{d\varepsilon}\left(E_{tan}\right) = 2\frac{d}{d\varepsilon}\left(E_{sec}\right) + \varepsilon \frac{d^2}{d\varepsilon^2}\left(E_{sec}\right).$$

Thus the tangent modulus is more than twice as sensitive to stiffness changes as the secant modulus.

The failure of the least squares procedure to adequately model the derivatives is manifest in figure 34. The polynomial derivative curve does not conform to the backward difference results. The plots of the $[45/90/-45/0]_S$ laminate response (fig. 35) show a more gradual stiffness loss and Poisson's ratio change, which initiates at the 0.006 strain level. Although an initial edge replicate of one specimen shows the presence of 90° ply cracks at zero stress, possibly due to specimen machining, the earliest indication of additional splitting in 90° plies

occurs in an edge replicate taken at a strain of 0.0063. Delaminations do not appear below a strain of 0.007 and do not grow extensively at higher strains. For this laminate, the polynomial derivative curves agree with the finite difference results. Both quasi-isotropic laminates exhibit splitting in the 90° plies, but the laminate with the two adjacent 90° plies begins to split at a lower strain than the one with isolated 90° plies, which are not at the surface.

The plot of the tangent modulus for the $[90/0]_{2S}$ laminate (fig. 36) shows a slight stiffness drop and a great deal of scatter starting at a strain of 0.004, while the corresponding plot for the $[0/90]_{2S}$ laminate (fig. 37) exhibits nearly the same stiffness loss, but displays comparatively little scatter. The 90° plies of the $[0/90]_{2S}$ laminate, two of which are adjacent, appear to begin splitting at the same strain as the 90° plies of the $[90/0]_{2S}$ laminate, each of which is isolated from the others. Two of the 90° plies in the $[90/0]_{2S}$ laminate are at the surface, however, and are each constrained by only one adjacent ply. The relative proximity of the 90° plies to the surface mounted strain gages apparently determines the relative magnitude of the scatter. Plots of the $[0_2/90/0]_S$ and $[90_2/0/90]_S$ tangent moduli shown in figures 38 and 39 appear to support this. The $[90_2/0/90]_S$ laminate, with two adjacent 90° plies at each surface, shows a stiffness drop and considerable scatter at a strain of about 0.0035. The tangent modulus plot in figure 39 indicates the inability of the polynomial to model derivatives when the data is ill-behaved.

Stiffness and Poisson's ratio plots for the $[90/45/90/-45]_S$, $[45/90/-45/90]_S$, and $[45/90/-45/90]_{2S}$ laminates shown in figures 40, 41, and 42 exhibit nearly identical behavior. The stiffness of each laminate drops at approximately the same 0.005 level of strain while scatter increases in the Poisson's ratio plots at that strain. Two of the laminates have two adjacent 90° plies at the center while the other has isolated 90° plies at the surface.

With the exception of the plots for the end-tabbed specimens, the tangent modulus and Poisson's ratio plots for the $[0/45/0/-45]_S$, $[45/0/-45/0]_S$, and $[45/0/-45/0]_{2S}$ laminates shown in figures 43, 44, 45, and 46 are similar. The source of the scatter in the plots of figure 46 is not apparent.

The error in the stacking sequence of laminate number five (see table I) had no discernable effect on the moduli and Poisson's ratios plotted in figures 47 and 48. In each case the polynomial adequately modeled the material behavior by smoothing scatter while retaining the essential character of the data.

A comparison of figures 49 and 50 shows that end-tabs, in addition to improving strength, reduce data scatter and enable the polynomial to accurately fit the tangent modulus and Poisson's ratio for the $[0_2/45/0_2/-45/0_2]_S$ laminate. Since this laminate is composed primarily of 0° plies, it is not surprising that the stiffness increases with increasing strain as in the $[0]_8$ laminate. The plots of the $[90_2/45/90_2/-45/90_2]_S$ stiffness and Poisson's ratio shown in figure 51 show linear behavior to a strain of about 0.0035 at which point the laminate suffers a substantial stiffness loss. The 90° plies at the surface of the laminate again contribute to data scatter.

The $[(90/0)_2/45/0/-45/0]_S$ laminate plots in figure 52 show stiffness drop and scatter at a strain of about 0.005 because of the 90° plies at the surface. The $[(0/90)_2/45/90/-45/90]_S$ laminate, with two adjacent 90° plies at the center, also exhibits a stiffness drop at a strain of 0.005, as seen in figure 53, but comparatively little scatter.

Experimental values of Young's modulus and Poisson's ratio for each laminate were calculated using the linear terms of the least squares polynomials for each specimen. These laminate elastic values and the average ultimate tensile strength of each laminate are displayed in figures 54, 55, and 56 in the form of Cordell (ref. 6) plots. Cordell plots are two-dimensional projections of three-dimensional plots presented so as to enable the viewer to visualize the original 3-D form. Data points in each figure are plotted as symbols. A fourth order polynomial surface, plotted as solid lines, was determined for each figure by the method of least squares to aid in visualizing the behavior of the laminate constants presented. In some cases there are laminates which have different stacking sequences but possess the same percentages of 0° plies, 90° plies, and ±45° plies. In the plots of Young's modulus and Poisson's ratio, the differences between experimental values in these cases are so slight as to be inconsequential and the fourth order surfaces were calculated using all the data points. It is obvious from figure 56, however, that two laminates with the same percentages of 0° plies,

90° plies, and ±45° plies can have substantially different strengths. The surface plotted in figure 56 was fit only to the greatest value corresponding to a given ply composition. Although the plots in figures 54 and 56 appear to have the same general shape, examination of table V will show that failure strains vary among the different laminates.

Laminate Analysis

Classical laminate analysis was performed for each laminate in this study. Values of Young's modulus and Poisson's ratio from the analysis appear in table V with experimentally determined values. Although classical laminate analysis predicts laminate constants to within a few percent of measured values in most cases, there are several substantial deviations which must be explained. The largest of these, the error in the $[90]_8$ Poisson's ratio prediction, suggests that the omission of transverse sensitivity corrections may have led to biases in strain data which appear as incorrect experimental laminate constants. Although the transverse sensitivity coefficient is unknown, a typical value of 1 percent is sufficient to account for the Poisson's ratio errors for the $[90]_8$, $[0_2/90/0]_S$, $[90/45/90/-45]_S$, $[45/90/-45/90]_S$, $[45/90/-45/90]_{2S}$, and $[\pm45/90/\mp45/90/\pm45/90/\pm45]_T$ laminates. The Poisson's ratio error for the $[90_2/45/90_2/-45/90_2]_S$ laminate is only halved by a transverse sensitivity of 1 percent and other errors are relatively unaffected.

While the transverse sensitivity of the strain gages appears to be responsible for at least part of the disagreement between experimental and laminate analysis values of elastic constants, it is not sufficient to explain all of the errors. Another possible source of error is the least squares curve fitting procedure from which experimental laminate constants are determined. As mentioned earlier, there appear to be cases in which the polynomials poorly model the slopes of the stress-strain curves. The most obvious examples are the Poisson's ratio plot of the $[45/0/-45/90]_S$ laminate in figure 34 and the tangent modulus plot of the $[90_2/0/90]_S$ laminate in figure 39 for which the polynomial curves and finite difference points clearly differ.

SUMMARY OF RESULTS

The tensile behavior of a variety of T300/5208 graphite/epoxy laminates was examined. Stress-strain curves were plotted for each specimen for uniaxial monotonic loading to failure. Fourth order polynomial curves were fit to the data in order to get average stress-strain curves. Stiffness and Poisson's ratio, obtained by differentiating the stress-strain polynomials, were plotted against longitudinal strain for each laminate. Experimentally determined values of Young's modulus and Poisson's ratio were compared with classical laminate analysis results.

Except for a few laminates, classical laminate analysis and experiments gave the same elastic constants. Predictions and measurements of Poisson's ratio differed for only a few laminates with very low Poisson's ratios. A combination of low transverse strain and the failure to account for the transverse sensitivity of the foil strain gages appeared to be primarily responsible for the difference rather than any inherent limitation of the laminate analysis. Measured and predicted values of Young's modulus differed in cases where sharp changes in the slope of the stress-strain curve limited the ability of the polynomial to model the slope. Overall, the laminate analysis results were within the experimental accuracy of the measurements.

Sharp changes in the slopes of stress-strain curves occurred only for laminates containing 90° plies. Laminates with four adjacent 90° plies at the center or two adjacent 90° plies at the surface exhibited stiffness drops at a strain approximately equal to the ultimate tensile strain of the $[90]_8$ laminate. Those with two adjacent 90° plies at the center or isolated 90° plies at the surface showed stiffness loss at strains between 0.004 and 0.005 while laminates with isolated 90° plies not at the surface experienced stiffness loss at strains between 0.006 and 0.007.

While the polynomial method did not adequately model the slopes of ill-behaved stress-strain curves, it accurately modeled the slopes of the $[0]_8$, $[90]_8$, and $[\pm 45]_{2S}$ stress-strain curves from which lamina elastic constants were determined. Because differences between laminate analysis predictions and experimental data analysis results appear to be due to data analysis limitations, it is felt that laminate elastic constants from the laminate analysis should be used when initial moduli are required.

Because of the large variety of laminates, there appears to be no simple failure model which can accurately predict tensile strength in every case. In several cases, delamination growth or gripping difficulties caused laminates to fail at unexpectedly low strains. Because tapered end-tabs exert tensile stresses normal to the specimen surfaces, their use improved gripping only for the $[0_2/45/0_2/-45/0_2]_S$ laminate which has compressive interlaminar normal stresses when tested in tension. In most instances failure strains fell in the range of 0.9 percent to 1.1 percent for both matrix and fiber dominated layups.

REFERENCES

1. Whitney, J. M.; and Kim, R. Y.: Effect of Stacking Sequence on the Notched Strength of Laminated Composites. Composite Materials: Testing and Design (Fourth Conference). ASTM STP 617, American Society for Testing and Materials, 1977, pp. 229-242.

2. Sova, J. A.; and Poe, C. C., Jr.: Tensile Stress-Strain Behavior of Boron/Aluminum Laminates. NASA TP-1117, 1978, p. 26.

3. Draper, N. R.; and Smith, H.: Applied Regression Analysis. Second ed. John Wiley & Sons, Inc., 1981, pp. 91-92.

4. Jones, R. M.: Mechanics of Composite Materials. Scripta Book Company, 1975.

5. Rosen, B. W.: A Simple Procedure for Experimental Determination of the Longitudinal Shear Modulus of Unidirectional Composites. Journal of Composite Materials, Vol. 6, October 1972, pp. 552-554.

6. Cordell, T. M.: The Cordell Plot: A Way to Determine Composite Properties. SAMPE Journal, Vol. 13, No. 6, Nov/Dec 1977, pp. 14-19.

7. Oplinger, D.: Studies of Tensile Specimens for Composite Material Testing. Proceedings of the Technical Co-Operation Program (TTCP) Subgroup P - Materials Technology, Technical Panel 3 - Organic Materials, Ottawa, Canada, May 1978.

8. Pagano, N. J.; and Pipes, R. B.: Some Observations on the Interlaminar Strength of Composite Laminates. International Journal of Mechanical Sciences, Vol. 15, 1973, pp. 679-688.

9. O'Brien, T. K.; Ryder, J. T.; and Crossman, F. W.: Stiffness, Strength, Fatigue Life Relationships for Composite Laminates. Proceedings of the 7th Annual Mechanics of Composites Review, Dayton, Ohio, October 1981, pp. 38-43.

TABLE I. - LAMINATES

LAMINATE NUMBER	SHEET	LAMINATE STACKING SEQUENCE	
		AS ORDERED	AS DELIVERED
2	A,B,C,D	$[90/45/90/-45]_S$	$[90/45/90/-45]_S$
3	A,B,C,D	$[\pm 45]_{2S}$	$[\pm 45]_{2S}$
4	A	$[45/0/-45/90]_S$	$[45/90/-45/0]_S$
	B,C,D	$[45/0/-45/90]_S$	$[45/0/-45/90]_S$
5	A,B,C	$[\pm 45/0/\pm 45/\bar{0}]_S$	$[\pm 45/0/\mp 45/0/\pm 45/0/\pm 45]_T$
	D	$[\pm 45/0/\pm 45/\bar{0}]_S$	$[\pm 45/0/\pm 45/\bar{0}]_S$
6	A,B,C,D	$[90/0]_{2S}$	$[90/0]_{2S}$
7	A,B,C,D	$[(90/0)_2/45/0/-45/0]_S$	$[(90/0)_2/45/0/-45/0]_S$
8	A,B,C,D	$[45/0/-45/0]_S$	$[45/0/-45/0]_S$
9	A,B,C,D	$[45/0/-45/0]_{2S}$	$[45/0/-45/0]_{2S}$
10	A,B,C,D	$[0_2/90/0]_S$	$[0_2/90/0]_S$
11	A,B,C,D	$[0_2/45/0_2/-45/0_2]_S$	$[0_2/45/0_2/-45/0_2]_S$
12	A,B,C,D	$[0]_8$	$[0]_8$

TABLE II. - MATERIAL CHARACTERISTICS

Laminate Number	Sheet	Thickness, mm	V_f, %	Moisture, %
2	A	1.07	67.5	0.7
	B	1.04	66.9	0.9
	C	1.12	66.1	1.0
	D	1.04	64.6	0.7
3	A	1.12	66.0	0.6
	B	1.12	64.6	0.9
	C	1.12	65.0	0.8
	D	1.09	64.4	0.8
4	A	1.14	62.6	0.7
	B	1.12	62.2	0.9
	C	1.12	64.2	0.9
	D	1.17	64.4	0.7
5	A	1.57	62.5	0.6
	B	1.57	63.5	0.6
	C	1.55	63.2	0.6
	D	1.57	61.0	0.8
6	A	1.14	62.2	0.7
	B	1.14	63.6	0.9
	C	1.17	62.3	0.8
	D	1.14	62.7	0.8
7	A	2.29	62.5	0.6
	B	2.26	63.4	0.8
	C	2.16	65.4	0.6
	D	2.16	63.8	0.6

TABLE II. - CONCLUDED

Laminate Number	Sheet	Thickness, mm	V_f, %	Moisture, %
8	A	1.12	65.7	0.6
	B	1.09	64.4	0.9
	C	1.09	65.2	0.6
	D	1.12	64.7	0.7
9	A	2.24	62.7	0.5
	B	2.18	62.1	0.7
	C	2.18	61.2	0.5
	D	2.24	62.7	0.6
10	A	1.09	62.8	0.7
	B	1.09	62.5	0.9
	C	1.09	62.8	0.5
	D	1.09	62.9	0.7
11	A	2.24	62.4	0.5
	B	2.18	62.7	0.7
	C	2.18	64.0	0.4
	D	2.18	63.6	0.6
12	A	1.19	61.6	0.6
	B	1.19	62.9	0.8
	C	1.19	63.3	0.6
	D	1.19	63.9	0.7

TABLE III. - TENSILE STRESS-STRAIN PARAMETERS

Specimen Number	a_{0xx}	a_{1xx}, GPa^{-1}	a_{3xx}, GPa^{-3}	a_{4xx}, GPa^{-4}	R^2_{xx}	a_{0xy}	a_{1xy}, GPa^{-1}	a_{3xy}, GPa^{-3}	a_{4xy}, GPa^{-4}	R^2_{xy}
(A) $[0]_8$										
12A2D	-0.000008	0.007984	-0.000539	0.000241	0.999998	-0.000008	-0.002732	0.000344	-0.000147	0.999960
12B2D	.000028	.007849	-.000574	.000254	.999996	-.000011	-.002355	.000286	-.000108	.999986
12C2D	.000002	.007543	-.000480	.000204	.999998	-.000022	-.002354	.000335	-.000151	.999969
12D2D	-.000008	.008000	-.000611	.000305	.999997	-.000009	-.002403	.000384	-.000190	.999969
Average	0.000004	0.007844	-0.000551	0.000251	--	-0.000013	-0.002461	0.000337	-0.000149	--
(B) $[0]_8$ tested with end tabs										
12A6D	0.000036	0.007640	-0.000504	0.000200	0.999985	-0.000039	-0.002237	0.000321	-0.000132	0.999975
12B6D	.000030	.007590	-0.000502	.000226	.999981	-.000047	-.002392	.000360	-.000164	.999973
12C6D	.000058	.007560	-.000501	.000244	.999992	-.000024	-.002385	.000401	-.000197	.999989
12D6D	.000038	.007678	-.000660	.000351	.999995	-.000009	-.002430	.000415	-.000206	.999994
Average	0.000041	0.007617	-0.000542	0.000255	--	-0.000030	-0.002361	0.000374	-0.000175	--
(C) $[90]_8$										
12A2E	-0.000055	0.091677	44.8045	-1122.93	0.999282	-0.000001	-0.001378	-1.29771	28.3715	0.487095
12B2E	-.000099	.093973	27.2694	-674.15	.998667	-.000008	-.000441	-4.48054	96.6977	.874665
12C2E	(a)	(a)	(a)	(a)	(a)	(a)	(a)	(a)	(a)	(a)
12D2E	-.000065	.090772	38.7606	-1002.55	.998404	.000010	-.002449	5.21003	-140.309	.583636
Average	-0.000073	0.092141	36.9448	-933.21	--	0.0	-0.001423	-0.18941	-5.0799	--

[a]Parameters not determined because of insufficient data.

TABLE III. - CONTINUED

Specimen Number	a_{0xx}	a_{1xx}, GPa^{-1}	a_{3xx}, GPa^{-3}	a_{4xx}, GPa^{-4}	R^2_{xx}	a_{0xy}	a_{1xy}, GPa^{-1}	a_{3xy}, GPa^{-3}	a_{4xy}, GPa^{-4}	R^2_{xy}
(D) $[\pm 45]_{2S}$										
3A2D	-0.000095	0.051266	-0.307545	8.73014	0.999815	0.000045	-0.037572	0.082679	-7.06284	0.999795
3B2D	-.000036	.049278	.542667	4.08179	.999526	.000065	-0.036852	.108815	-7.73062	.999864
3C2D	-.000061	.049534	.602761	3.35371	.999423	.000050	-.038369	.031741	-7.04677	.999930
3D2D	-.000044	.049747	.489131	4.74174	.999448	.000080	-.038504	.354106	-9.63648	.999816
Average	-0.000059	0.049956	0.331754	5.22685	--	0.000060	-0.037824	0.144335	-7.86918	--
(E) $[\pm 45]_{2S}$										
3A2E	-0.000079	0.050027	-0.284407	8.05195	0.999879	0.000088	-0.038452	0.465900	-9.05145	0.999663
3B2E	-.000085	.049583	-.197236	7.40266	.999908	.000087	-.040442	.585472	-10.09255	.999586
3C2E	-.000049	.052892	.975107	2.62297	.999391	.000044	-.035326	-.321907	-5.37215	.999992
3D2E	-.000055	.050012	.284195	5.71111	.999534	.000107	-.040193	.921760	-12.24709	.999128
Average	-0.000067	0.050629	0.194415	5.94717	--	0.000082	-0.038603	0.412806	-9.19081	--
(F) $[45/0/-45/90]_S$										
4A2E	-0.000064	0.020595	-0.078631	0.240327	0.999560	0.000055	-0.007238	0.072758	-0.206606	0.988363
4B2D	-.000041	.020477	-.060419	.204262	.999692	.000009	-.006004	.007018	-.026688	.999743
4C2D	-.000037	.020269	-.051617	.165626	.999709	.000061	-.006659	.038092	-.109762	.998184
4D2D	-.000054	.020339	-.076720	.240454	.999656	.000064	-.007002	.063251	-.180584	.995769
Average	-0.000049	0.020420	-0.066847	0.212667	--	0.000047	-0.006726	0.045280	-0.130910	--

TABLE III. - CONTINUED

Specimen Number	a_{0xx}	a_{1xx}, GPa^{-1}	a_{3xx}, GPa^{-3}	a_{4xx}, GPa^{-4}	R^2_{xx}	a_{0xy}	a_{1xy}, GPa^{-1}	a_{3xy}, GPa^{-3}	a_{4xy}, GPa^{-4}	R^2_{xy}
(G) $[45/90/-45/0]_S$										
4A2D	-0.000011	0.019067	-0.005120	0.018309	0.999977	0.000005	-0.005595	-0.002565	0.001927	0.999988
4B2E	-.000007	.019117	-.006745	.019862	.999964	.000009	-.005705	-.002316	.001662	.999981
4C2E	-.000018	.020204	-.014597	.034336	.999965	.000006	-.005900	-.001737	.000190	.999982
4D2E	0.0	.018467	-.005086	.015886	.999939	.000001	-.005705	-.002274	.001898	.999976
Average	-0.000009	0.019214	-0.007887	0.022098	--	0.000005	-0.005726	-0.002223	0.001419	--
(H) $[90/0]_{2S}$										
6A2D	-0.000016	0.014533	-0.009690	0.018227	0.999993	0.000032	-0.000816	0.004268	-0.007112	0.938259
6B2D	.000013	.013544	-.002376	.002831	.999931	.000015	-.000732	.001604	-.001186	.996516
6C2D	-.000048	.014395	-.013528	.018166	.999866	.000012	-.000602	.000574	.000030	.992033
6D2D	.000008	.013489	-.001373	.003162	.999872	-.000009	-.000595	.000341	.000528	.996116
Average	-0.000011	0.013990	-0.006742	0.010597	--	0.000013	-0.000686	0.001697	-0.001935	--
(J) $[0/90]_{2S}$										
6A2E	0.000012	0.013926	-0.000809	0.002193	0.999975	0.000018	-0.000634	0.001405	-0.000883	0.992503
6B2E	.000019	.013837	-.001622	.003710	.999978	.000011	-.000562	.000637	.000178	.988584
6C2E	.000008	.013841	.000738	-.000236	.999964	-.000003	-.000633	.001257	-.000746	.992962
6D2E	.000032	.013606	.001775	-.001550	.999981	.000016	-.000679	.001439	-.000985	.993412
Average	0.000018	0.013803	0.000021	0.001029	--	0.000011	-0.000627	0.001185	-0.000609	--

TABLE III. - CONTINUED

Specimen Number	a_{0xx}	a_{1xx},GPa^{-1}	a_{3xx},GPa^{-3}	a_{4xx},GPa^{-4}	R^2_{xx}	a_{0xy}	a_{1xy},GPa^{-1}	a_{3xy},GPa^{-3}	a_{4xy},GPa^{-4}	R^2_{xy}
(K) $[0_2/90/0]_S$										
10A2D	0.000015	0.009672	-0.001045	0.000764	0.999991	0.000004	-0.000742	0.000199	0.000021	0.999071
10B2D	-.000005	.009880	-.001155	.000838	.999992	-.000007	-.000750	.000116	.000119	.999458
10C2D	-.000112	.010069	-.001281	.000746	.999998	.000026	-.000562	.000080	-.000009	.999601
10D2D	-.000001	.009959	-.000785	.000495	.999996	.000021	-.000890	.000449	-.000174	.998787
Average	-0.000026	0.009895	-0.001067	0.000711	--	.000011	-.000736	.000211	-.000011	--
(L) $[90_2/0/90]_S$										
10A2E	0.000075	0.021361	0.193830	-0.417164	0.999692	0.000022	-0.000908	0.015414	-0.027652	0.902251
10B2E	.000177	.020478	.189558	-.424839	.998275	.000018	-.000682	.013369	-.023448	.611944
10C2E	.000005	.024013	.107271	-.235270	.999591	.000007	-.000644	.007760	-.010310	.883699
10D2E	.000054	.023695	.090570	-.164033	.999551	.000006	-.000995	.020673	-.040618	.940597
Average	0.000078	0.022387	0.145307	-0.310327	--	0.000013	-0.000807	0.014304	-0.025507	--
(M) $[90/45/90/-45]_S$										
2A2D	-0.000092	0.047199	-1.32199	9.8500	0.997742	0.000016	-0.008975	0.136759	-1.18632	0.999155
2B2D	-.000125	.049214	-1.43223	10.8178	.997515	.000044	-.009763	.266637	-1.96199	.999506
2C2D	-.000160	.052497	-2.19396	14.7036	.997845	-.000004	-.009497	.220732	-1.67750	.999470
2D2D	-.000104	.048461	-1.34077	10.3443	.996804	.000009	-.009166	.199300	-1.56136	.999388
Average	-0.000120	0.049343	-1.57224	11.4289	--	0.000016	-0.009350	0.205857	-1.59679	--

TABLE III. - CONTINUED

Specimen Number	a_{0xx}	a_{1xx}, GPa^{-1}	a_{3xx}, GPa^{-3}	a_{4xx}, GPa^{-4}	R^2_{xx}	a_{0xy}	a_{1xy}, GPa^{-1}	a_{3xy}, GPa^{-3}	a_{4xy}, GPa^{-4}	R^2_{xy}
(N) $[45/90/-45/90]_S$										
8A2E	-0.000152	0.050317	-2.04099	14.8734	0.999222	0.000010	-0.008874	0.242344	-1.88013	0.999133
8B2E	-.000172	.052823	-2.31638	15.6263	.996849	.000032	-.010208	.416085	-2.99439	.998837
8C2E	-.000070	.046978	-1.29561	9.6602	.999638	.000009	-.008915	.171998	-1.39202	.999650
8D2E	-.000179	.050551	-2.10216	14.8717	.999092	.000062	-.009652	.368997	-2.58139	.998031
Average	-0.000143	0.050167	-1.93879	13.7579	--	0.000028	-0.009412	0.299856	-2.21198	--
(O) $[45/90/-45/90]_{2S}$										
9A2E	-0.000006	0.045128	-0.67534	6.54505	0.999047	-0.000011	-0.008496	0.065237	-0.79898	0.998674
9B2E	-.000122	.050183	-1.81714	12.67008	.998690	-.000008	-.009078	.211586	-1.61912	.999488
9C2E	-.000050	.048897	-1.11600	8.74676	.998445	-.000004	-.008876	.091570	-.92396	.999026
9D2E	-.000099	.048799	-1.38947	9.53658	.99320	-.000003	-.009054	.174705	-1.28628	.999658
Average	-0.000069	0.048252	-1.24949	9.37462	--	-0.000007	-0.008876	0.135775	-1.15709	--
(P) $[0/45/0/-45]_S$										
2A2E	-0.000016	0.013552	-0.000672	0.000530	0.999999	0.000024	-0.008392	-0.001921	0.001148	0.999995
2B2E	-.000008	.012885	-.000563	0.000339	0.999999	-.000002	-.008286	-.001884	.001274	.999998
2C2E	-.000017	.012830	-.000407	.000163	.999998	.000016	-.008380	-.001599	.001078	.999997
2D2E	.000004	.013193	-.000690	.000541	.999998	.000005	-.008542	-.001856	.001177	.999996
Average	-0.000009	0.013115	-0.000583	0.000393	--	0.000011	-0.008400	-0.001815	0.001169	--

TABLE III. - CONTINUED

Specimen Number	a_{0xx}	a_{1xx},GPa^{-1}	a_{3xx},GPa^{-3}	a_{4xx},GPa^{-4}	R^2_{xx}	a_{0xy}	a_{1xy},GPa^{-1}	a_{3xy},GPa^{-3}	a_{4xy},GPa^{-4}	R^2_{xy}
(Q) $[45/0/-45/0]_S$										
8A2D	-0.000024	0.013034	-0.001228	0.001168	0.999996	-0.000006	-0.007630	-0.001694	0.001383	0.999997
8B2D	-0.000003	.013056	-.001501	.001822	.999994	-.000011	-.008425	-.001626	.001152	.999992
8C2D	-.000004	.012997	-.002737	.003641	.999998	.000013	-.008788	-.002234	.001177	.999997
8D2D	-.000003	.013056	-0.000884	.000732	.999998	.000022	-.008936	-.001752	.001299	.999998
Average	-0.000009	0.013036	-0.001588	0.001841	--	0.000005	-0.008445	-0.001827	0.001253	--
(R) $[45/0/-45/0]_{2S}$										
9A2D	0.000034	0.013103	-0.002300	0.002142	0.999998	-0.000002	-0.009411	0.000155	-0.000751	0.999999
9B2D	-.000022	.012931	-.001205	.001017	.999998	.000010	-.008305	-.001397	.000984	.999999
9C2D	.000155	.013705	-.002324	.001830	.999999	.000007	-.008859	-.000270	.000036	.999999
9D2D	-.000029	.012754	-.001036	.000655	.999998	.000001	-.008357	-.001300	.001004	.999998
Average	0.000035	0.013123	-0.001716	0.001411	--	0.000004	-0.008733	-0.000703	0.000318	--
(S) $[45/0/-45/0]_{2S}$ tested with end tabs										
9A3D	-0.000003	0.012846	-0.001896	0.001822	0.999969	0.0	-0.008266	-0.000774	0.000281	0.999978
9B3D	-.000008	.012624	-.000276	-.000430	.999972	.000003	-.007946	-.001929	.002033	.999974
9C3D	-.000002	.013078	-.000233	-.000759	.999978	0.0	-.008529	-.002257	.002521	.999975
9D3D	-.000016	.012779	-.001777	.001490	.999960	.000003	-.008274	-.001238	.001212	.999962
Average	-0.000007	0.012832	-0.001046	0.000531	--	0.000002	-0.008254	-0.001550	0.001512	--

TABLE III. - CONTINUED

Specimen Number	a_{0xx}	a_{1xx}, GPa^{-1}	a_{3xx}, GPa^{-3}	a_{4xx}, GPa^{-4}	R^2_{xx}	a_{0xy}	a_{1xy}, GPa^{-1}	a_{3xy}, GPa^{-3}	a_{4xy}, GPa^{-4}	R^2_{xy}
(T) $[\pm 45/0/\mp 45/0/\pm 45/0/\pm 45]_T$										
5A2D	-0.000018	0.020870	0.007992	-0.007403	0.999998	-0.000011	-0.013571	-0.014515	0.013779	0.999998
5B2D	-.000014	.019149	.006166	-.004594	.999999	-.000003	-.013187	-.013300	.010053	.999996
5C2D	-.000005	.019648	.004942	-.004224	.999998	.000014	-.013410	-.013872	.015457	.999998
5D2D[b]	-.000002	.019522	.004827	-.004702	.999999	.000012	-.012773	-.009116	.007768	.999988
Average	-0.000010	0.019797	0.005982	-.005231	--	0.000003	-0.013235	-0.012701	0.011764	--
(U) $[\pm 45/90/\mp 45/90/\pm 45/90/\pm 45]_T$										
5A2E	-0.000081	0.040467	-0.222561	1.83689	0.999928	0.000044	-0.013994	0.059080	-0.623788	0.999930
5B2E	-.000046	.039073	-.138916	1.54680	.999937	.000003	-.012765	.003680	-.407922	.999930
5C2E	-.000036	.040315	-.183805	1.53043	.999979	-.000007	-.014119	.010184	-.375622	.999970
5D2E[c]	-.000040	.039365	-.066713	.85229	.999990	.000036	-.013715	-.015828	-.200684	.999922
Average	-0.000051	0.039805	-0.152999	1.44160	--	0.000019	-0.013648	0.014279	-0.402004	--
(V) $[0_2/45/0_2/-45/0_2]_S$										
11A2D	0.000006	0.009963	-0.001778	0.001488	0.999990	0.000003	-0.005265	-0.000050	0.000020	0.999999
11B2D	-.000002	.009924	-.000965	.000691	.999982	-.000022	-.005381	-.000062	.000048	.999999
11C2D	-.000016	.009744	-.001221	.000926	.999996	.000003	-.005407	.000122	-.000294	.999981
11D2D	-.000011	.009585	-.000868	.000437	.999998	-.000004	-.005392	-.000131	.000120	.999995
Average	-0.000006	0.009804	-0.001208	0.000886	--	-0.000005	-0.004186	-0.000030	-0.000027	--

[b]Different layup: $[\pm 45/0/\pm 45/\overline{0}]_S$ [c]Different layup: $[\pm 45/90/\pm 45/\overline{90}]_S$

TABLE III. - CONTINUED

Specimen Number	a_{0xx}	a_{1xx}, GPa^{-1}	a_{3xx}, GPa^{-3}	a_{4xx}, GPa^{-4}	R^2_{xx}	a_{0xy}	a_{1xy}, GPa^{-1}	a_{3xy}, GPa^{-3}	a_{4xy}, GPa^{-4}	R^2_{xy}
(W) $[0_2/45/0_2/-45/0_2]_S$ tested with end tabs										
11A6D	0.000030	0.009372	-0.000774	0.000445	0.999995	-0.000026	-0.005146	-0.000122	0.000046	0.999997
11B6D	.000026	.009423	-.000862	.000445	.999996	-.000016	-.005171	-.000050	.000025	.999997
11C6D	.000008	.009681	-.000922	.000450	.999999	-.000028	-.005259	.000072	-.000040	.999998
11D6D	.000023	.009474	-.001087	.000643	.999993	-.000013	-.005259	.000236	-.000243	.999956
Average	0.000022	0.009488	-0.000911	0.000496	--	-0.000021	-0.005209	0.000034	-0.000053	--
(X) $[90_2/45/90_2/-45/90_2]_S$										
11A2E	-0.000043	0.062657	-4.03664	54.4694	0.997706	-0.000015	-0.005315	0.201073	-2.94882	0.997862
11B2E	-.000043	.065051	-6.95329	94.6553	.997251	-.000009	-.004560	-.508579	4.60618	.989498
11C2E	-.000141	.071931	-9.80587	109.7312	.996549	.000006	-.005373	.143504	-1.98642	.998029
11D2E	-.000239	.074656	-9.62243	94.0970	.991249	-.000021	-.005151	.151246	-2.81785	.999344
Average	-0.000117	0.068574	-7.60456	88.2382	--	-0.000010	-0.005100	-0.003189	-0.78673	--
(Y) $[(90/0)_2/45/0/-45/0]_S$										
7A2D	-0.000007	0.012652	0.000055	-0.000692	0.999954	-0.000008	-0.002754	0.000501	-0.000300	0.999898
7B2D	-.000014	.012882	-.005494	.006319	.999915	.000004	-.002584	.000349	-.000208	.999988
7C2D	-.000008	.012490	.002390	-.002414	.999911	-.000025	-.002713	.000472	-.000345	.999936
7D2D	-.000008	.012609	.002428	-.002698	.999926	.000013	-.002795	.000762	-.000682	.999729
Average	-0.000009	0.012658	-0.000155	0.000129	--	-0.000004	-0.002712	0.000521	-0.000384	--

TABLE III. - CONCLUDED

Specimen Number	a_{0xx}	a_{1xx}, GPa^{-1}	a_{3xx}, GPa^{-3}	a_{4xx}, GPa^{-4}	R^2_{xx}	a_{0xy}	a_{1xy}, GPa^{-1}	a_{3xy}, GPa^{-3}	a_{4xy}, GPa^{-4}	R^2_{xy}
(Z) $[(0/90)_2/45/90/-45/90]_S$										
7A2E	0.000018	0.020105	0.013406	0.001845	0.999763	-0.000002	-0.002683	0.000899	0.001089	0.999759
7B2E	.000056	.019818	.025694	-.026835	.999872	-.000007	-.002620	.002238	-.002802	.999930
7C2E	.000075	.020284	.018222	-.012405	.999816	-.000009	-.002683	.001870	-.001949	.999791
7D2E	.000050	.020416	.030877	-.037492	.999811	-.000003	-.002889	.003295	-.004353	.999807
Average	0.000050	0.020156	0.022050	-0.018722	--	-0.000005	-0.002719	0.002076	-0.002004	--

TABLE IV. - TENSILE ELASTIC PROPERTIES

Specimen Number	E_x, GPa	ν_{xy}	F_{tu}, MPa	ε_{tu}
(A) $[0]_8$				
12A2D	125.3	.3422	1291	.00977
12B2D	127.4	.3011	1265	.00933
12C2D	132.6	.3120	1250	.00890
12D2D	125.0	.3004	1136	.00855
Average	127.5	.3138	1236	.00914
(B) $[0]_8$ tested with tabs				
12A6D	130.9	.2928	1412	.01025
12B6D	131.7	.3152	1286	.00926
12C6D	132.3	.3155	1128	.00820
12D6D	130.2	.3165	1049	.00791
Average	131.3	.3100	1219	.00891
(C) $[90]_8$				
12A2E	10.91	.0150	37.72	.00369
12B2E	10.64	.0047	39.28	.00362
12C2E	b	b	11.58[a]	.00064[a]
12D2E	11.02	.0270	38.03	.00342
Average	10.85	.0154	38.34	.00358
(D) $[\pm 45]_{2S}$				
3A2D	19.51	.7329	158.7	.01273
3B2D	20.29	.7478	158.1	.01243
3C2D	20.19	.7746	158.5	.01215
3D2D	20.10	.7740	158.2	.01267
Average	20.02	.7571	158.4	.01249

[a]Not included in average.
[b]Elastic constants not determined because of insufficient data.

TABLE IV. - CONTINUED

Specimen Number	E_x, GPa	ν_{xy}	F_{tu}, MPa	ε_{tu}
(E) $[\pm 45]_{2S}$				
3A2E	19.99	.7686	167.0	.01329
3B2E	20.17	.8157	171.4	.01379
3C2E	18.91	.6679	139.9	.01092
3D2E	20.00	.8037	163.9	.01352
Average	19.75	.7625	160.6	.01288
(F) $[45/0/-45/90]_S$				
4A2E	48.56	.3514	421.8	.00928
4B2D	48.84	.2932	344.6	.00733
4C2D	49.34	.3285	373.7	.00799
4D2D	49.17	.3443	443.6	.00955
Average	48.97	.3294	395.9	.00854
(G) $[45/90/-45/0]_S$				
4A2D	52.45	.2934	506.0	.01004
4B2E	52.31	.2984	503.7	.00998
4C2E	49.50	.2920	482.1	.00972
4D2E	54.15	.3089	546.4	.01044
Average	52.05	.2980	509.6	.01004
(H) $[90/0]_{2S}$				
6A2D	68.81	.0561	292.4[a]	.00405[a]
6B2D	73.83	.0540	682.7	.00902
6C2D	69.47	.0418	683.5	.00923
6D2D	74.14	.0441	633.6	.00864
Average	71.48	.0490	666.6	.00897

[a]Not included in average.

TABLE IV. - CONTINUED

Specimen Number	E_x, GPa	ν_{xy}	F_{tu}, MPa	ε_{tu}
(J) $[0/90]_{2S}$				
6A2E	71.81	.0456	708.5	.01007
6B2E	72.27	.0407	628.7	.00868
6C2E	72.25	.0458	694.8	.00960
6D2E	73.50	.0499	734.4	.01011
Average	72.45	.0454	691.6	.00962
(K) $[0_2/90/0]_S$				
10A2D	103.4	.0767	1028	.00956
10B2D	101.2	.0759	1023	.00972
10C2D	99.32	.0558	1124	.01064
10D2D	100.4	.0894	1102	.01063
Average	101.1	.0744	1069	.01014
(L) $[90_2/0/90]_S$				
10A2E	46.81	.0425	365.6	.00990
10B2E	48.83	.0333	333.3	.00879
10C2E	41.64	.0268	371.7	.01010
10D2E	42.20	.0420	343.5	.00943
Average	44.67	.0361	353.5	.00955
(M) $[90/45/90/-45]_S$				
2A2D	21.19	.1902	177.2	.01021
2B2D	20.32	.1984	170.6	.00978
2C2D	19.05	.1809	179.2	.01116
2D2D	20.63	.1891	175.0	.01051
Average	20.27	.1895	175.5	.01042

TABLE IV. - CONTINUED

Specimen Number	E_x, GPa	ν_{xy}	F_{tu}, MPa	ε_{tu}
(N) $[45/90/-45/90]_S$				
8A2E	19.87	.1764	161.4	.00911
8B2E	18.93	.1933	163.9	.00939
8C2E	21.29	.1898	166.8	.00893
8D2E	19.78	.1909	162.8	.00928
Average	19.93	.1876	163.7	.00918
(O) $[45/90/-45/90]_{2S}$				
9A2E	22.16	.1883	189.9	.01185
9B2E	19.93	.1809	176.9	.01045
9C2E	20.45	.1815	188.3	.01193
9D2E	20.49	.1855	183.5	.01063
Average	20.72	.1840	184.7	.01122
(P) $[0/45/0/-45]_S$				
2A2E	73.79	.6192	801.2	.01073
2B2E	77.61	.6431	759.9	.00958
2C2E	77.95	.6532	826.2	.01037
2D2E	75.80	.6475	810.6	.01054
Average	76.25	.6405	799.5	.01031
(Q) $[45/0/-45/0]_S$				
8A2D	76.73	.5854	639.0	.00803
8B2D	76.59	.6452	591.1	.00755
8C2D	76.94	.6762	544.7	.00678
8D2D	76.59	.6845	653.7	.00838
Average	76.71	.6478	607.1	.00769

TABLE IV. - CONTINUED

Specimen Number	E_x, GPa	ν_{xy}	F_{tu}, MPa	ε_{tu}
(R) $[45/0/-45/0]_{2S}$				
9A2D	76.32	.7183	763.3	.00964
9B2D	77.34	.6422	706.1	.00899
9C2D	72.96	.6464	802.4	.01066
9D2D	78.41	.6552	742.5	.00916
Average	76.20	.6655	753.6	.00961
(S) $[45/0/-45/0]_{2S}$ tested with end tabs				
9A3D	77.84	.6435	624.8	.00780
9B3D	79.21	.6294	617.8	.00767
9C3D	76.46	.6521	616.6	.00789
9D3D	78.26	.6475	530.4[a]	.00659[a]
Average	77.93	.6432	619.7	.00779
(T) $[\pm45/0/\mp45/0/\pm45/0/\pm45]_T$				
5A2D	47.92	.6503	499.5	.01094
5B2D	52.22	.6887	522.2	.01037
5C2D	50.90	.6825	457.3	.00911
5D2D	51.22[c]	.6543[c]	512.2[c]	.01029[c]
Average	50.28	.6732	493.0	.01014
(U) $[\pm45/90/\mp45/90/\pm45/90/\pm45]_T$				
5A2E	24.71	.3458	224.2	.01094
5B2E	25.59	.3267	227.8	.01160
5C2E	24.80	.3502	225.9	.01087
5D2E	25.40[c]	.3484[c]	181.5[c]	.00759[c]
Average	25.03	.3411	226.0	.01114

[a]Not included in average.
[c]Not included in average; see Table I.

TABLE IV. - CONTINUED

Specimen Number	E_x, GPa	ν_{xy}	F_{tu}, MPa	ε_{tu}
(V) $[0_2/45/0_2/-45/0_2]_S$				
11A2D	100.4	.5285	738.8	.00711
11B2D	100.8	.5422	645.2	.00621
11C2D	102.6	.5549	889.5	.00809
11D2D	104.3	.5626	947.7	.00841
Average	102.0	.5469	805.3	.00745
(W) $[0_2/45/0_2/-45/0_2]_S$ tested with end tabs				
11A6D	106.7	.5491	1062	.00974
11B6D	106.1	.5488	1104	.00987
11C6D	103.3	.5433	1035	.00947
11D6D	105.6	.5551	948.3	.00888
Average	105.4	.5491	1046	.00949
(X) $[90_2/45/90_2/-45/90_2]_S$				
11A2E	15.96	.0848	107.9	.00985
11B2E	15.37	.0701	103.8	.01023
11C2E	13.90	.0747	105.5	.00892
11D2E	13.39	.0690	102.5	.00746
Average	14.58	.0744	104.9	.00912
(Y) $[(90/0)_2/45/0/-45/0]_S$				
7A2D	79.04	.2176	787.8	.00966
7B2D	77.63	.2006	767.1	.00954
7C2D	80.07	.2172	805.9	.01019
7D2D	79.31	.2217	767.9	.00980
Average	79.00	.2142	782.2	.00980

TABLE IV. - CONCLUDED

Specimen Number	E_x, GPa	ν_{xy}	F_{tu}, MPa	ε_{tu}
(Z) $[(0/90)_2/45/90/-45/90]_S$				
7A2E	49.74	.1334	445.6	.01005
7B2E	50.46	.1322	473.3	.01062
7C2E	49.30	.1323	459.3	.01042
7D2E	48.98	.1415	473.7	.01103
Average	49.61	.1349	463.0	.01053

TABLE V. - LAMINATE TENSILE ELASTIC CONSTANTS.

Laminate	E_x, GPa		Error%	ν_{xy}		Error%	F_{tu}, MPa	ε_{tu}
	Experimental	Laminate Analysis		Experimental	Laminate Analysis			
$[0]_8$	127.5	--	--	.3138	--	--	1236	.00914
$[0]_8$ [d]	131.3	--	--	.3100	--	--	1219	.00891
$[90]_8$	10.85[b]	--	--	.0154[b]	.0261	69.5	38.34[b]	.00358[b]
$[\pm 45]_{2S}$	19.88[a]	19.61	-1.4	.7598[a]	.7354	-3.2	159.5[a]	.01269[a]
$[45/0/-45/90]_S$	48.97	51.36	4.9	.3294	.3070	-6.8	395.9	.00854
$[45/90/-45/0]_S$	52.05	51.36	-1.3	.2980	.3070	3.0	509.6	.01004
$[90/0]_{2S}$	71.48	70.54	-1.3	.0490	.0482	-1.6	666.6[b]	.00897[b]
$[0/90]_{2S}$	72.45	70.54	-2.6	.0454	.0482	6.2	691.6	.00962
$[0_2/90/0]_S$	101.1	100.3	-0.8	.0744	.0836	12.4	1069	.01014
$[90_2/0/90]_S$	44.67	40.70	-8.9	.0361	.0339	-6.1	353.5	.00955
$[90/45/90/-45]_S$	20.27	23.32	15.0	.1895	.2011	6.1	175.5	.01042
$[45/90/-45/90]_S$	19.93	23.32	17.0	.1876	.2011	7.2	163.7	.00918
$[45/90/-45/90]_{2S}$	20.72	23.32	12.5	.1840	.2011	9.3	184.7	.01122

(a) average of 8 tests (b) average of 3 tests (d) tested with end tabs

TABLE V. - CONCLUDED

Laminate	E_x, GPa		Error%	ν_{xy}		Error%	F_{tu}, MPa	ε_{tu}
	Experimental	Laminate Analysis		Experimental	Laminate Analysis			
$[0/45/0/-45]_S$	76.25	75.29	-1.3	.6405	.6490	1.3	799.5	.01031
$[45/0/-45/0]_S$	76.71	75.29	-1.9	.6478	.6490	0.2	607.1	.00769
$[45/0/-45/0]_{2S}$	76.20	75.29	-1.2	.6655	.6490	-2.5	753.6	.00961
$[45/0/-45/0]_{2S}$ [d]	77.93	75.29	-3.4	.6432	.6490	0.9	619.7[b]	.00779[b]
$[\pm 45/0/\pm 45/\bar{0}]_S$	51.22[c]	50.04	-2.3	.6543[c]	.6983	6.7	512.2[c]	.01029[c]
$[\pm 45/0/\mp 45/0/\pm 45/0/\pm 45]_T$	50.28[b]	50.03	-0.5	.6732[b]	.6974	3.6	493.0[b]	.01014[b]
$[\pm 45/90/\pm 45/\overline{90}]_S$	25.40[c]	25.56	0.6	.3484[c]	.3567	2.4	181.5[c]	.00759[c]
$[\pm 45/90/\mp 45/90/\pm 45/90/\pm 45]_T$	25.03[b]	25.52	2.0	.3411[b]	.3557	4.1	226.0[b]	.01114[b]
$[0_2/45/0_2/-45/0_2]_S$	102.0	102.8	0.8	.5469	.5513	0.8	805.3	.00745
$[0_2/45/0_2/-45/0_2]_S$ [d]	105.4	102.8	-2.5	.5491	.5513	0.4	1046	.00949
$[90_2/45/90_2/-45/90_2]_S$	14.58	17.88	22.6	.0744	.0959	28.9	104.9	.00912
$[(90/0)_2/45/0/-45/0]_S$	79.00	76.42	-3.3	.2142	.2135	-0.3	782.2	.00980
$[(0/90)_2/45/90/-45/90]_S$	49.61	47.38	-4.5	.1349	.1324	-1.9	463.0	.01053

(b) average of 3 tests (c) one test (d) tested with end tabs

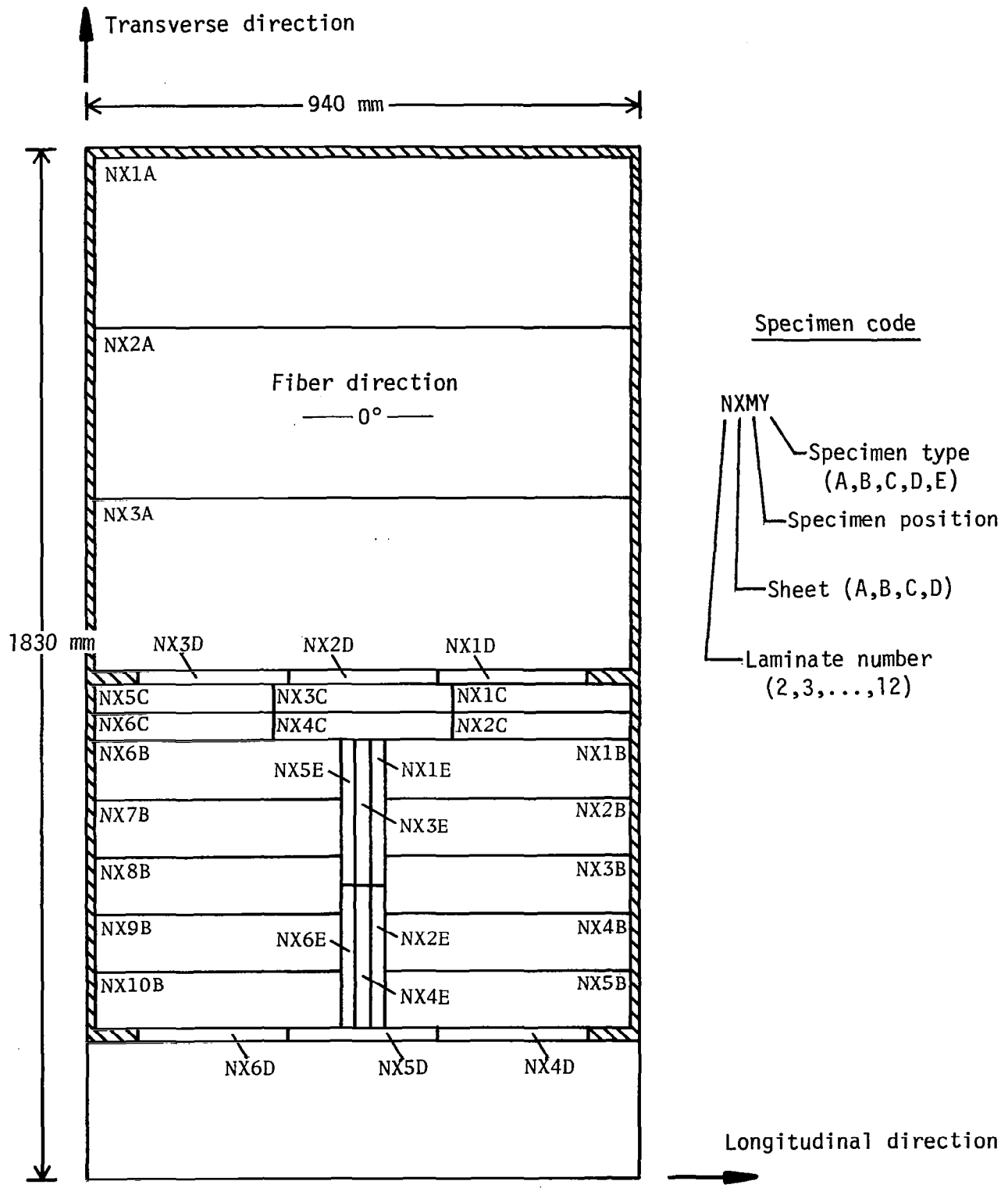

Figure 1. - Specimen layout and numbering system.

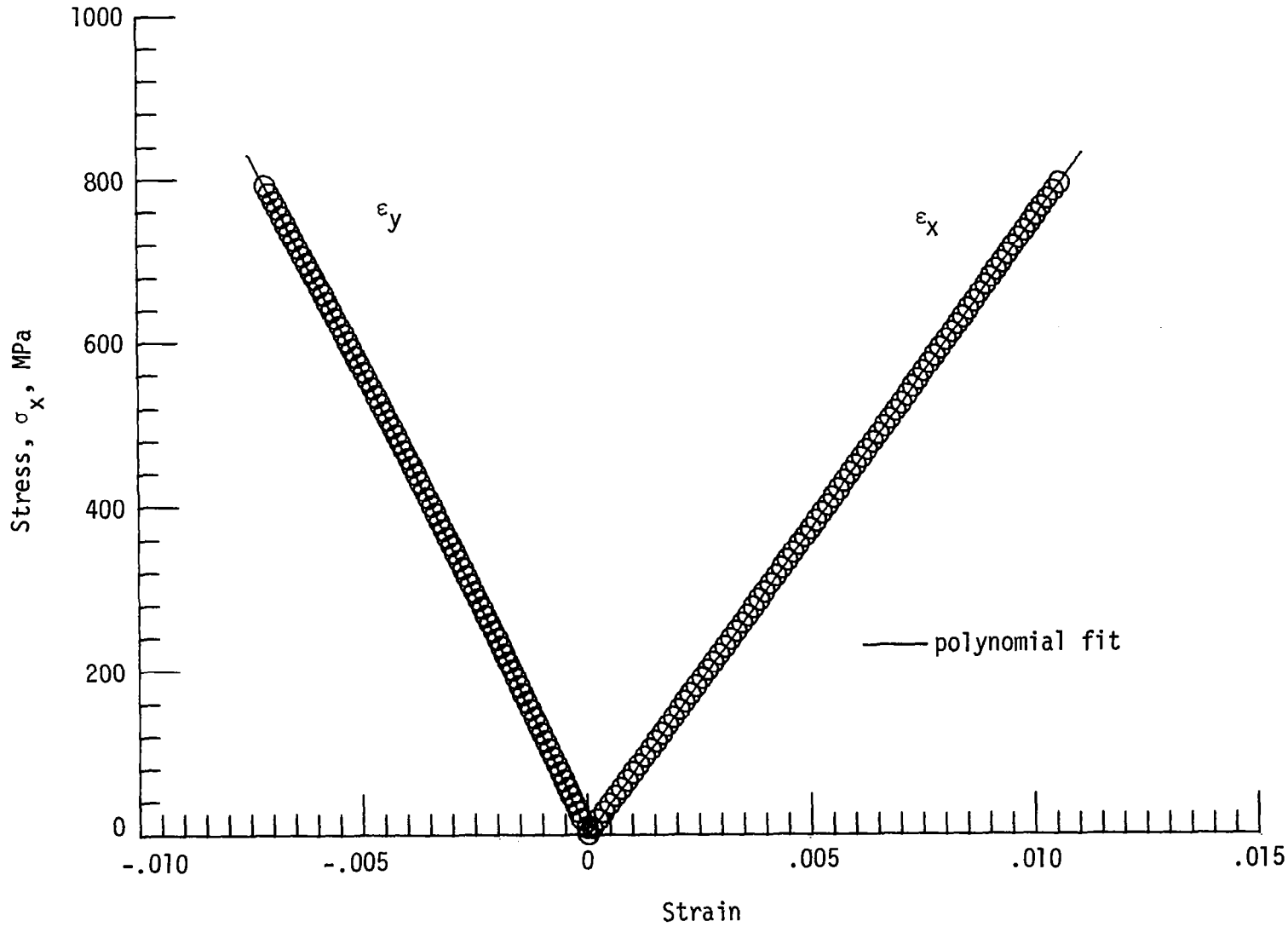

Figure 2. - Stress-strain curve for specimen 2A2E.

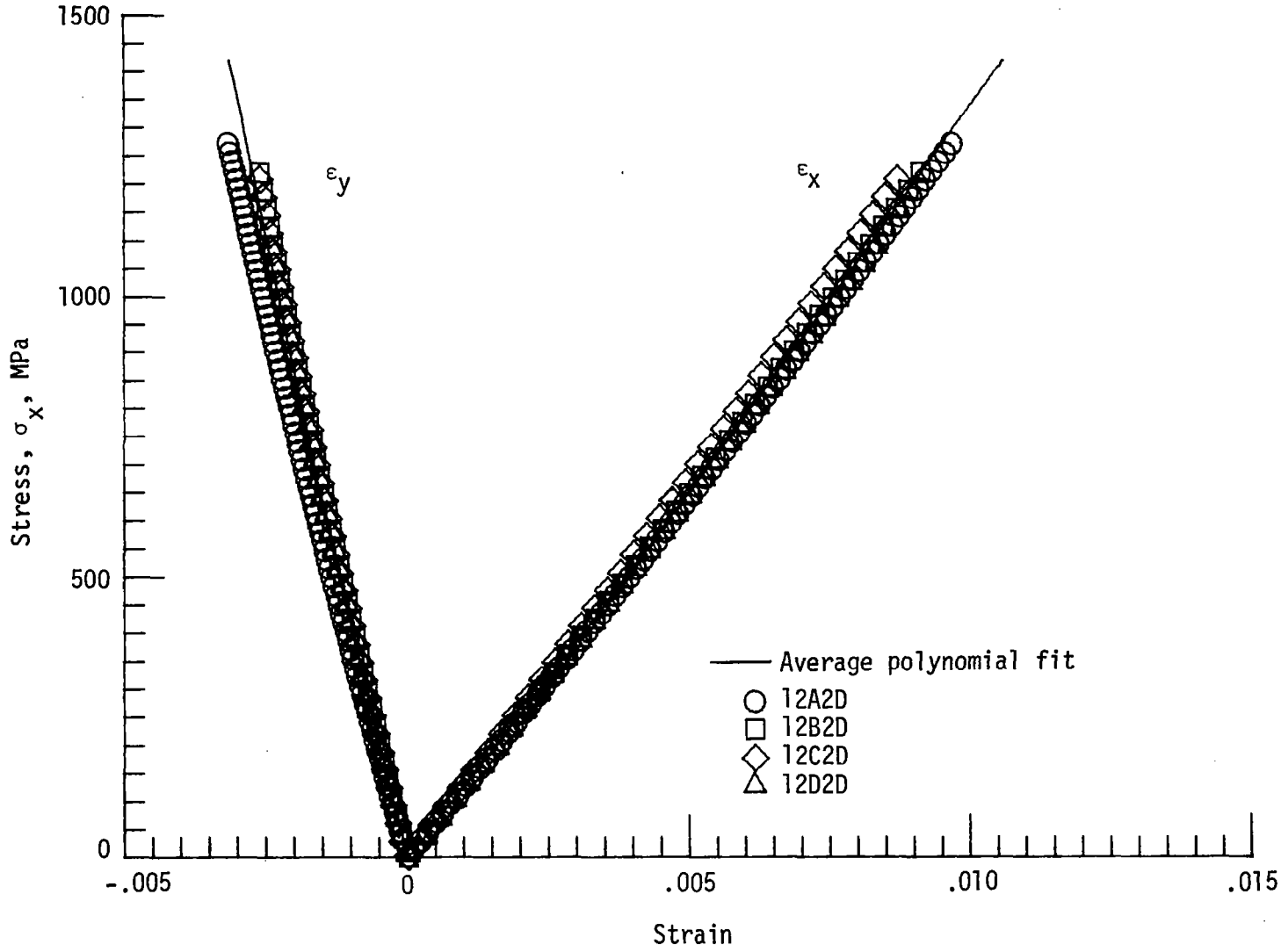

Figure 3. - Stress-strain curve for $[0]_8$ laminate.

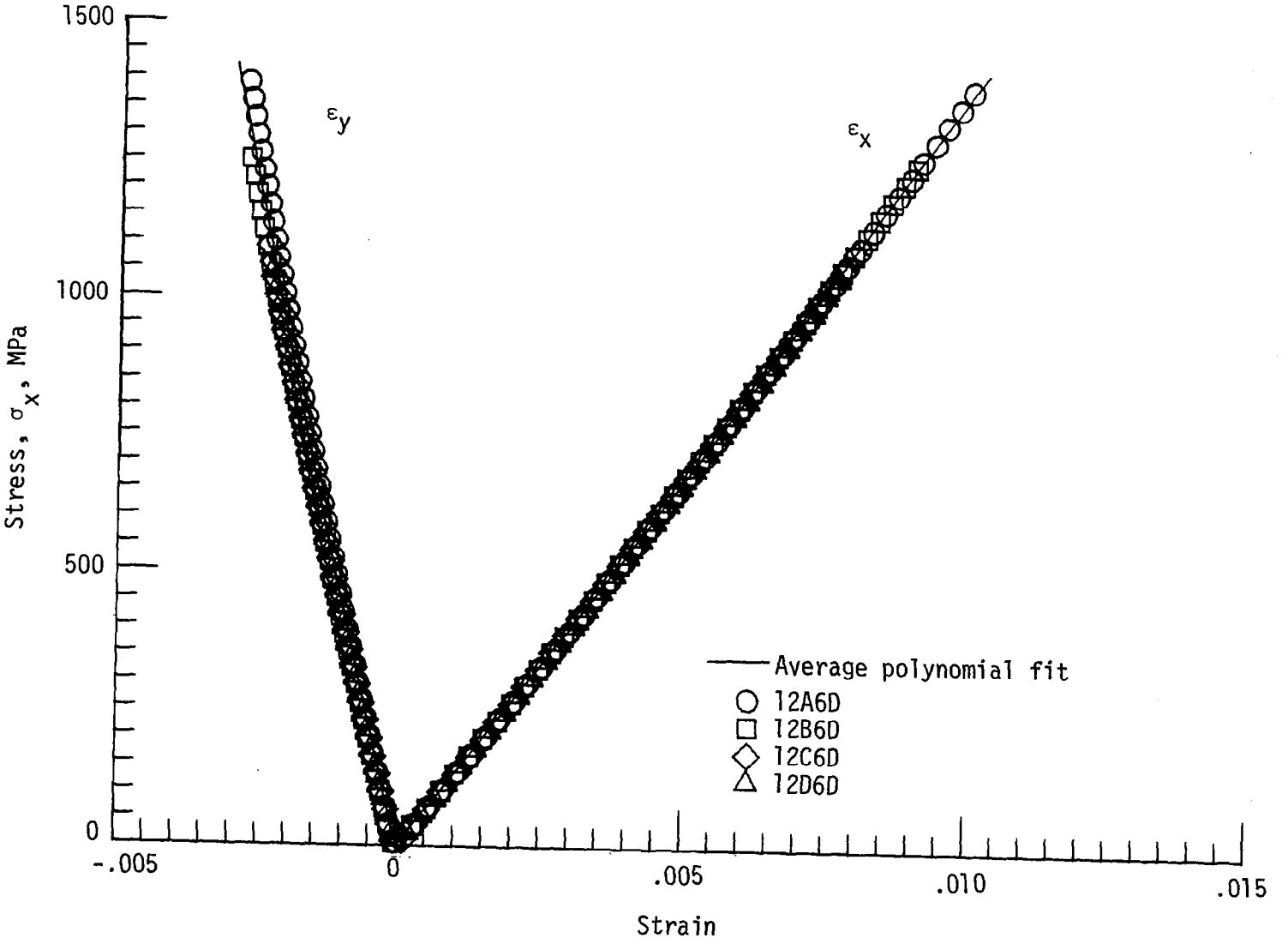

Figure 4. - Stress-strain curve for $[0]_8$ laminate tested with end tabs.

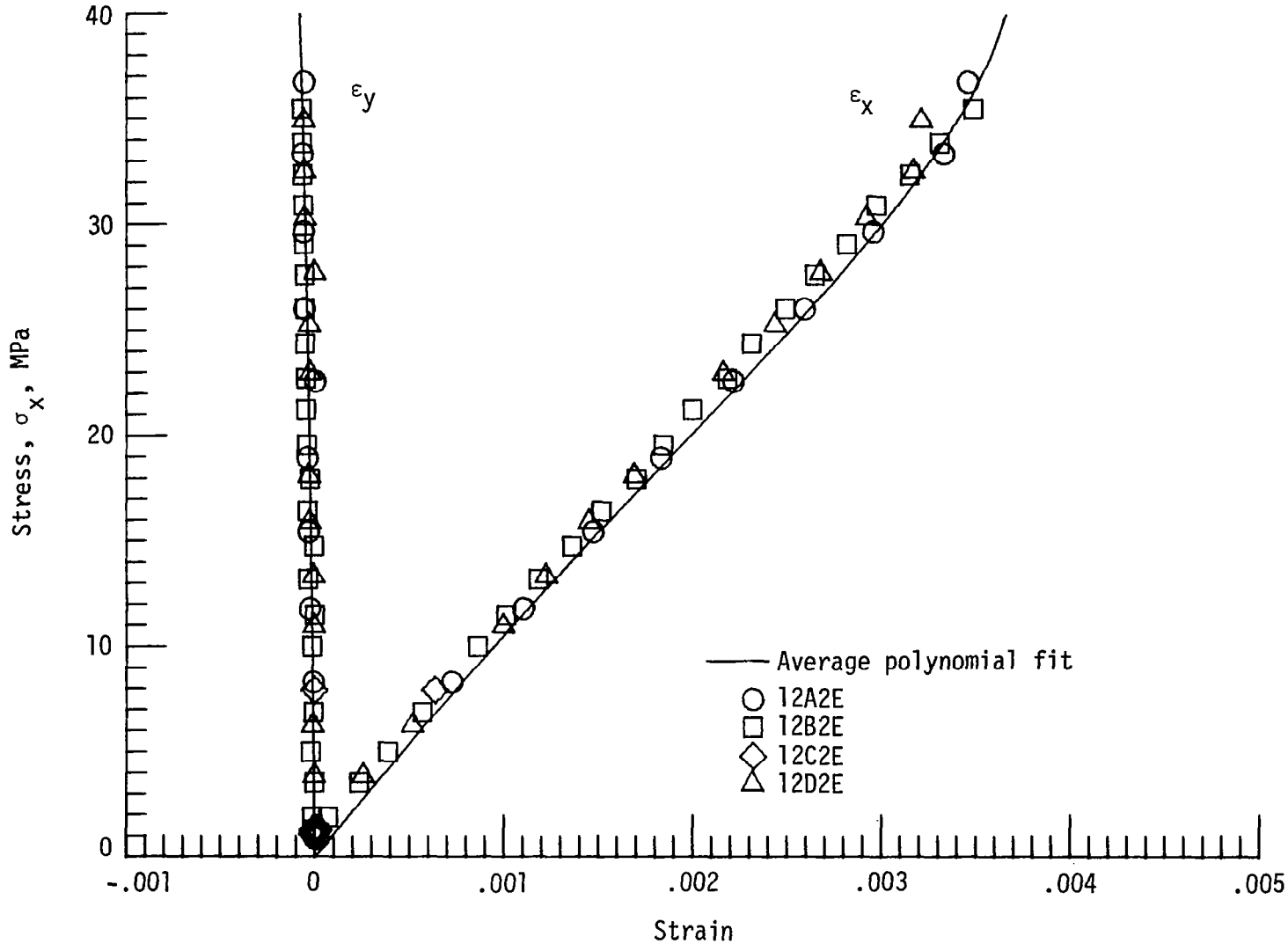

Figure 5. - Stress-strain curve for $[90]_8$ laminate.

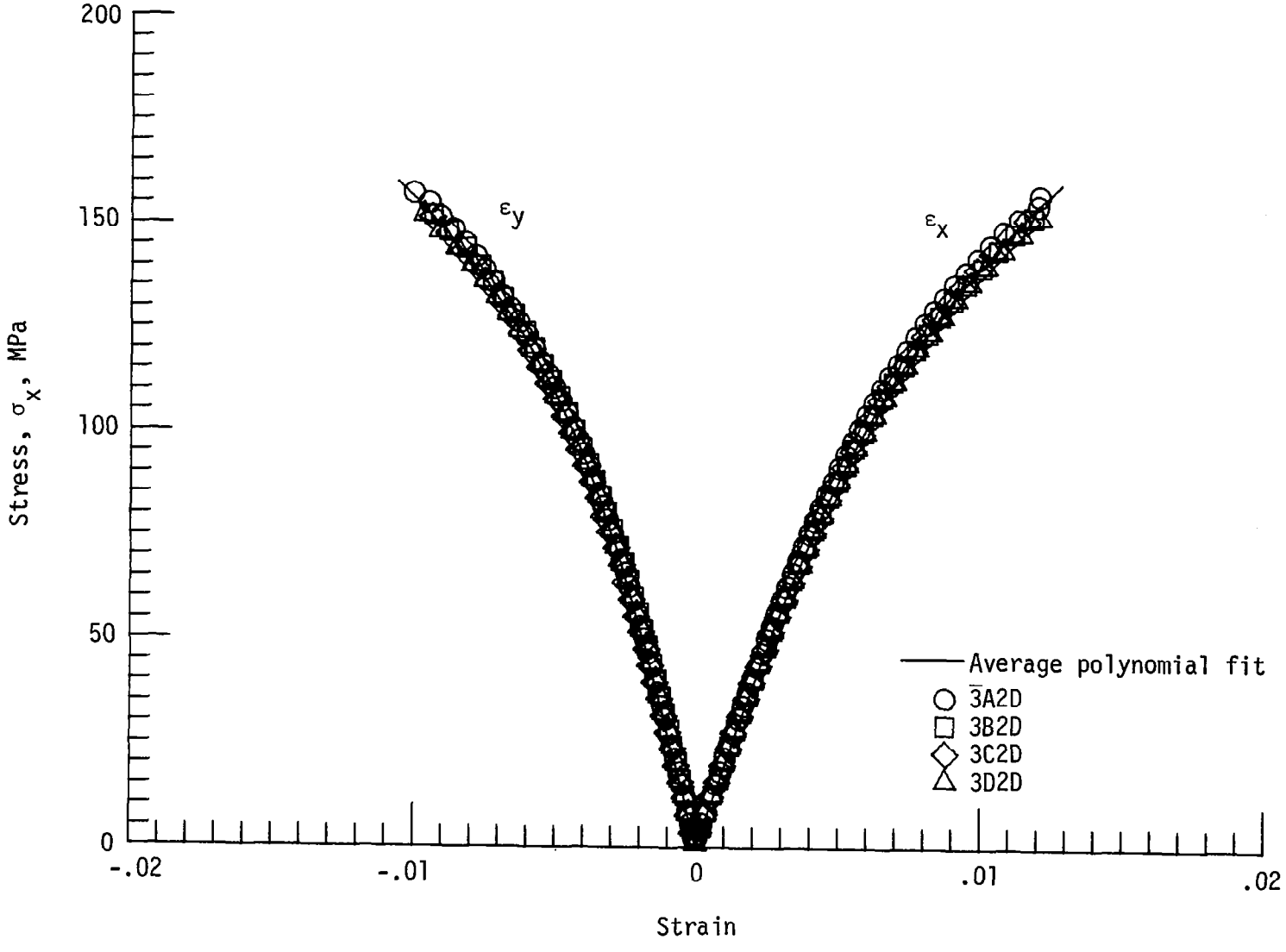

Figure 6. - Stress-strain curve for $[\pm 45]_{2S}$ laminate.

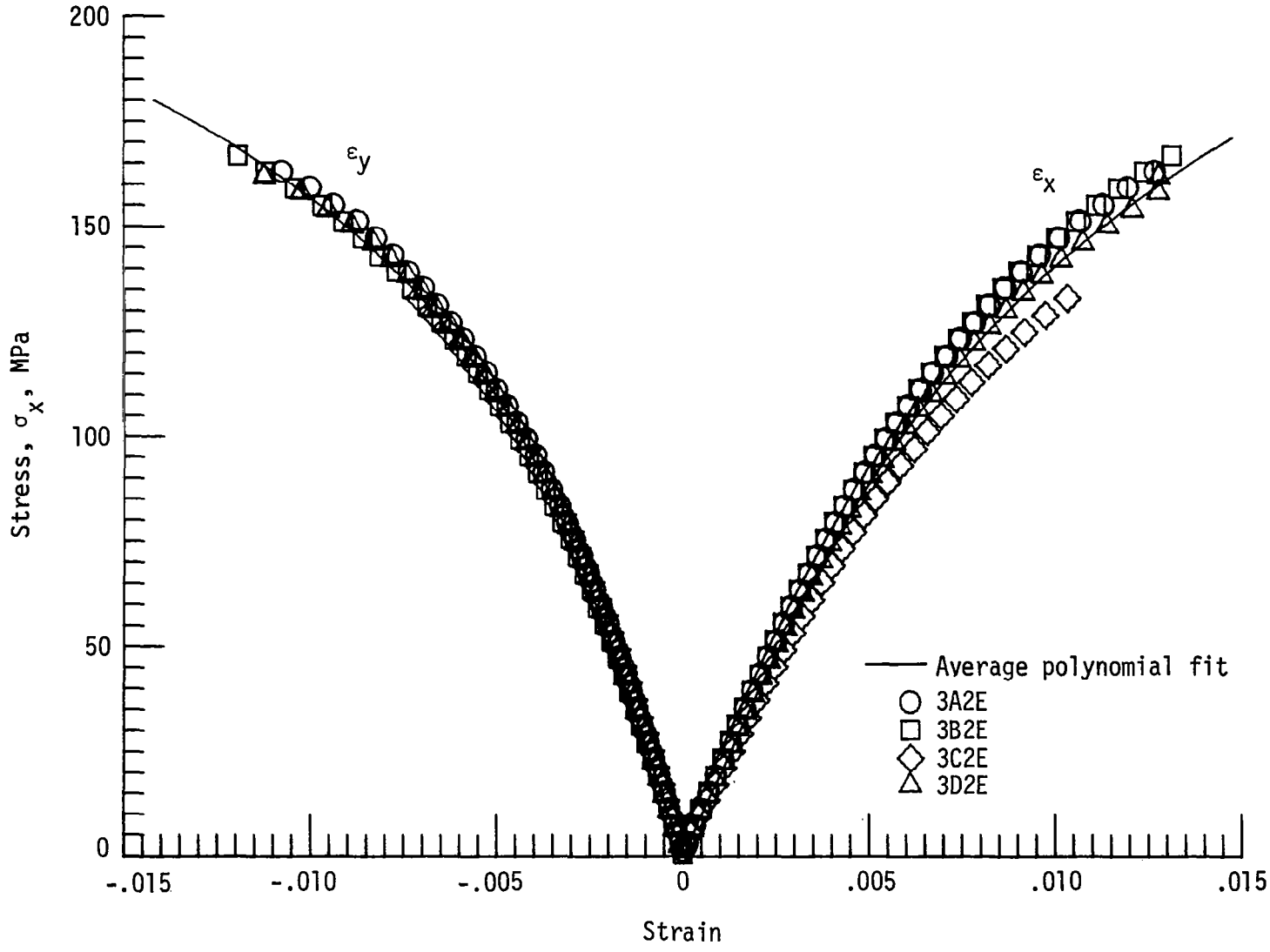

Figure 7. - Stress-strain curve for $[\pm 45]_{2S}$ laminate.

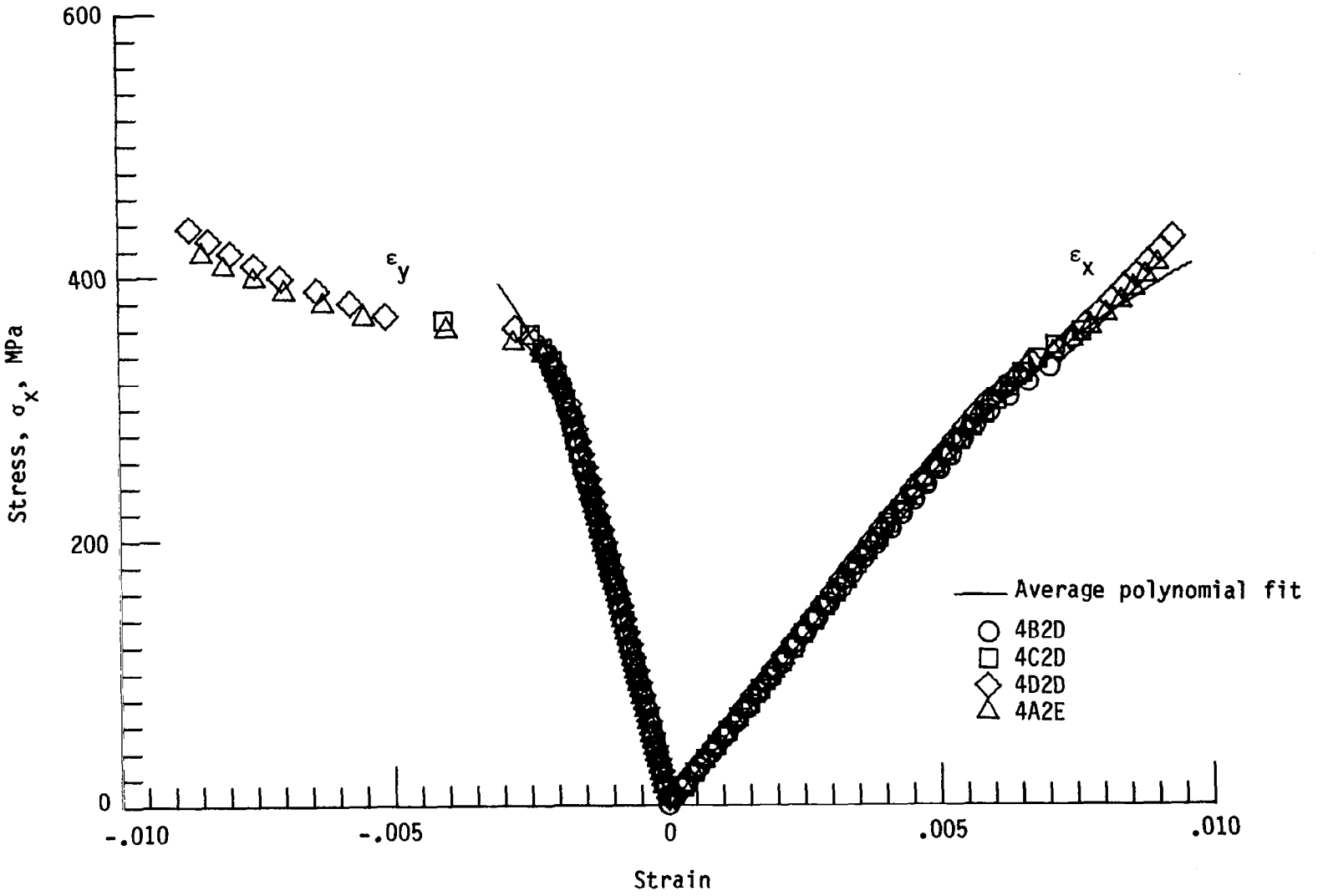

Figure 8. - Stress-strain curve for $[45/0/-45/90]_S$ laminate.

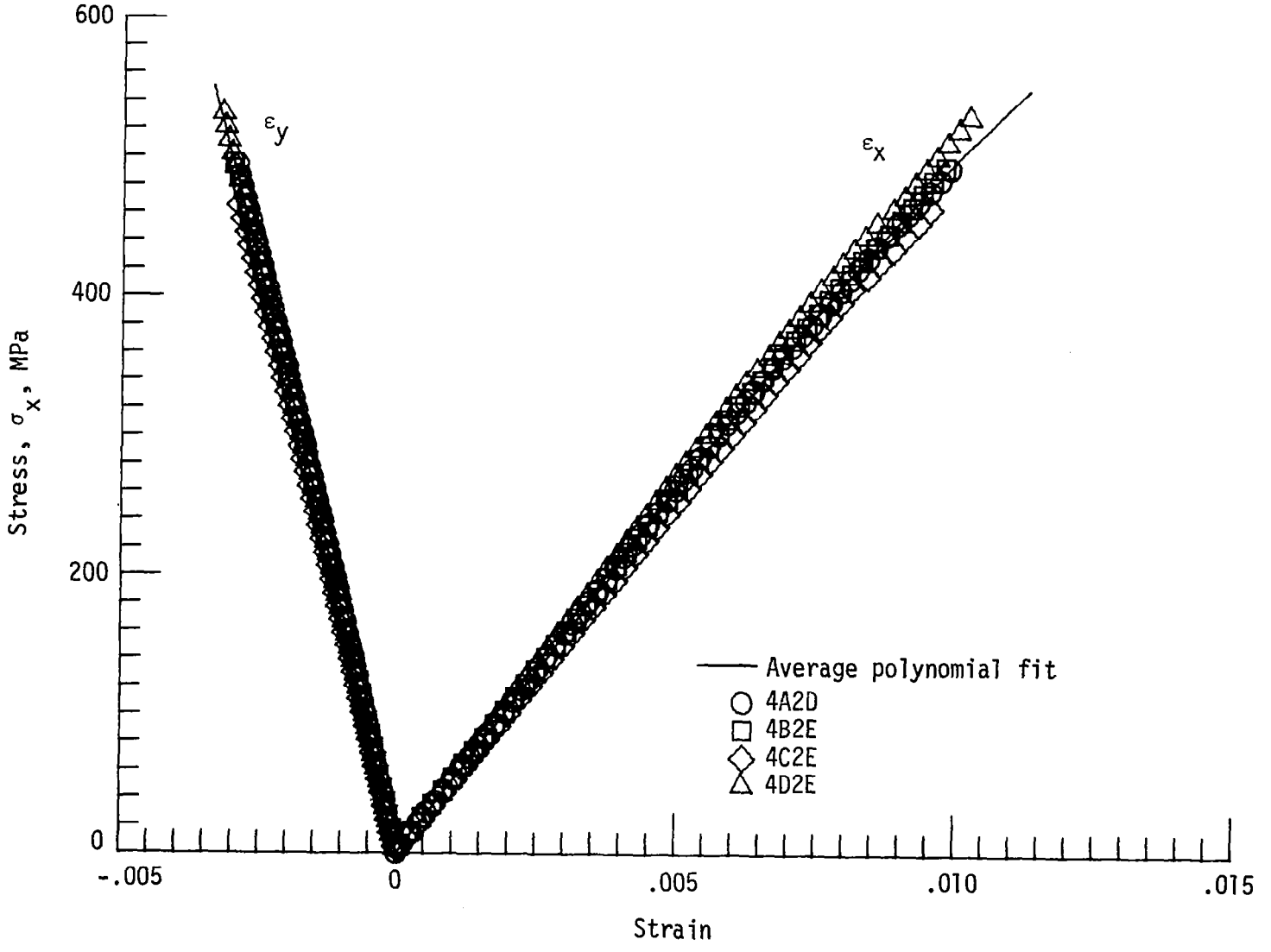

Figure 9. - Stress-strain curve for $[45/90/-45/0]_S$ laminate.

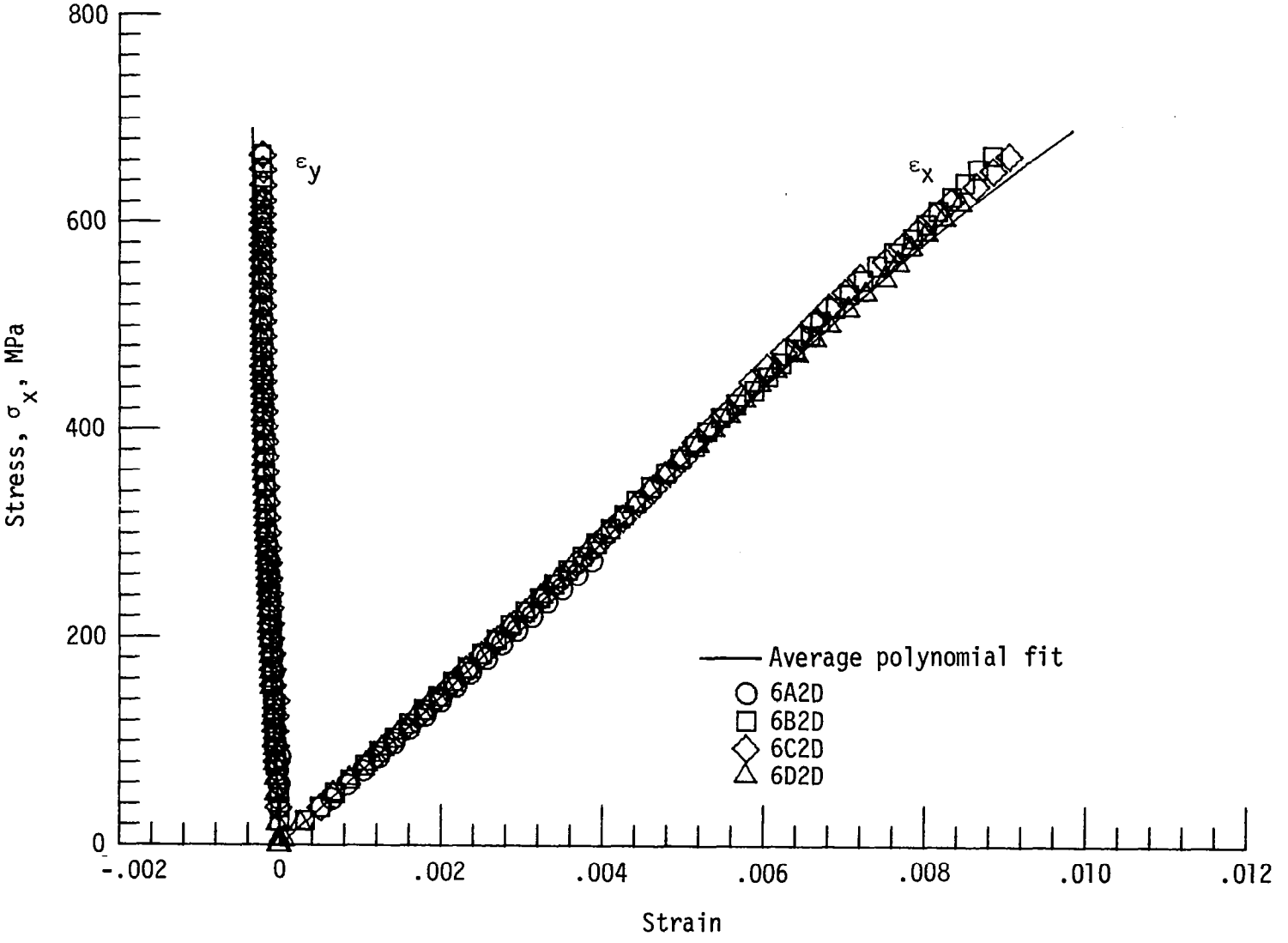

Figure 10. - Stress-strain curve for $[90/0]_{2S}$ laminate.

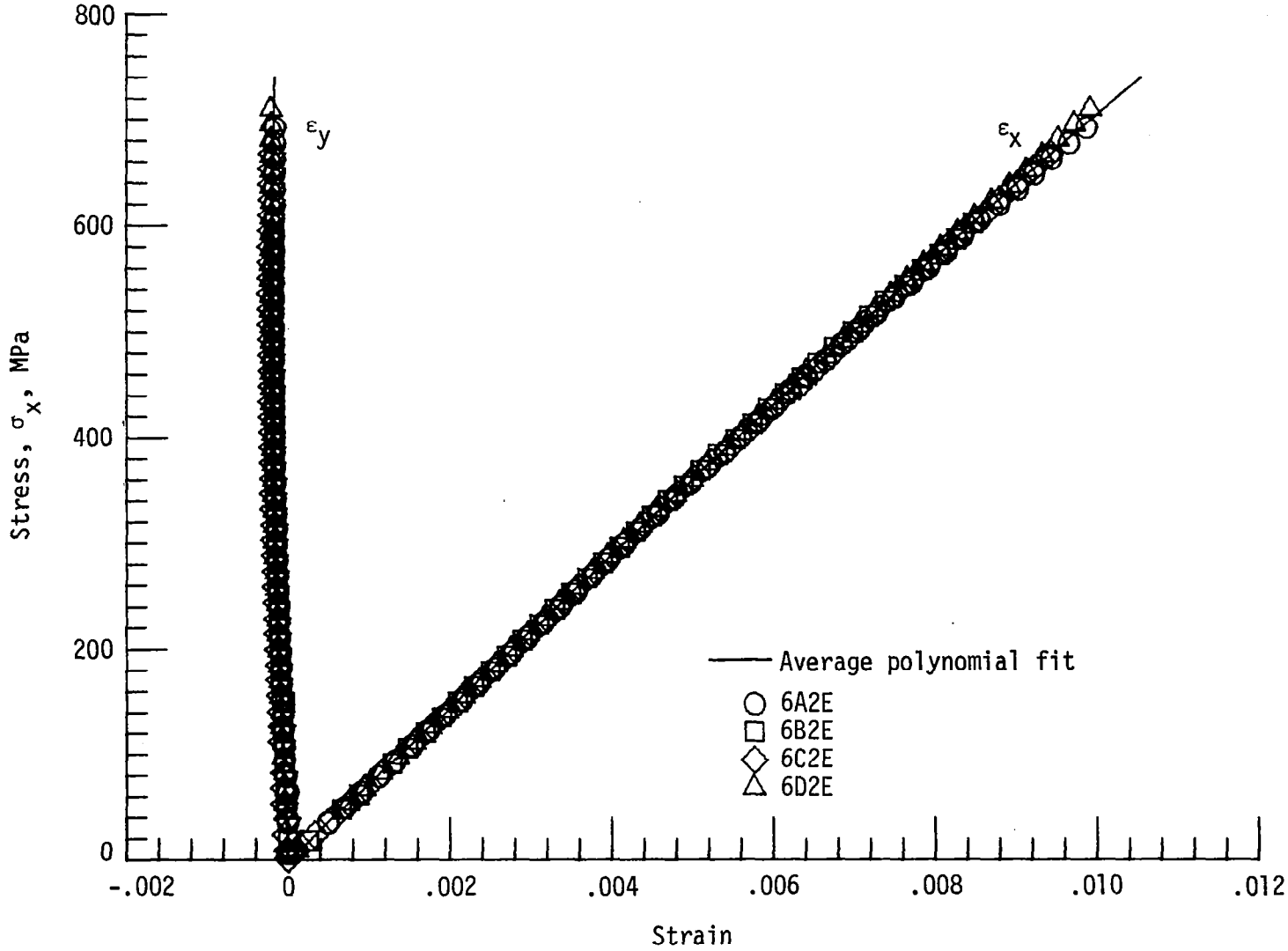

Figure 11. - Stress-strain curve for $[0/90]_{2S}$ laminate.

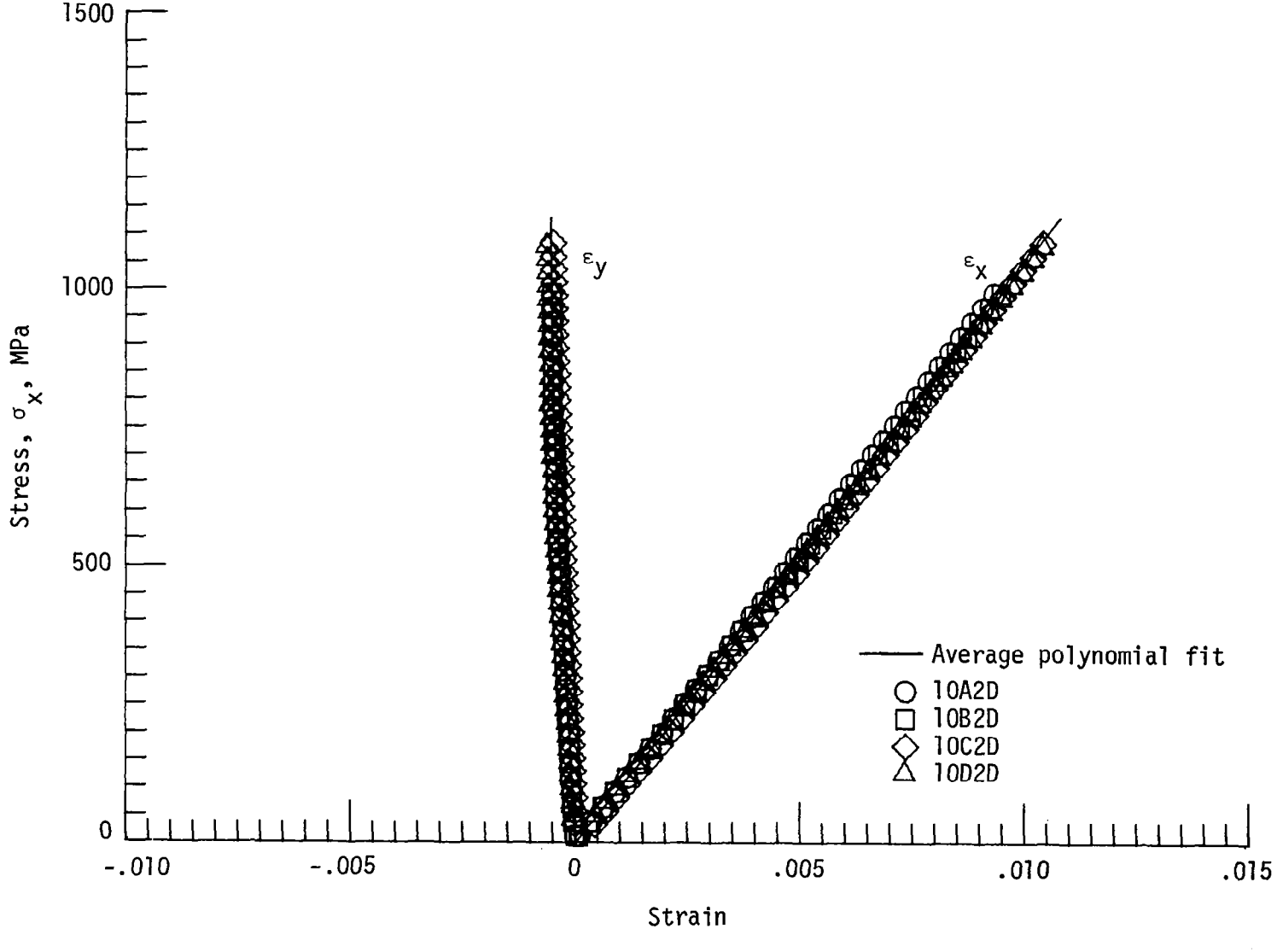

Figure 12. - Stress-strain curve for $[0_2/90/0]_S$ laminate.

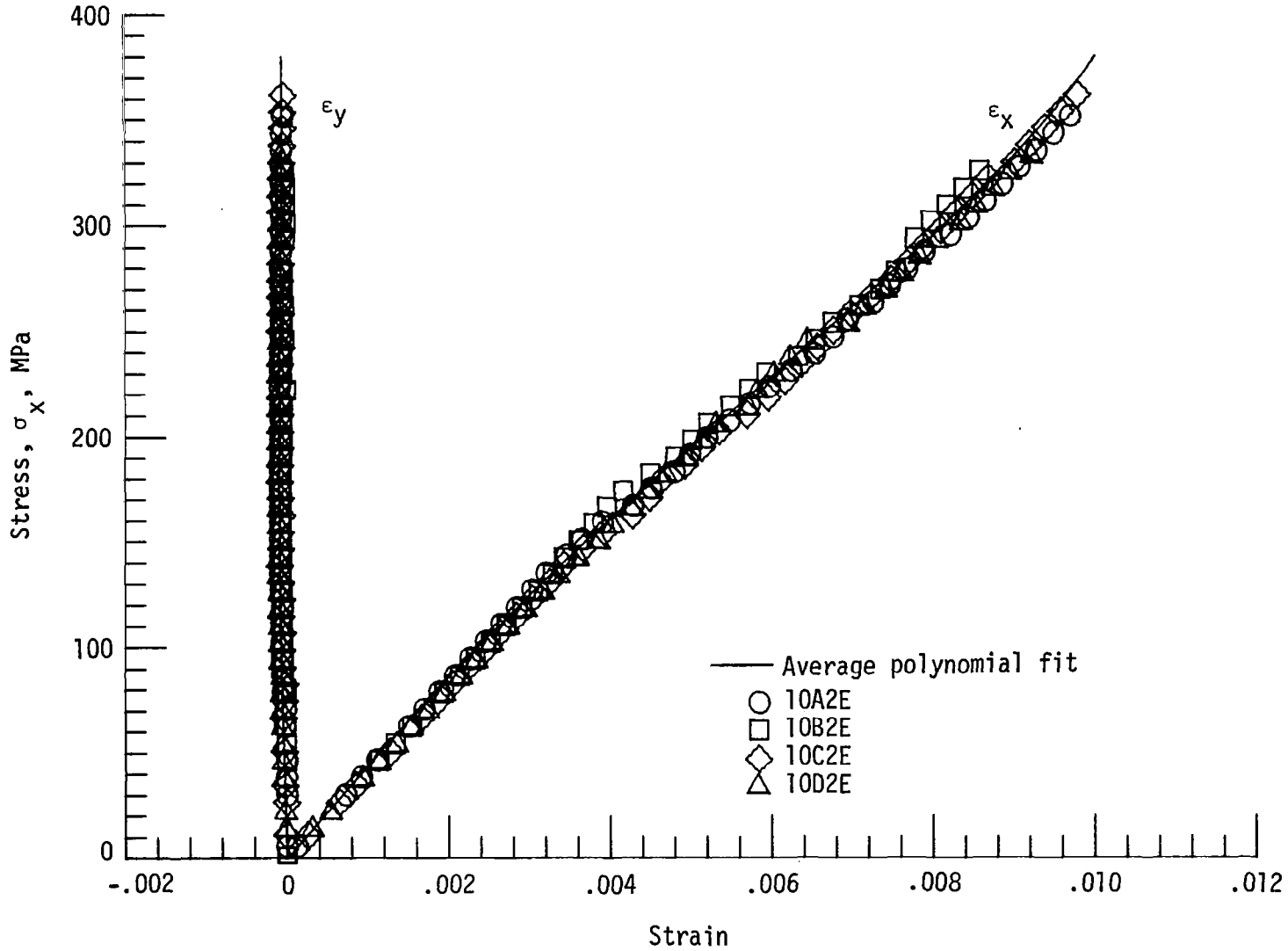

Figure 13. - Stress-strain curve for $[90_2/0/90]_S$ laminate.

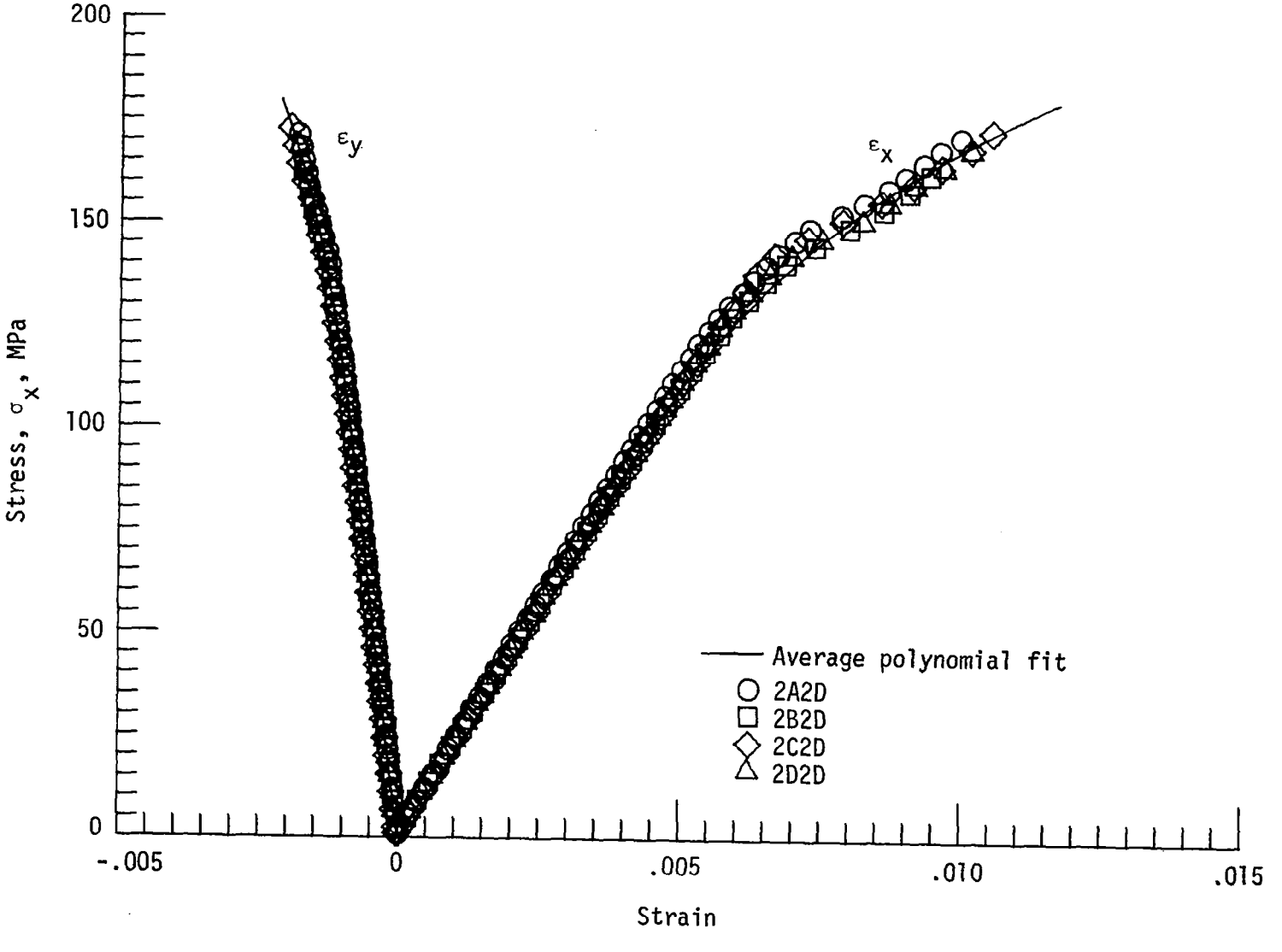

Figure 14. - Stress-strain curve for $[90/45/90/-45]_S$ laminate.

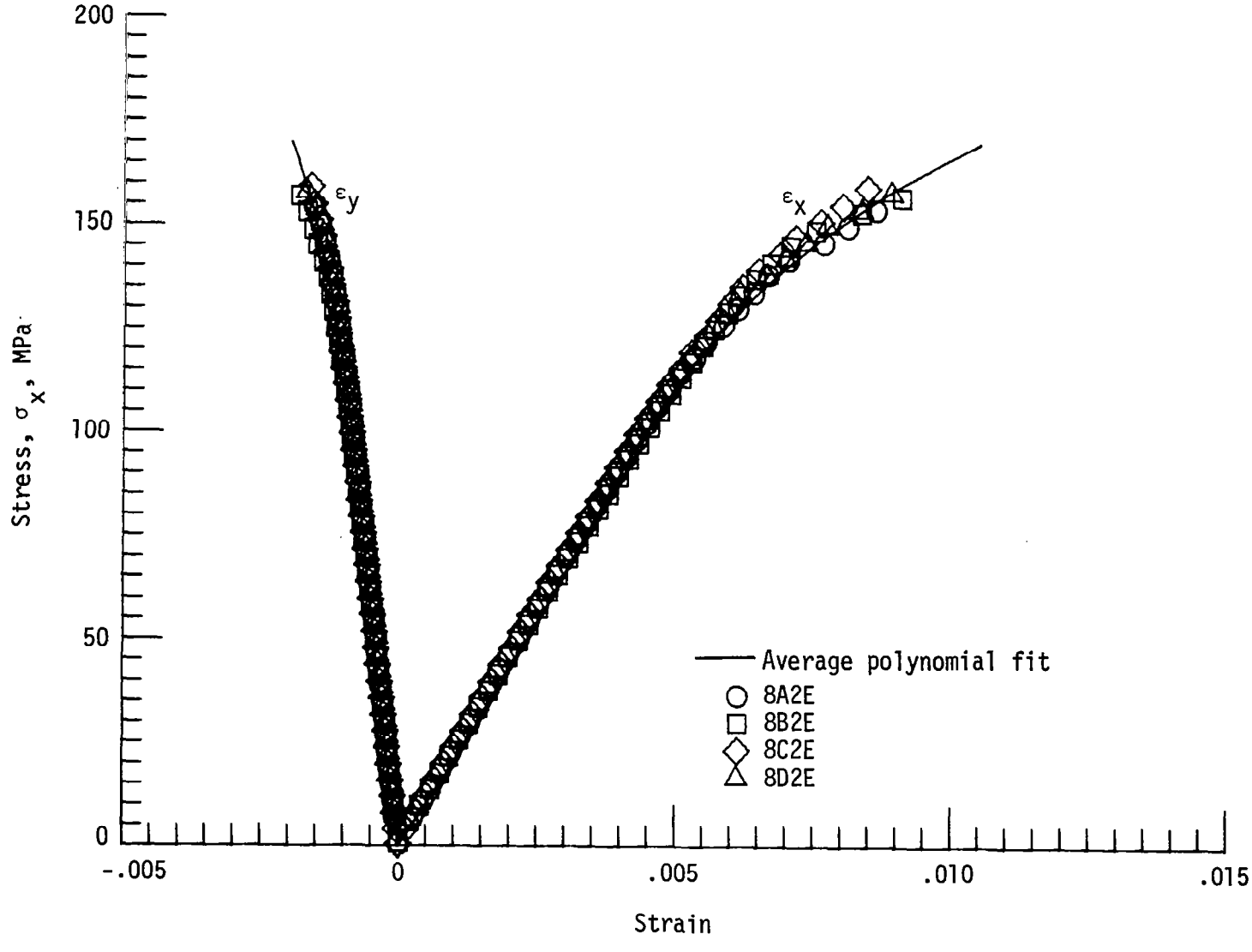

Figure 15. - Stress-strain curve for $[45/90/-45/90]_S$ laminate.

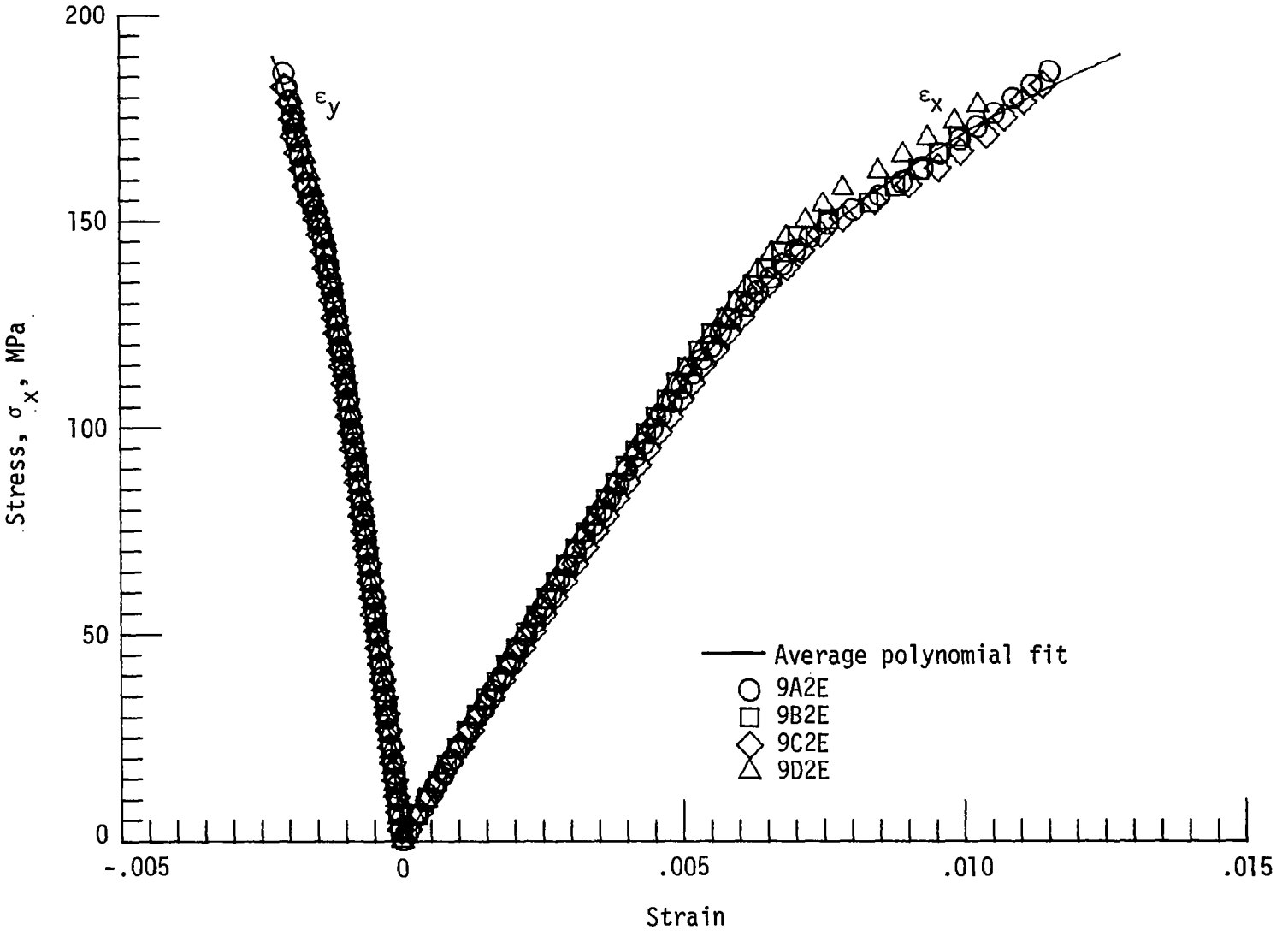

Figure 16. - Stress-strain curve for $[45/90/-45/90]_{2S}$ laminate.

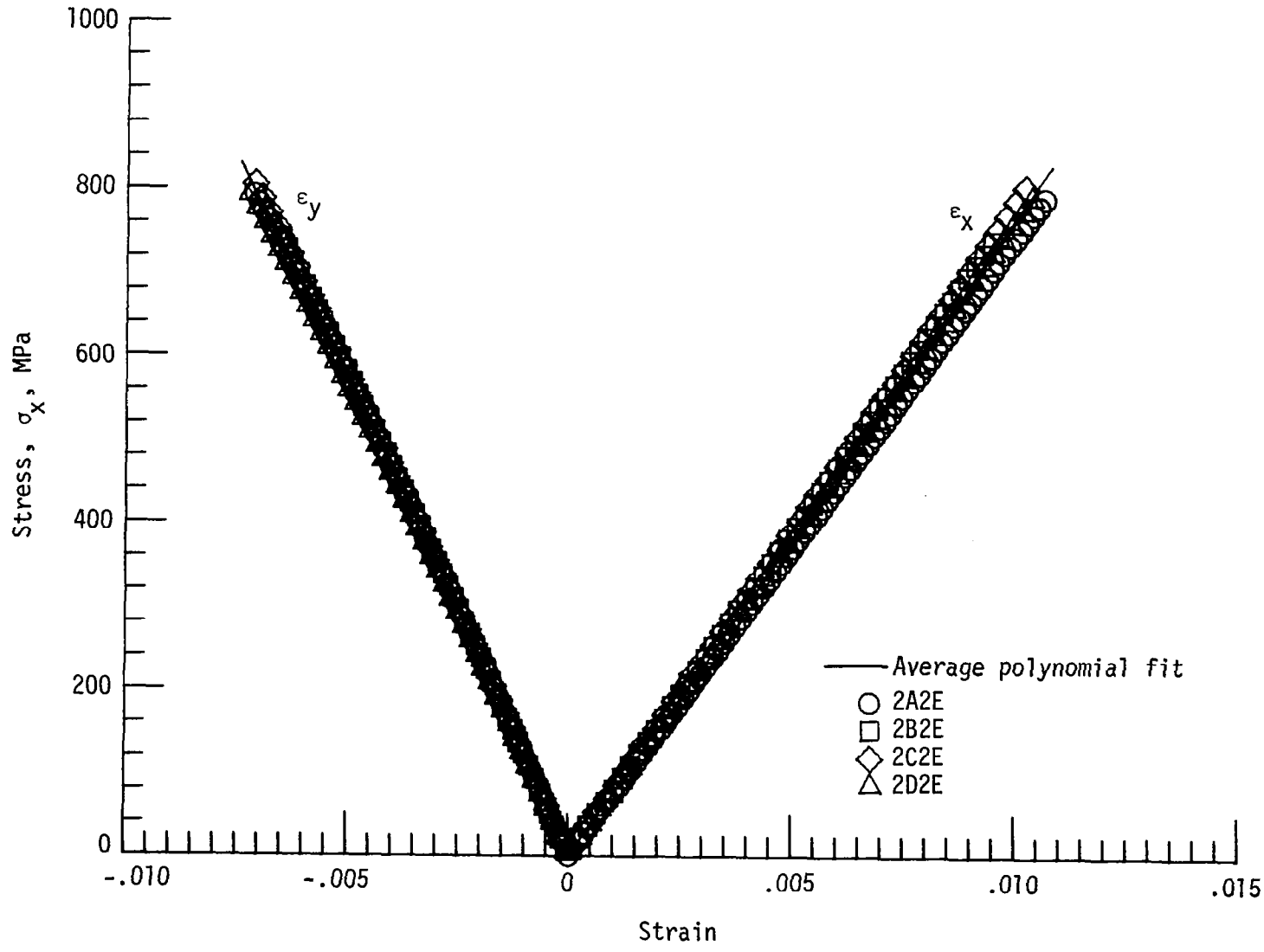

Figure 17. - Stress-strain curve for $[0/45/0/-45]_S$ laminate.

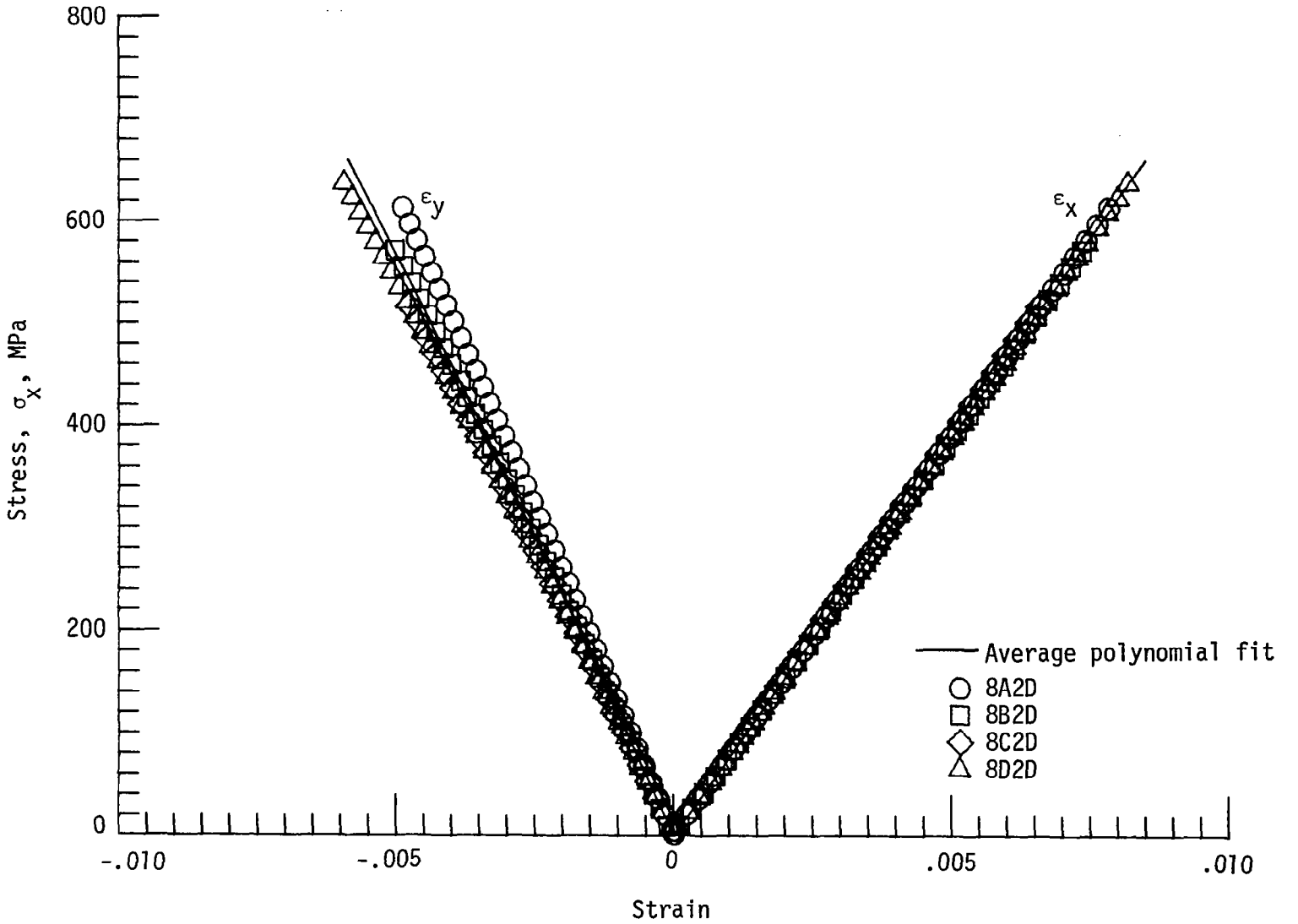

Figure 18. - Stress-strain curve for $[45/0/-45/0]_S$ laminate.

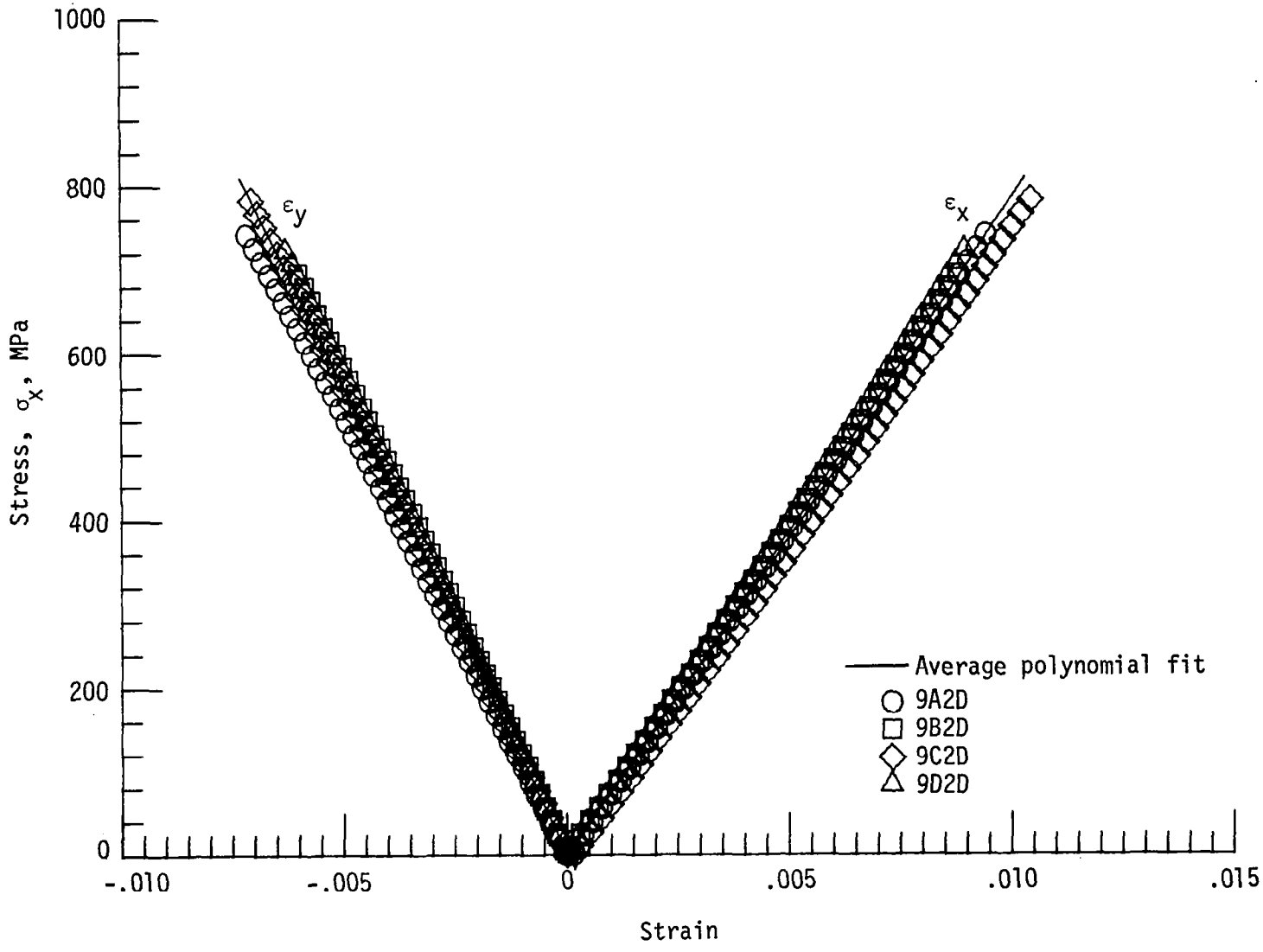

Figure 19. - Stress-strain curve for $[45/0/-45/0]_{2S}$ laminate.

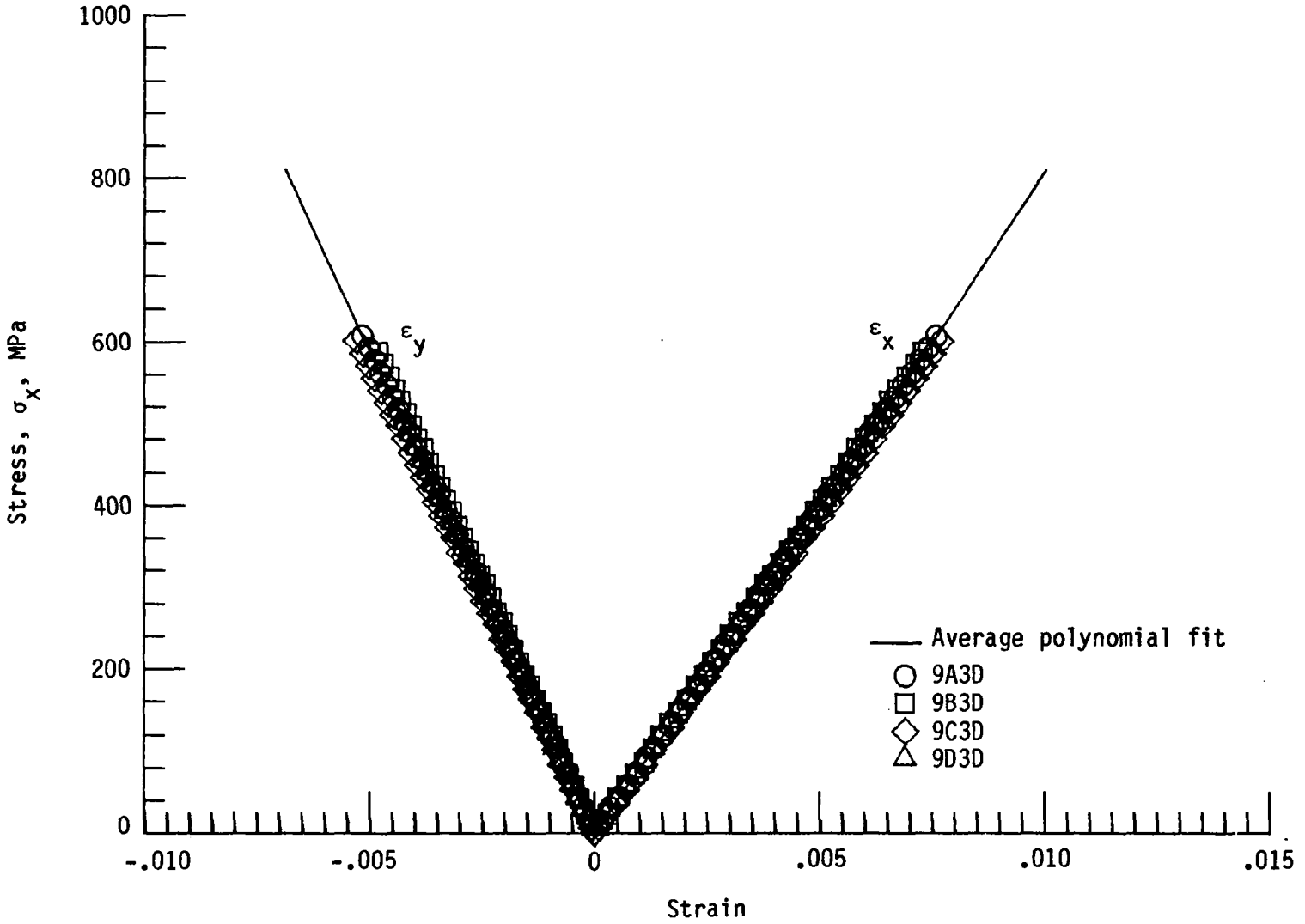

Figure 20. - Stress-strain curve for $[45/0/-45/0]_{2S}$ laminate tested with end tabs.

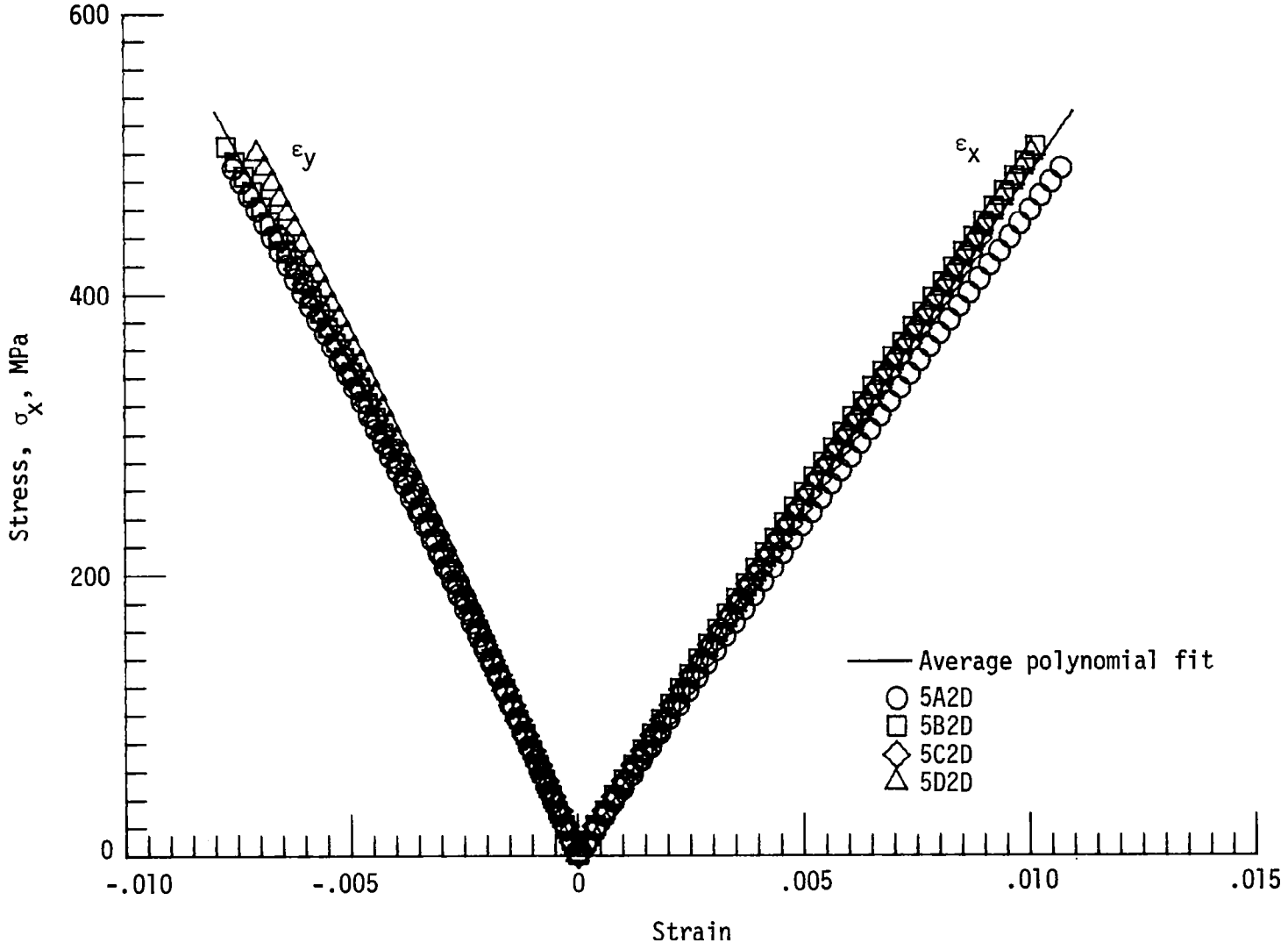

Figure 21. - Stress-strain curve for $[\pm 45/0/\pm 45/\bar{0}]_S$ and $[\pm 45/0/\bar{\mp} 45/0/\pm 45/0/\pm 45]_T$ laminates.

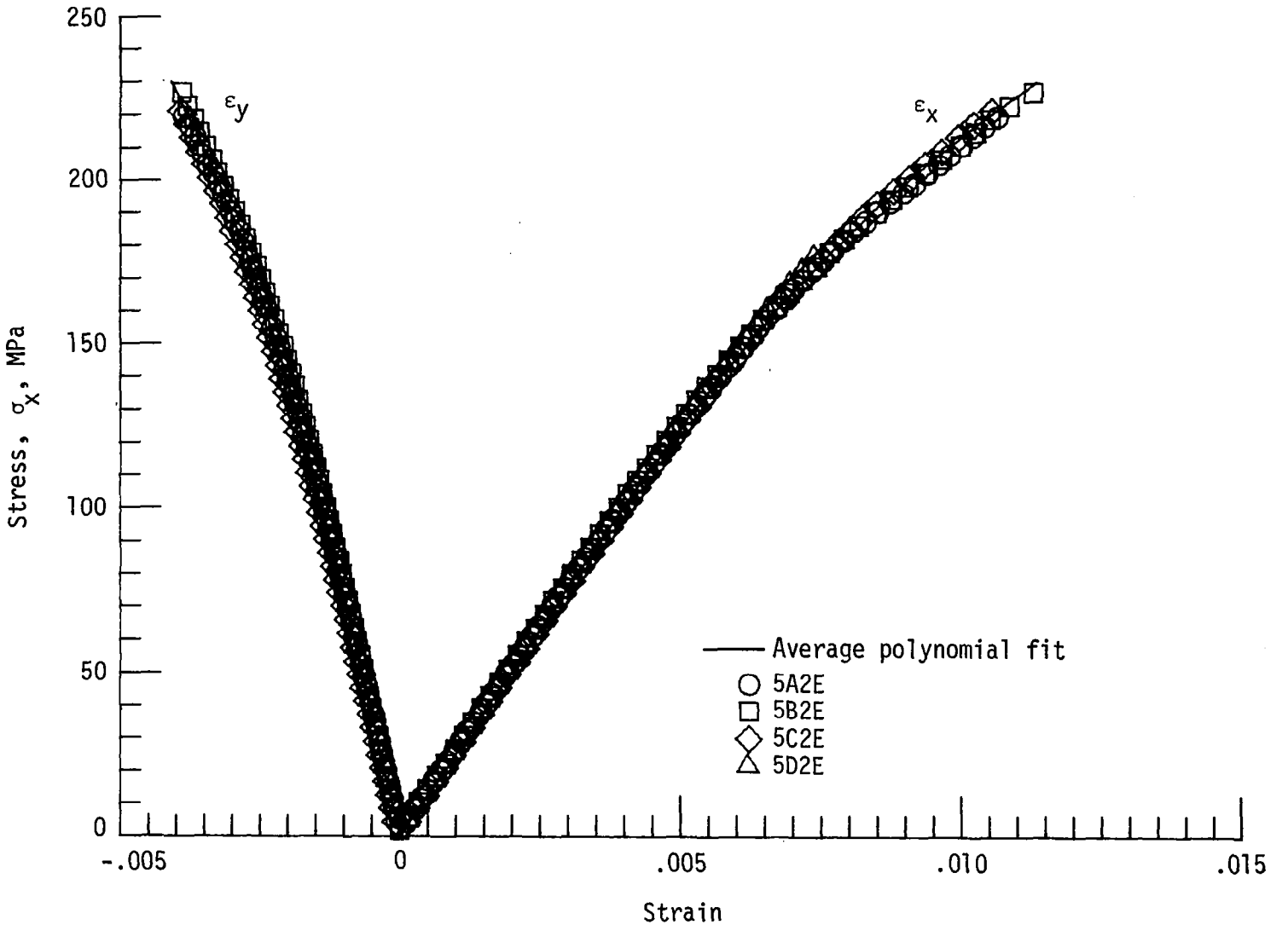

Figure 22. - Stress-strain curve for $[\pm 45/90/\pm 45/\overline{90}]_S$ and $[\pm 45/90/\mp 45/90/\pm 45/90/\pm 45]_T$ laminates.

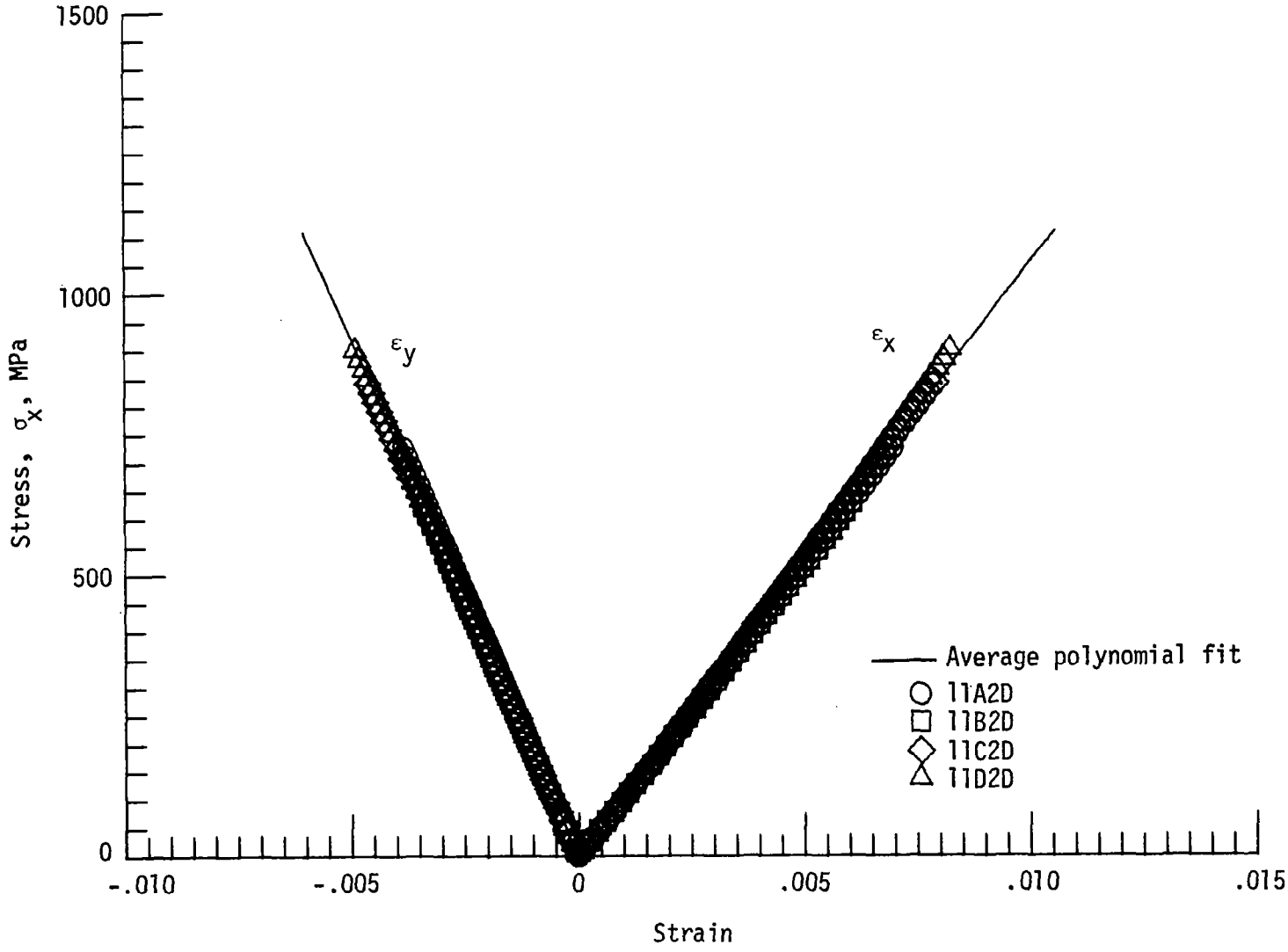

Figure 23. - Stress-strain curve for $[0_2/45/0_2/-45/0_2]_S$ laminate.

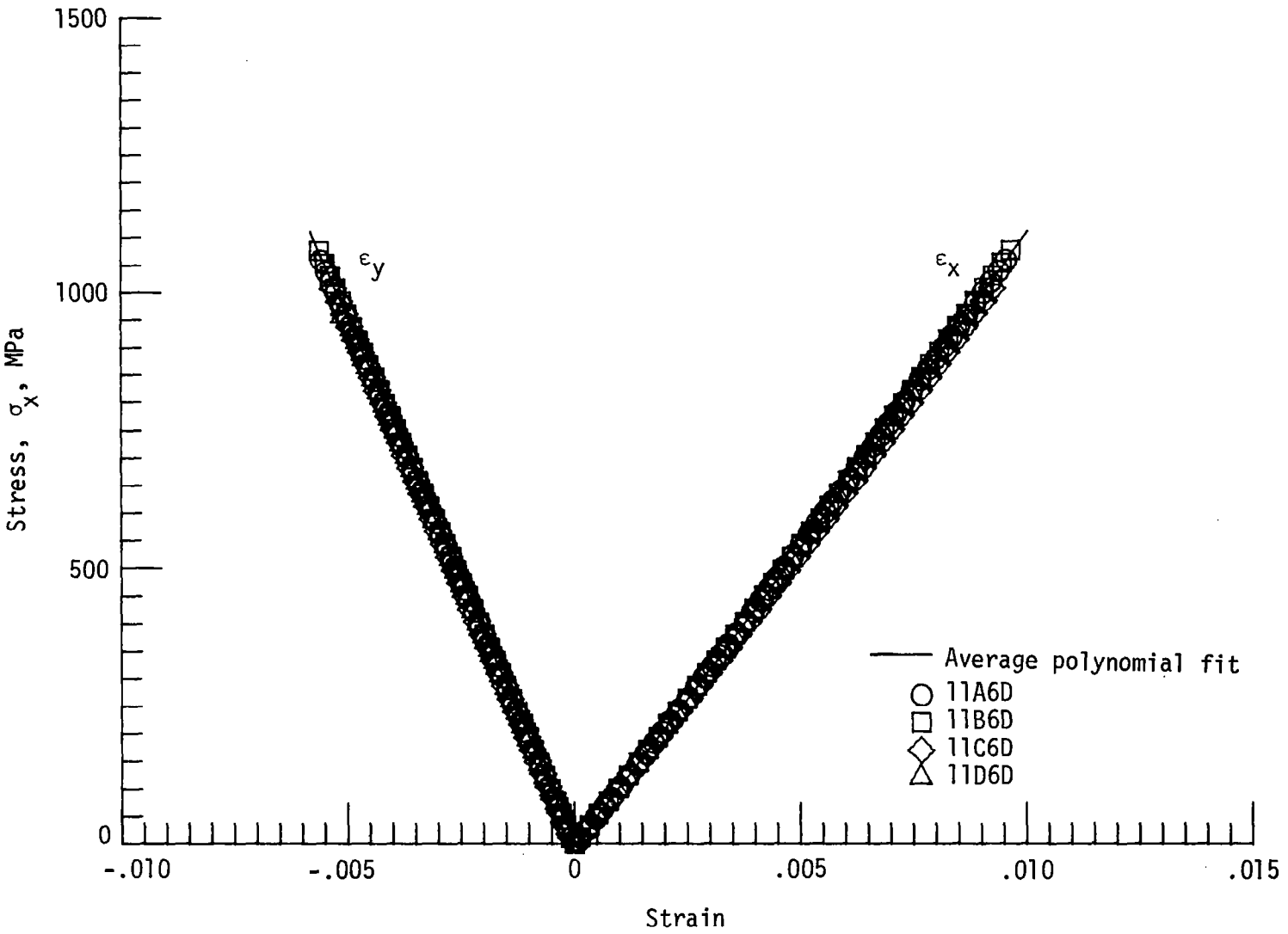

Figure 24. - Stress-strain curve for $[0_2/45/0_2/-45/0_2]_S$ laminate tested with end tabs.

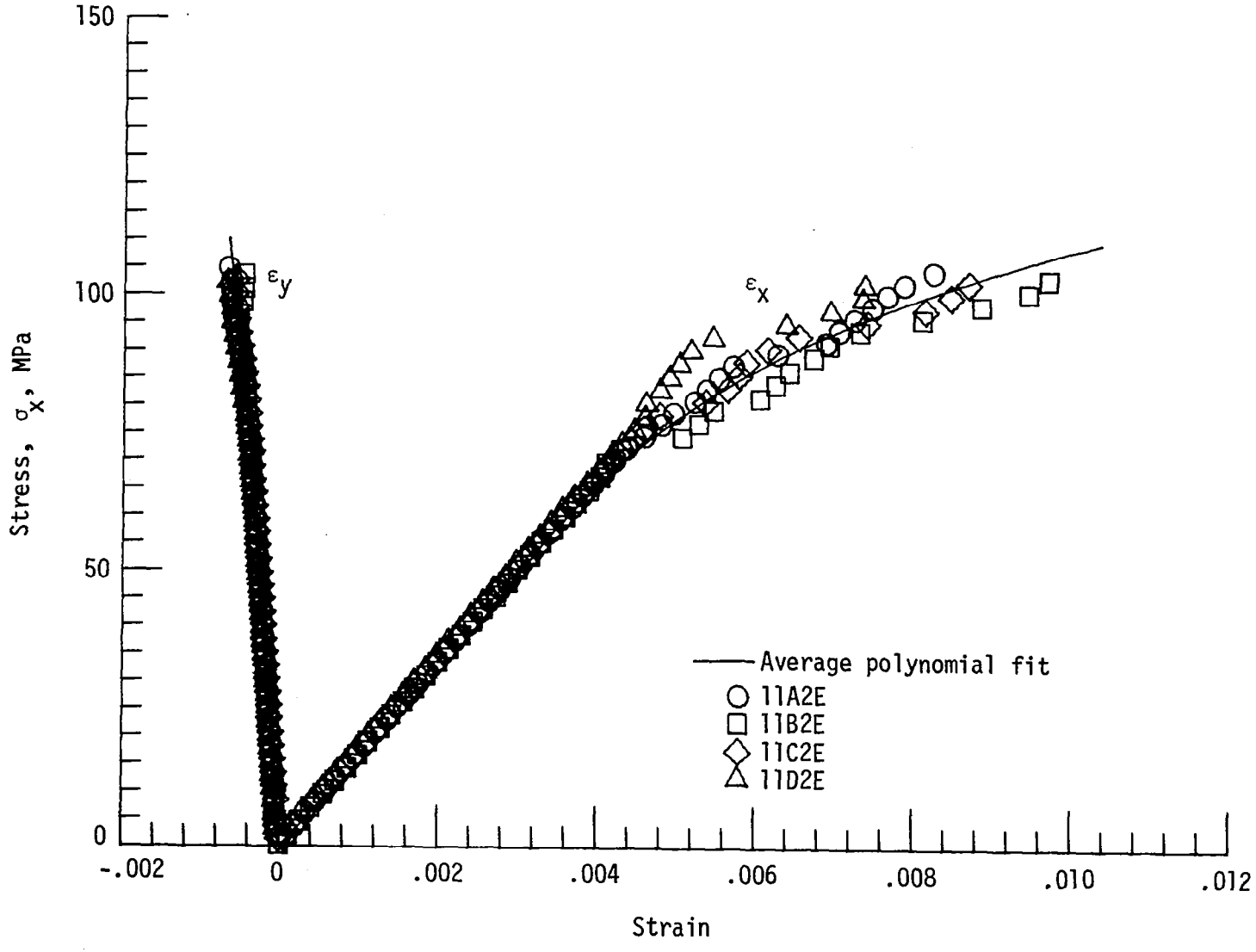

Figure 25. - Stress-strain curve for $[90_2/45/90_2/-45/90_2]_S$ laminate.

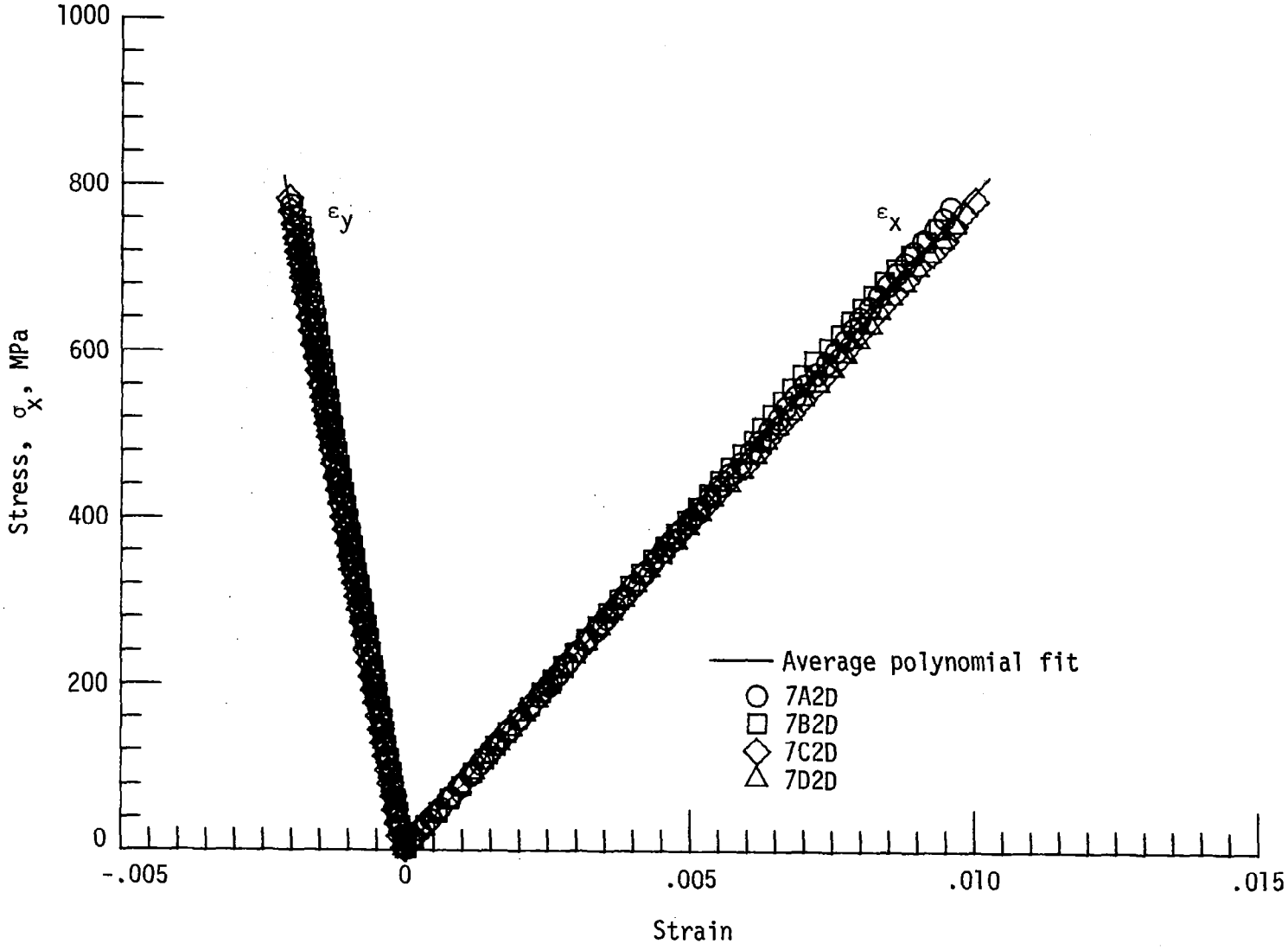

Figure 26. - Stress-strain curve for $[(90/0)_2/45/0/-45/0]_S$ laminate.

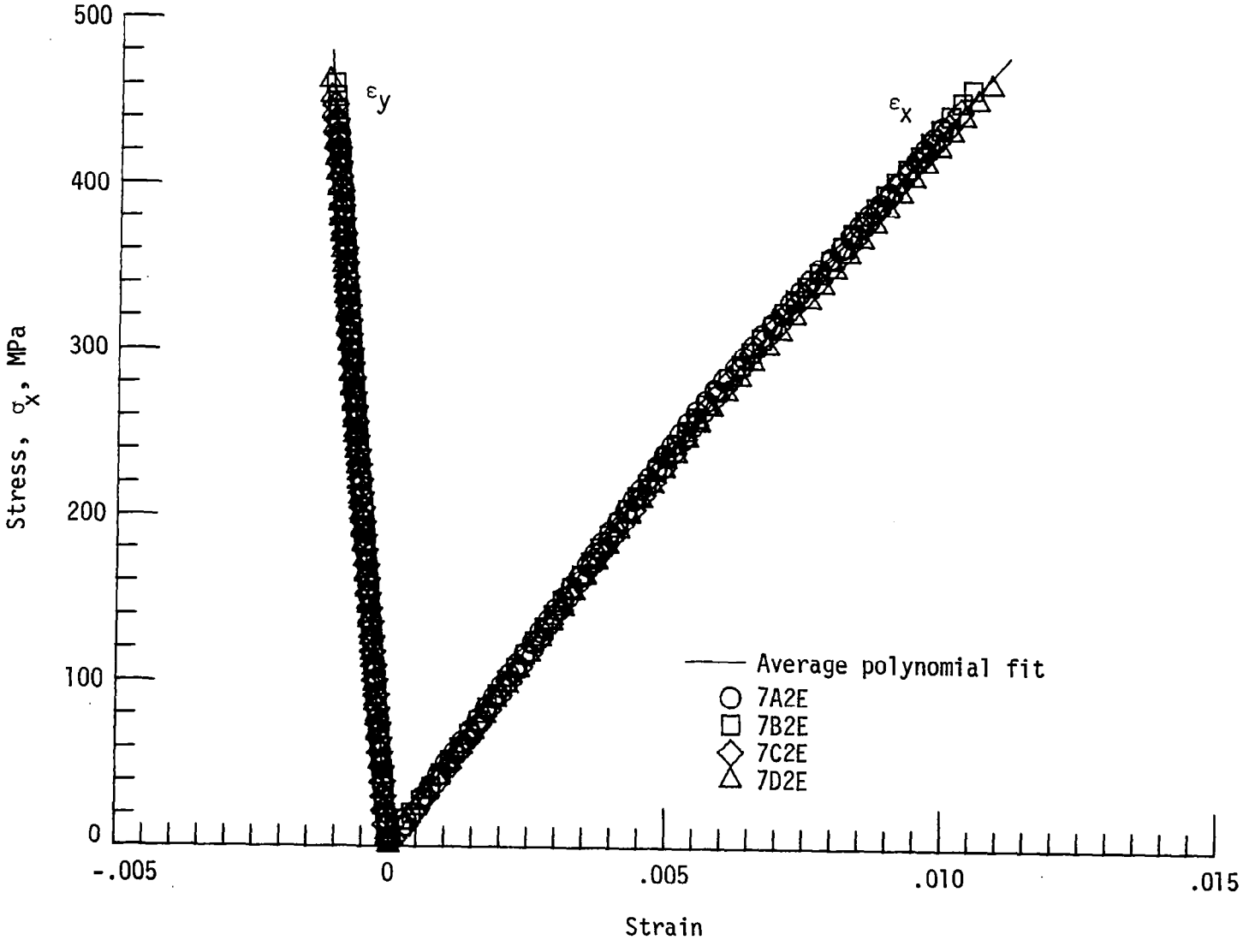

Figure 27. - Stress-strain curve for $[(0/90)_2/45/90/-45/90]_S$ laminate.

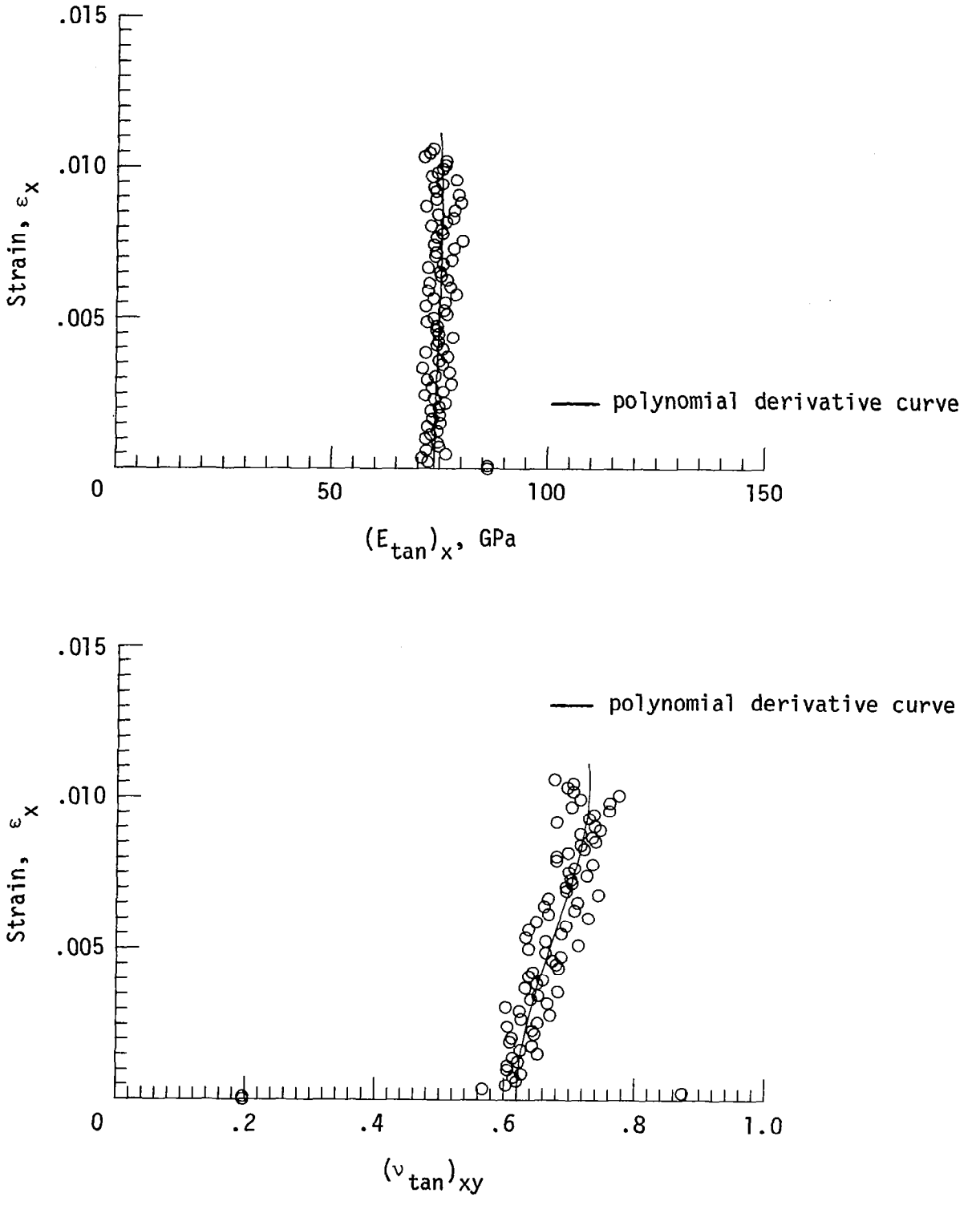

Figure 28. - Tangent modulus and Poisson's ratio for specimen 2A2E.

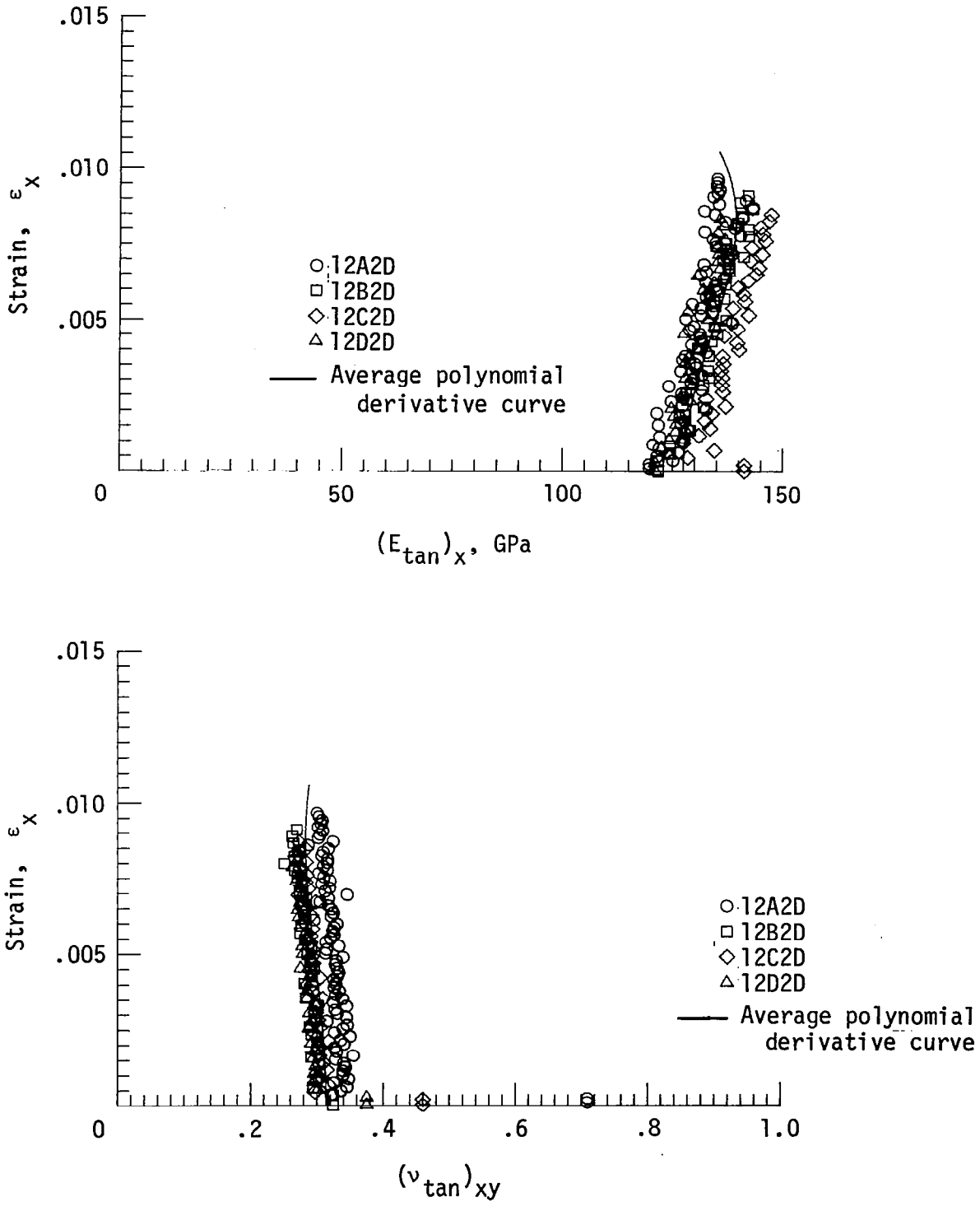

Figure 29. - Tangent modulus and Poisson's ratio for $[0]_8$ laminate.

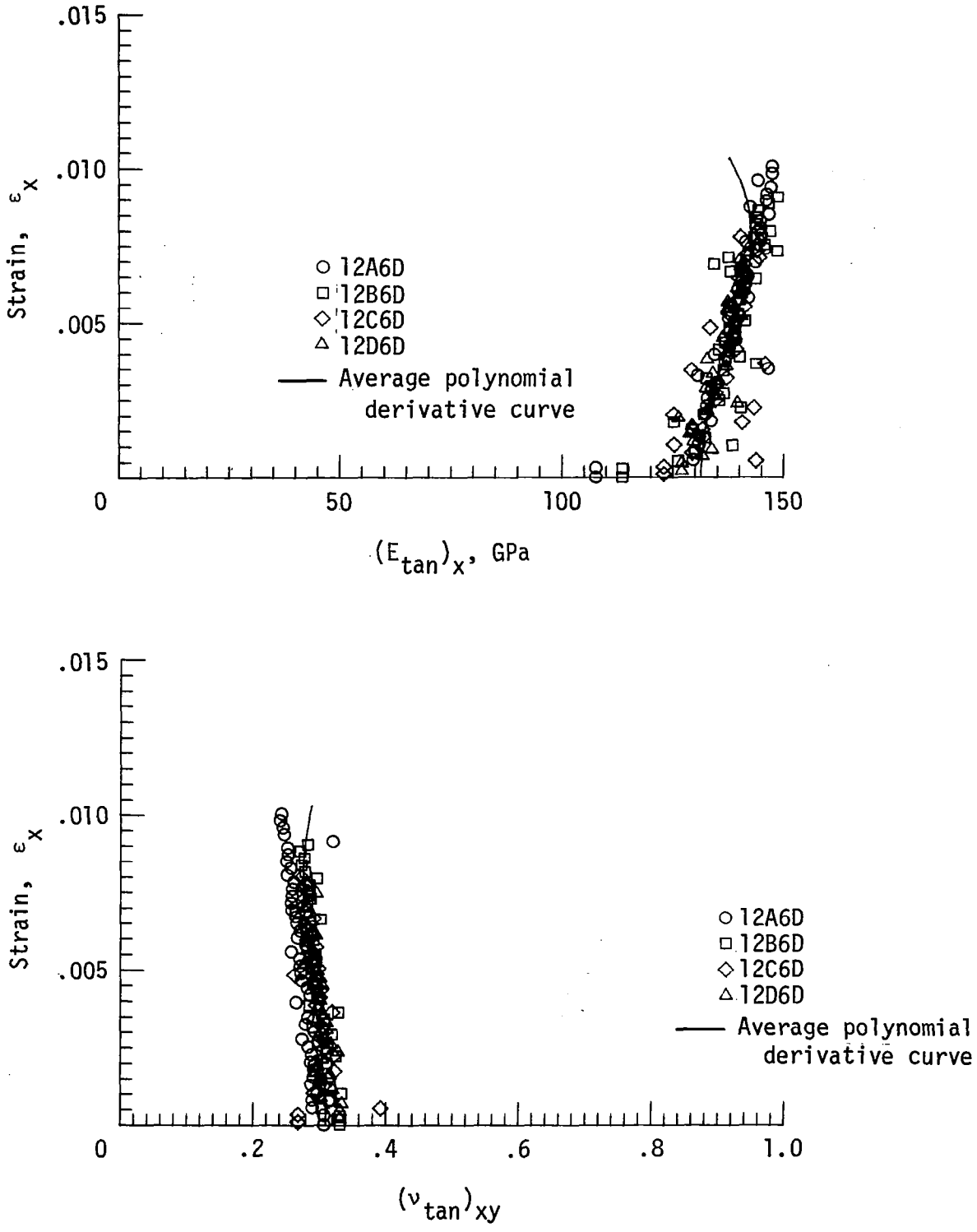

Figure 30. - Tangent modulus and Poisson's ratio for $[0]_8$ laminate tested with end tabs.

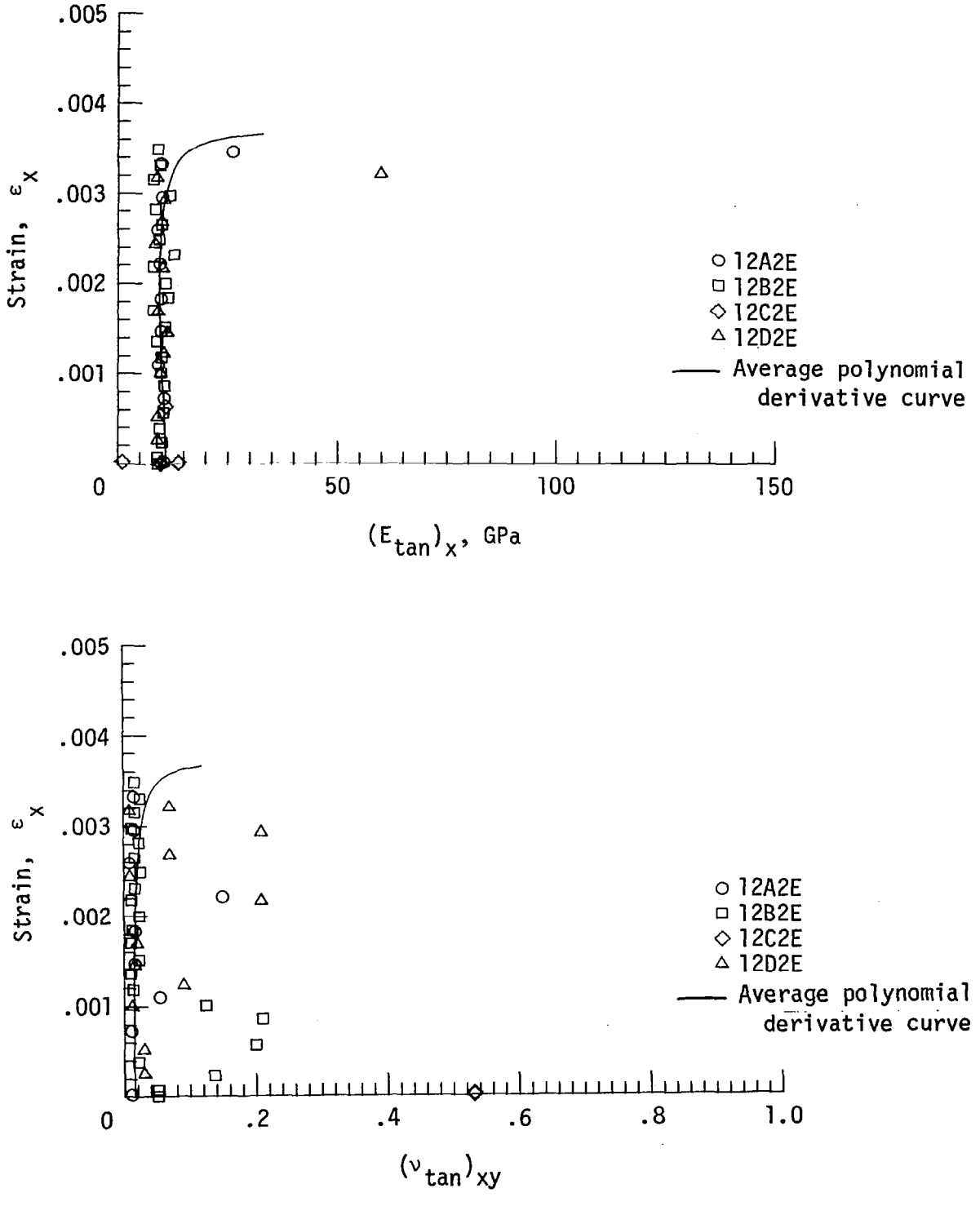

Figure 31. - Tangent modulus and Poisson's ratio for $[90]_8$ laminate.

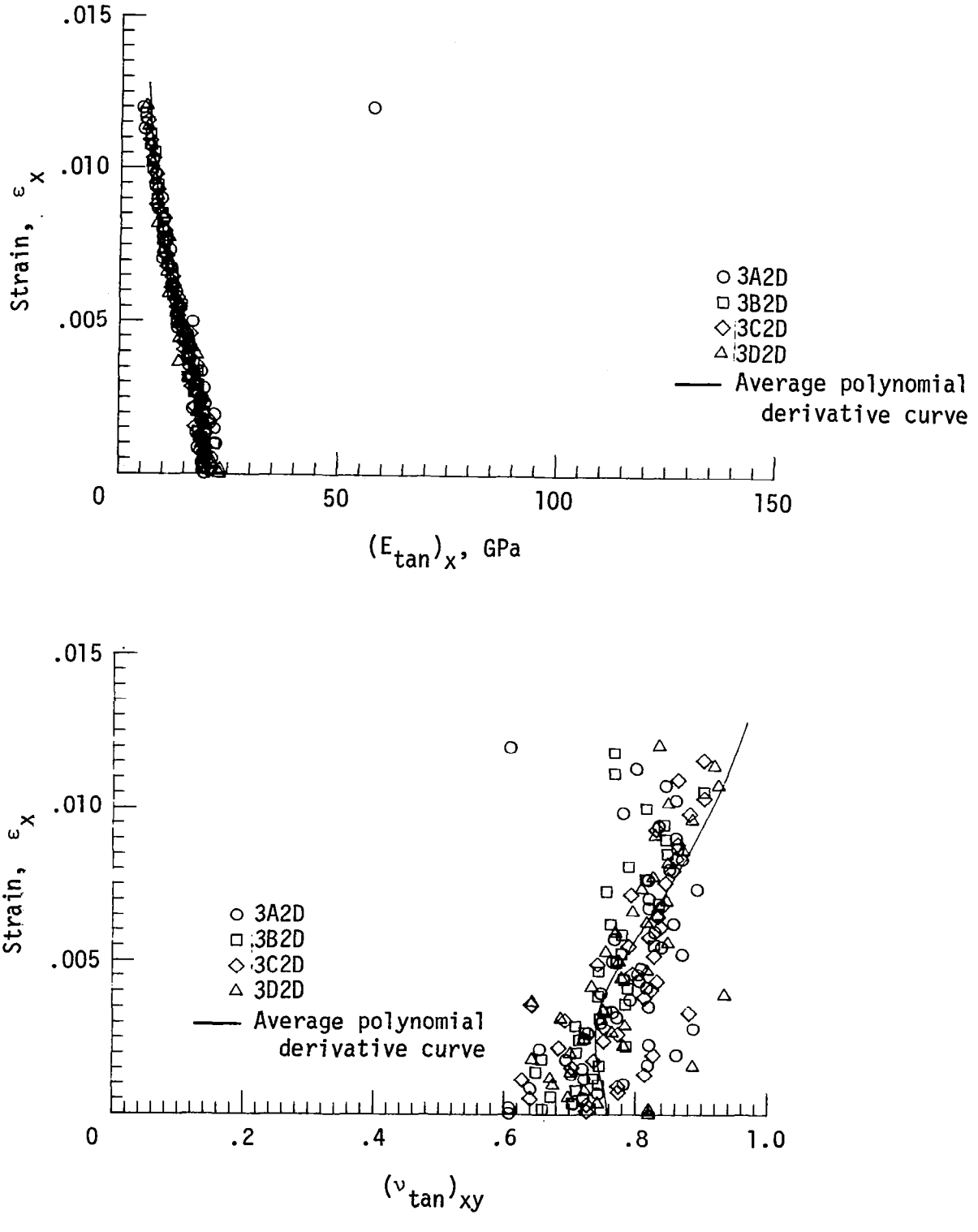

Figure 32. - Tangent modulus and Poisson's ratio for $[\pm 45]_{2S}$ laminate.

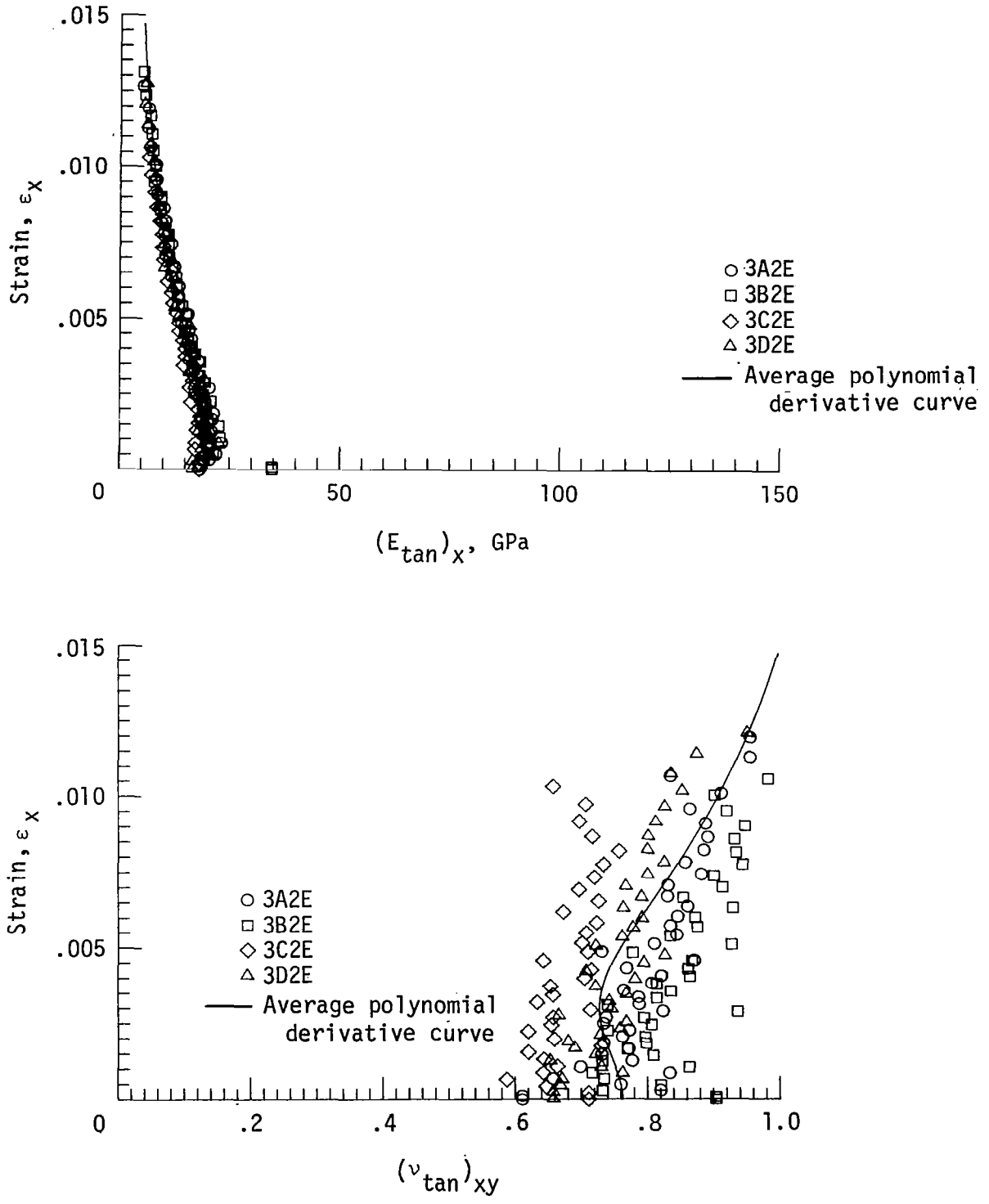

Figure 33. - Tangent modulus and Poisson's ratio for $[\pm 45]_{2S}$ laminate.

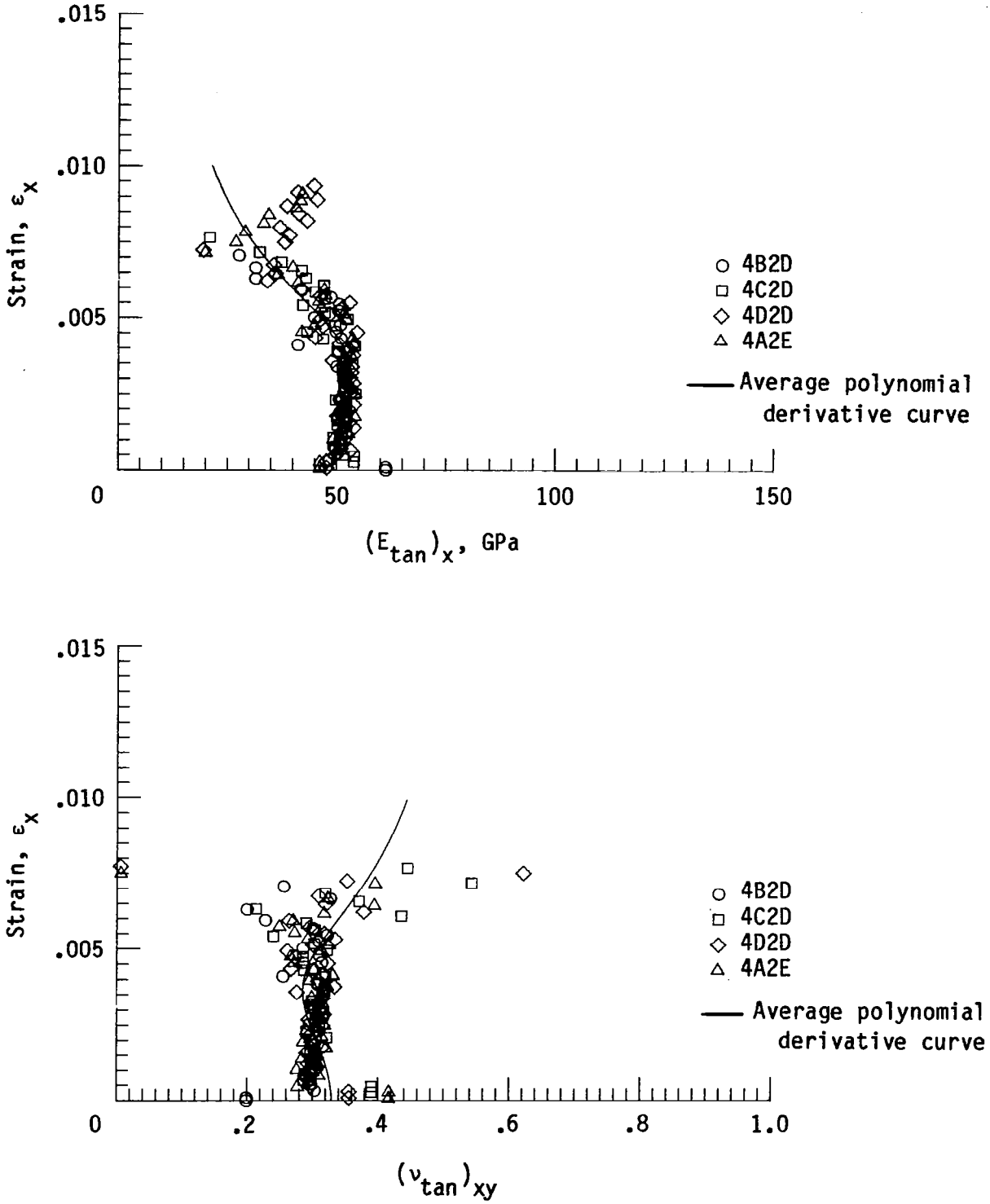

Figure 34. - Tangent modulus and Poisson's ratio for $[45/0/-45/90]_S$ laminate.

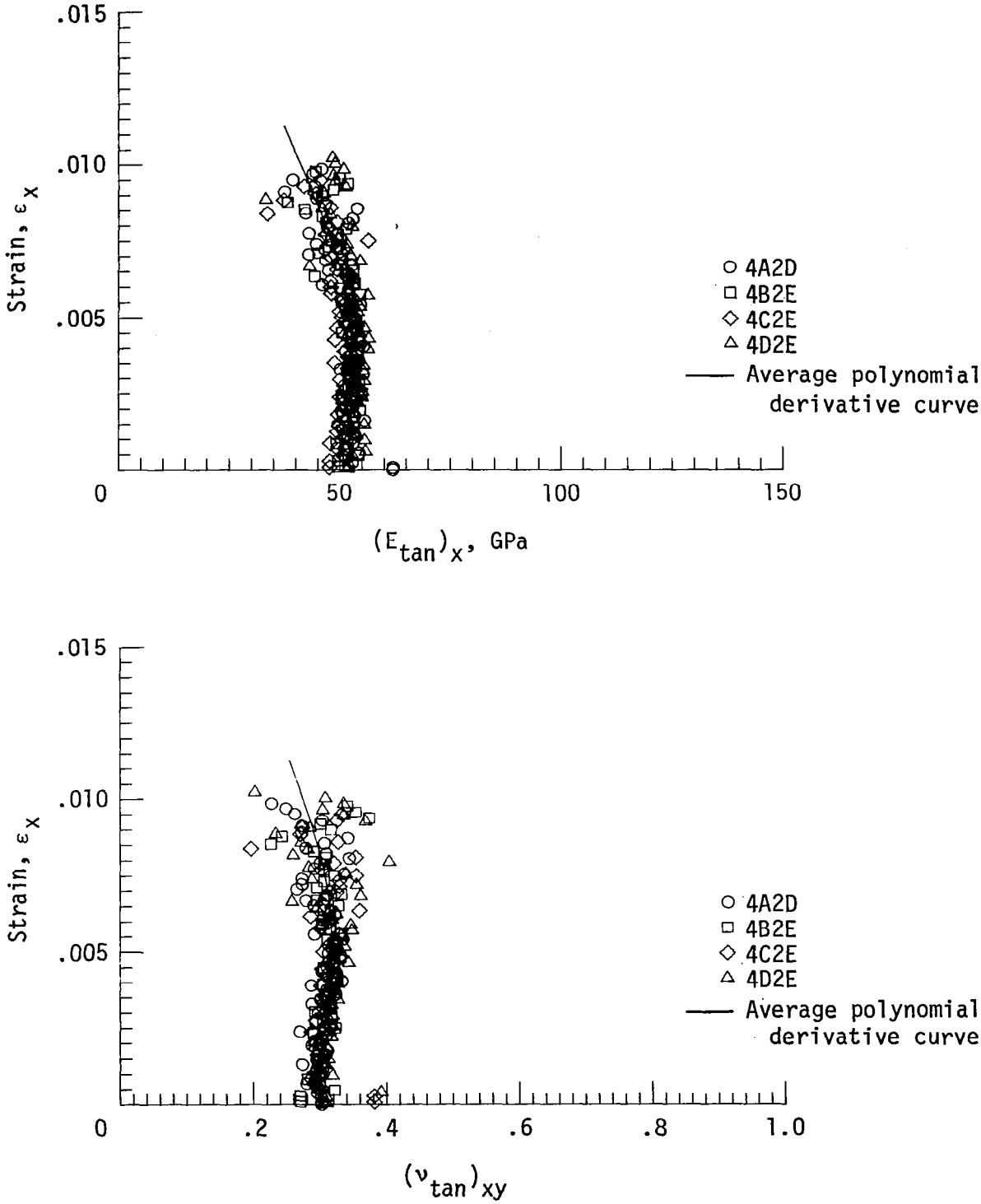

Figure 35. - Tangent modulus and Poisson's ratio for $[45/90/-45/0]_S$ laminate.

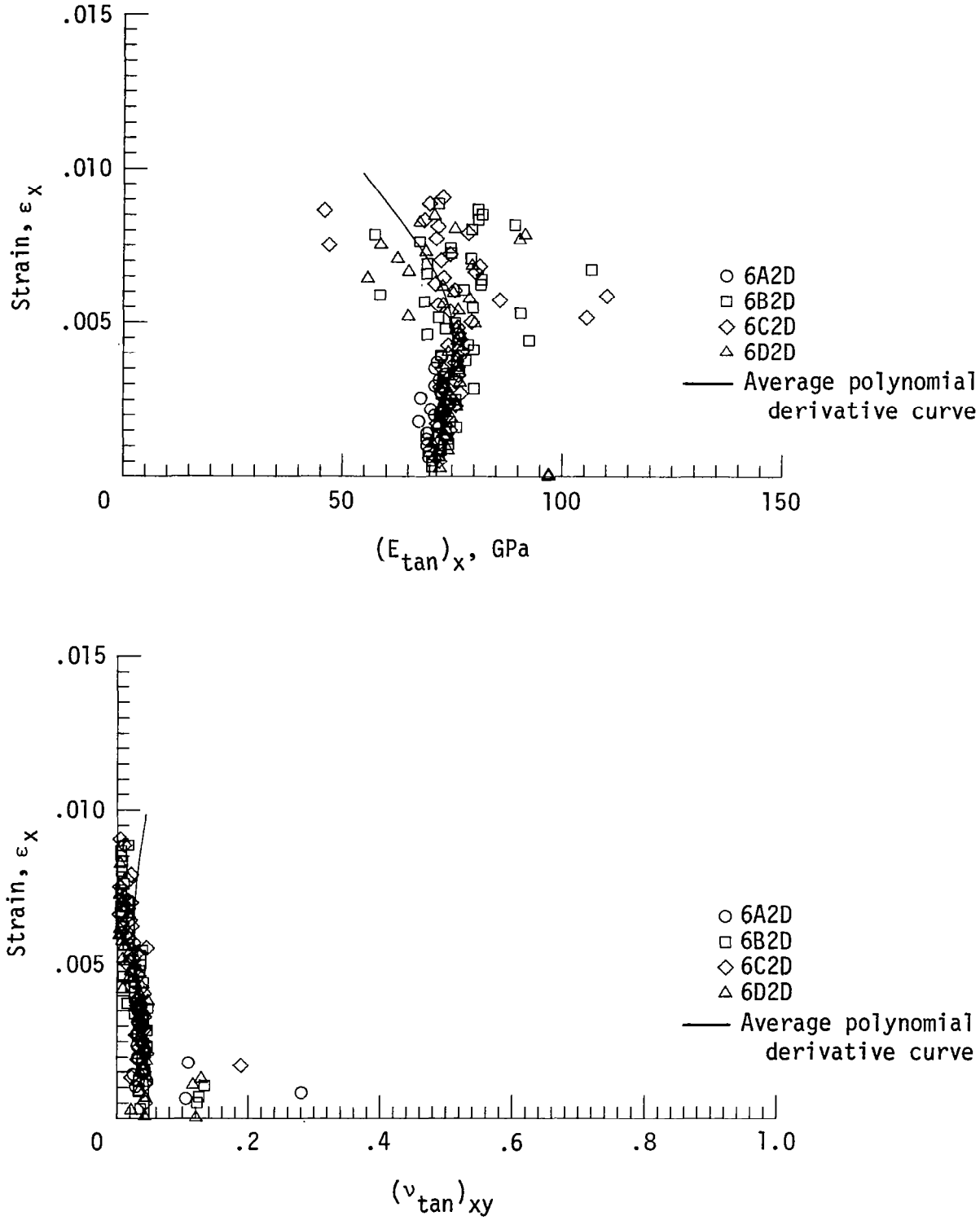

Figure 36. - Tangent modulus and Poisson's ratio for $[90/0]_{2S}$ laminate.

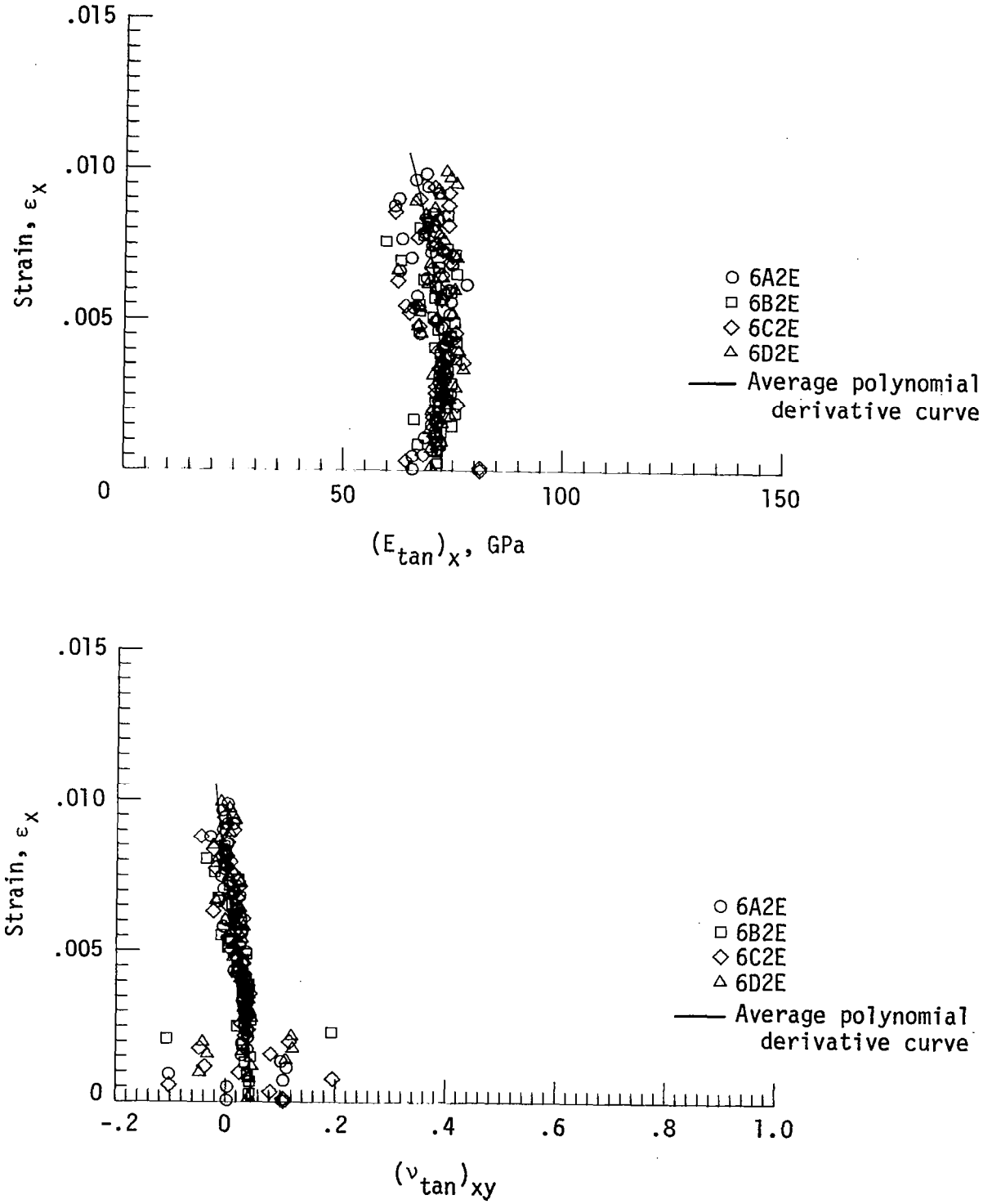

Figure 37. - Tangent modulus and Poisson's ratio for $[0/90]_{2S}$ laminate.

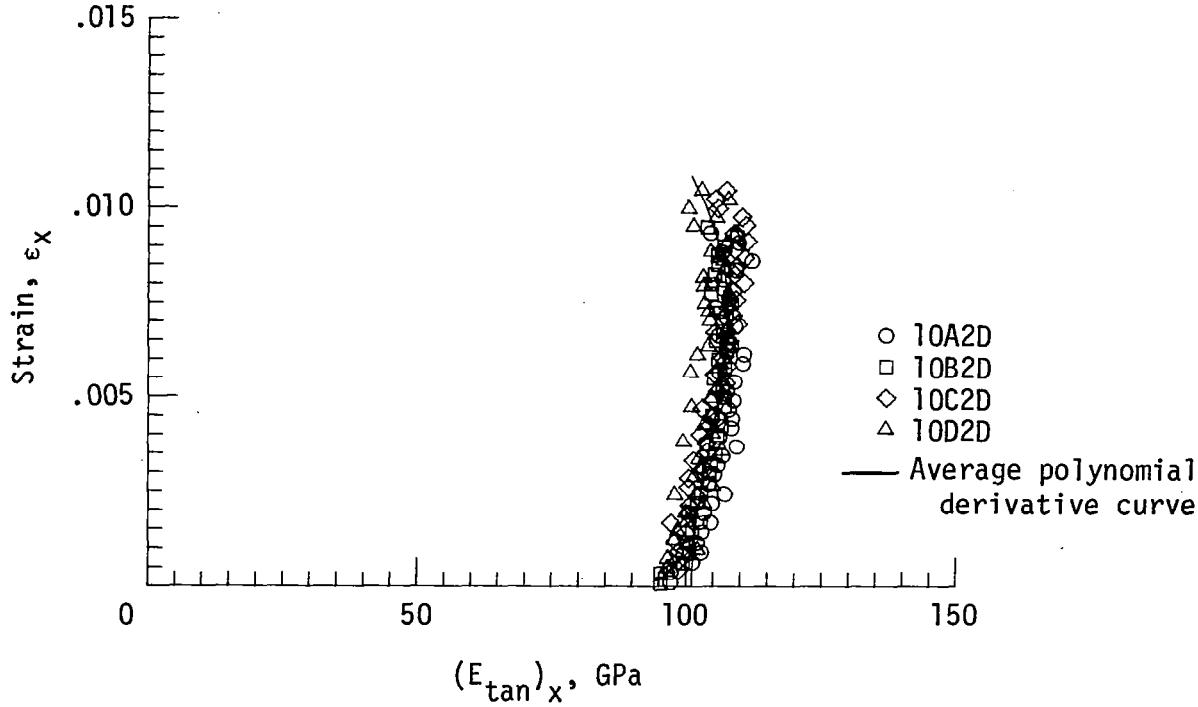

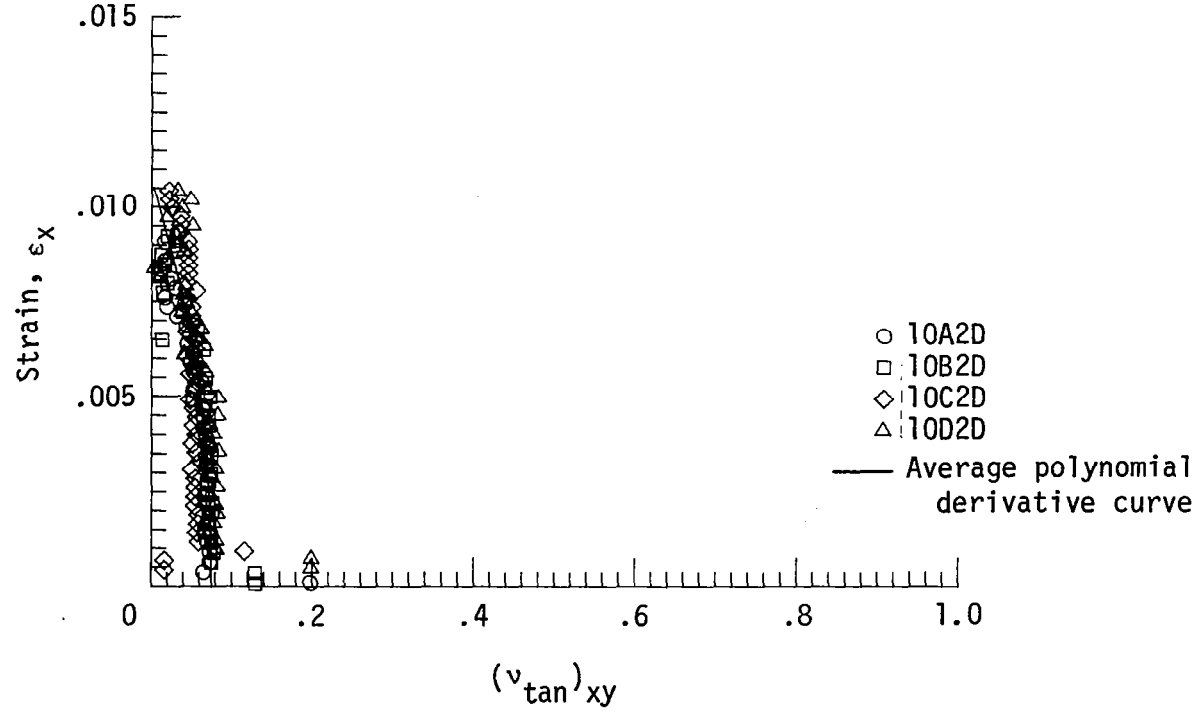

Figure 38. - Tangent modulus and Poisson's ratio for $[0_2/90/0]_S$ laminate.

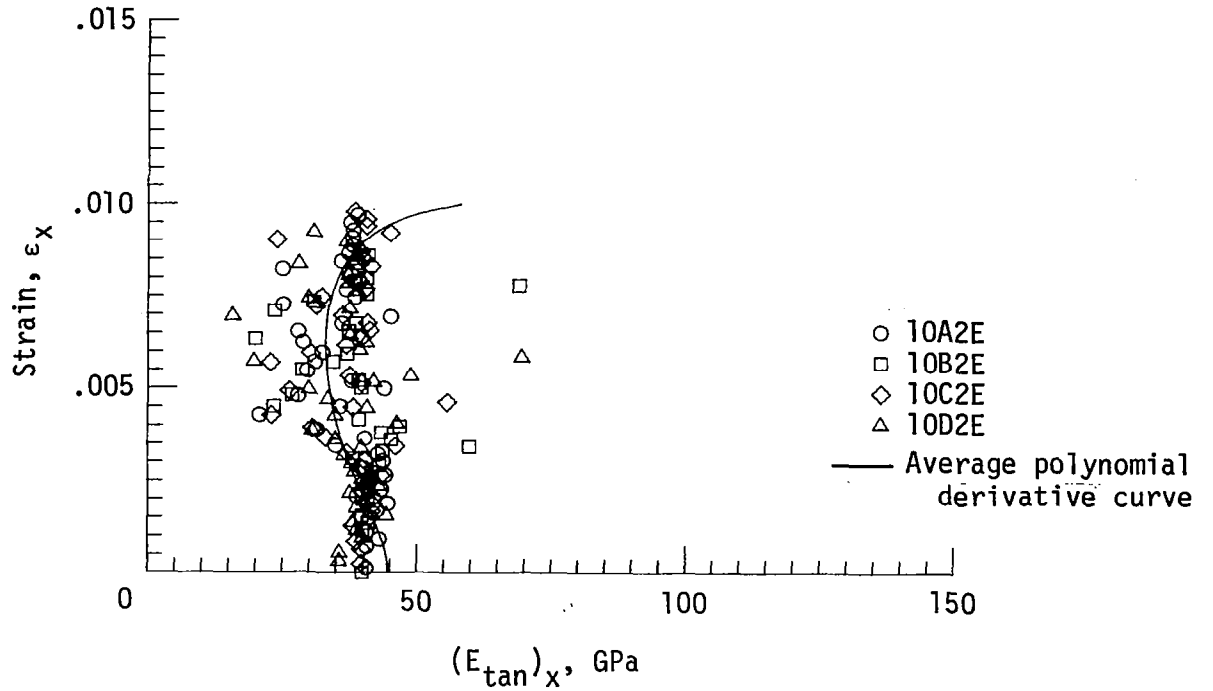

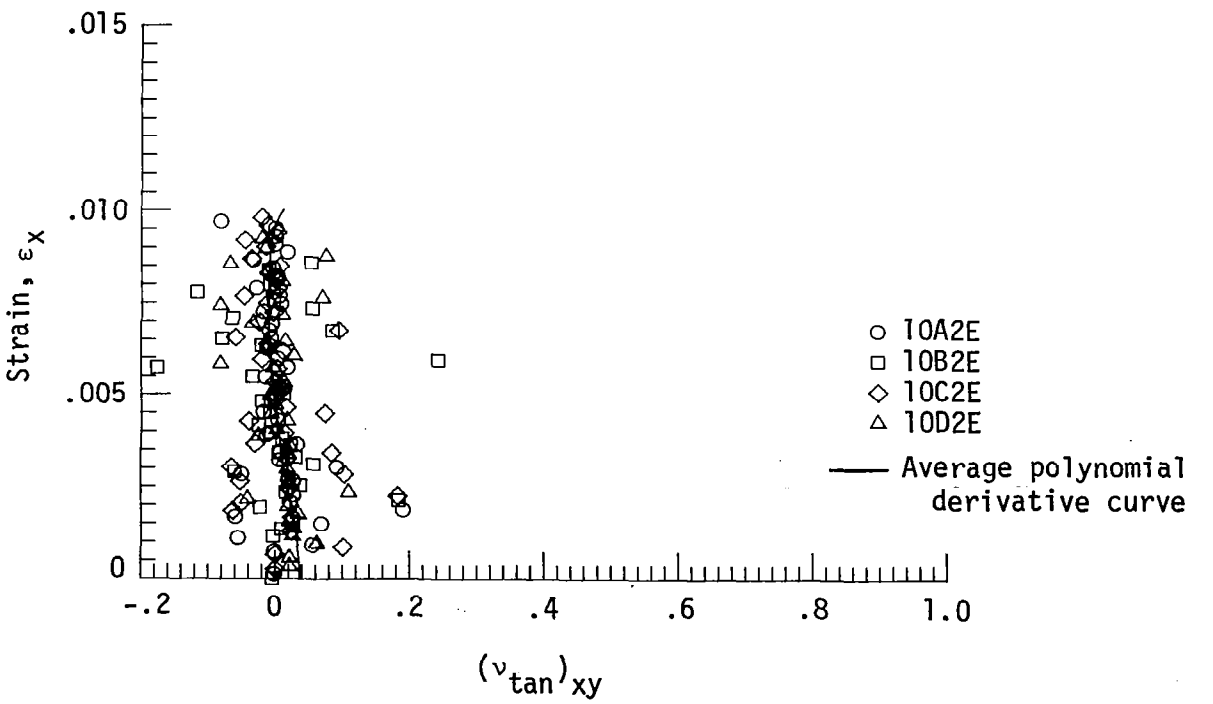

Figure 39. - Tangent modulus and Poisson's ratio for $[90_2/0/90]_S$ laminate.

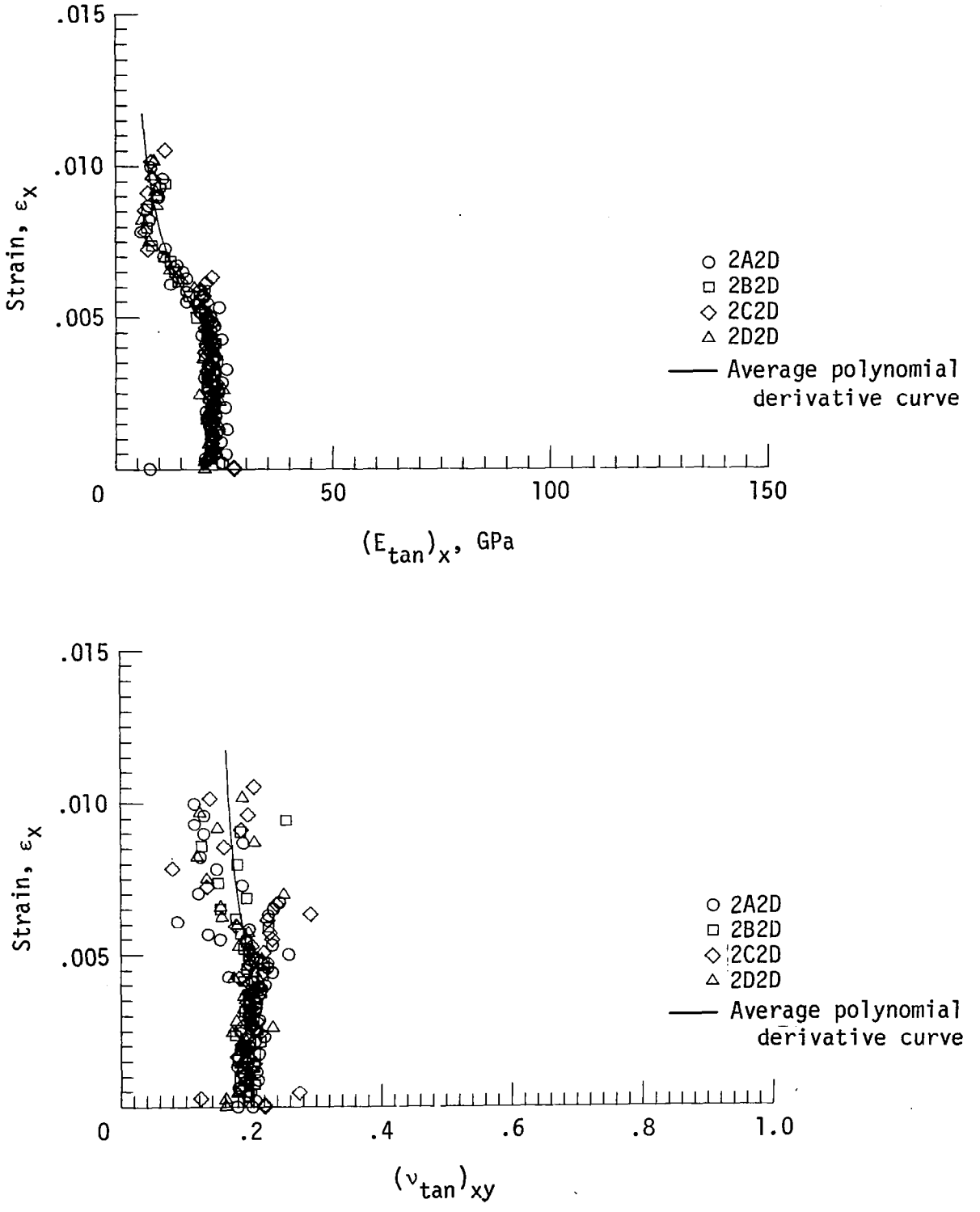

Figure 40. - Tangent modulus and Poisson's ratio for $[90/45/90/-45]_S$ laminate.

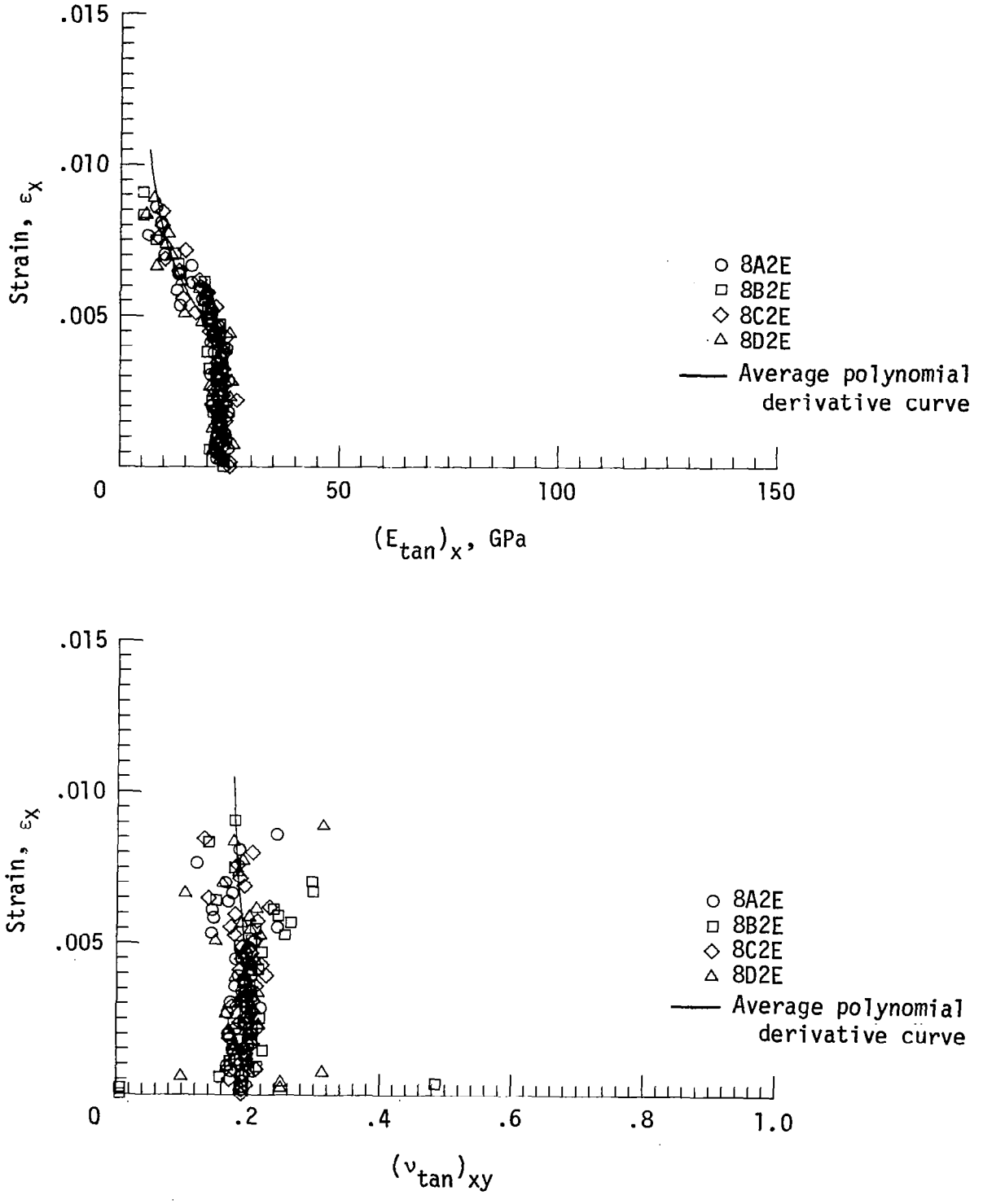

Figure 41. - Tangent modulus and Poisson's ratio for $[45/90/-45/90]_S$ laminate.

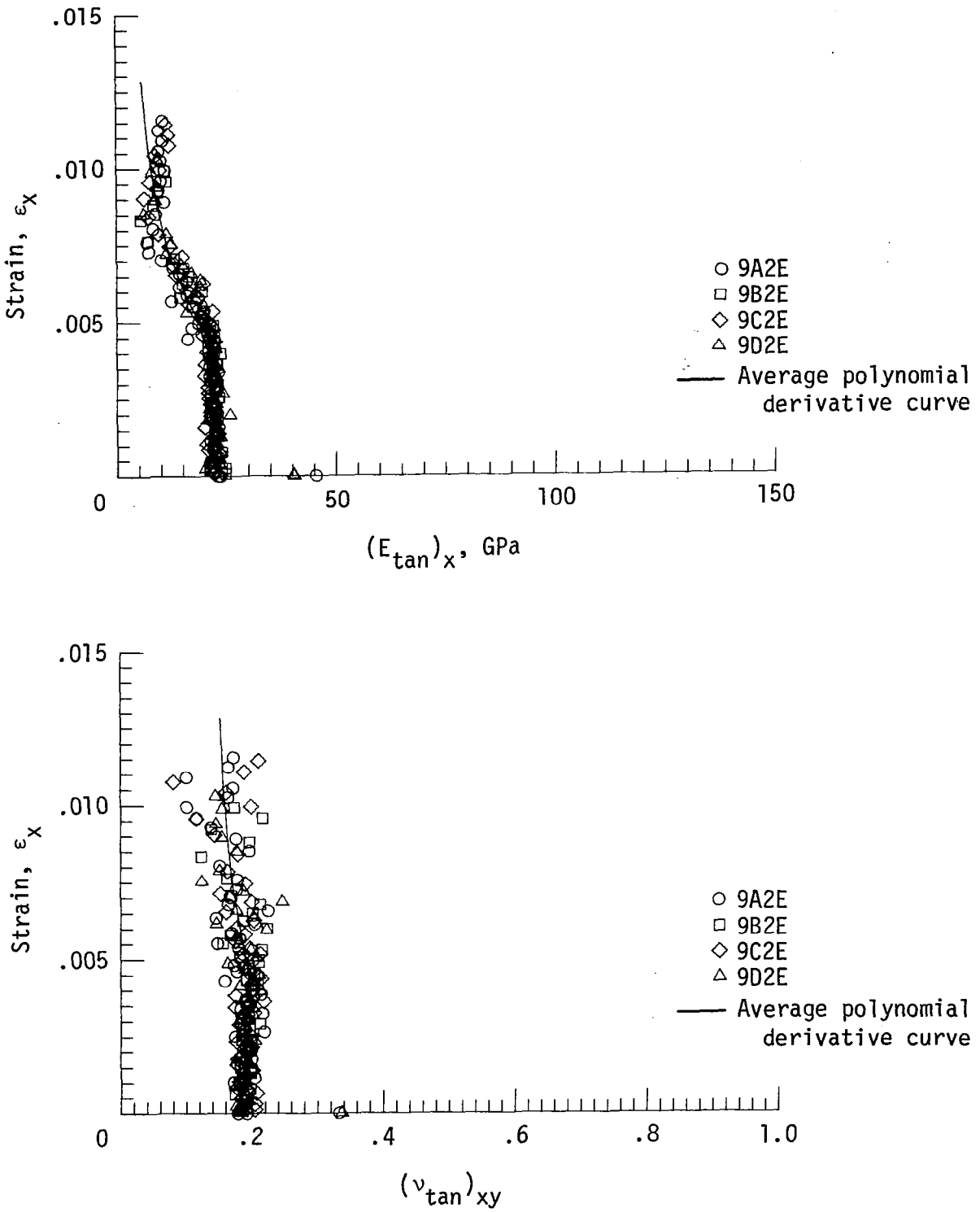

Figure 42. - Tangent modulus and Poisson's ratio for $[45/90/-45/90]_{2S}$ laminate.

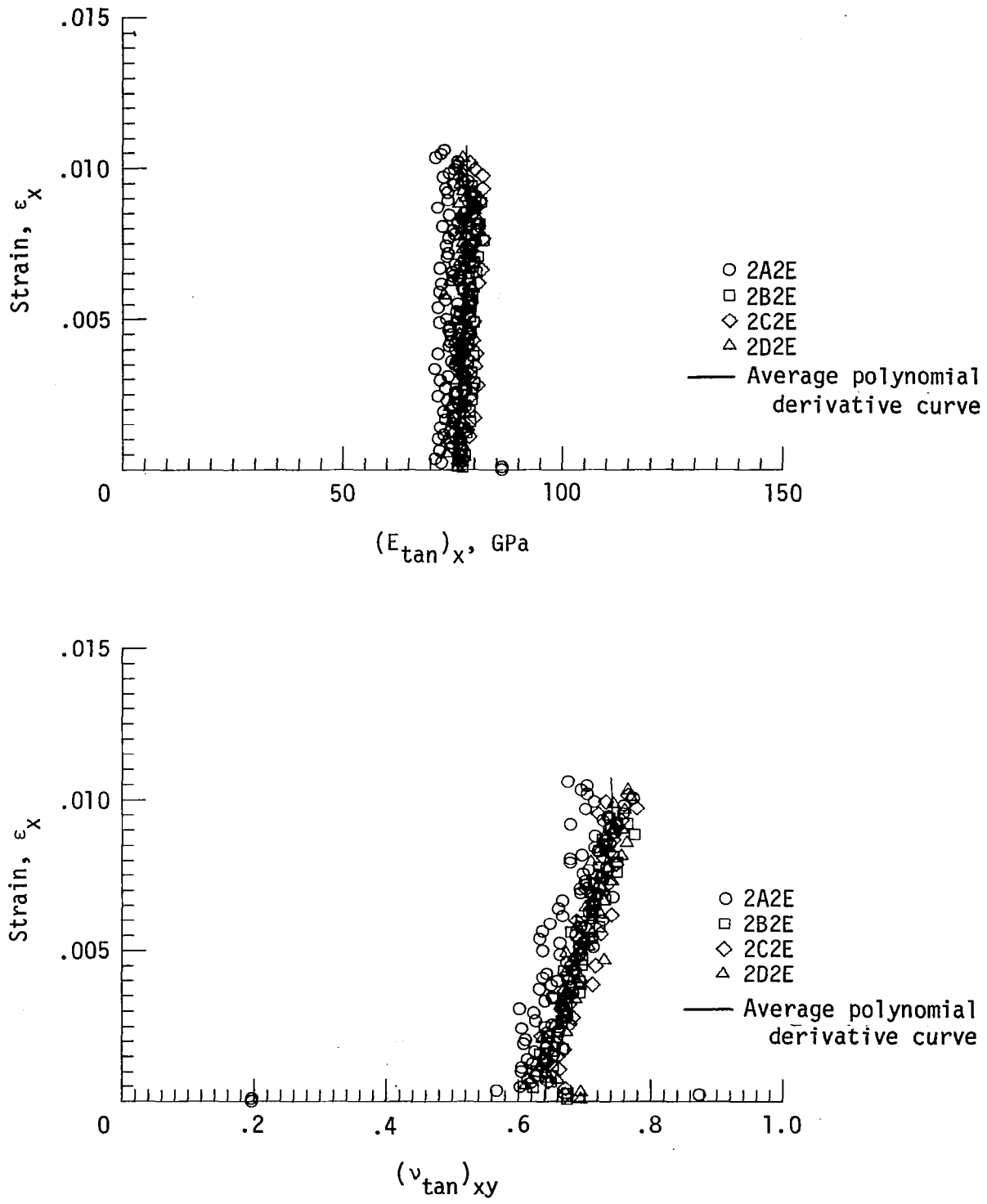

Figure 43. - Tangent modulus and Poisson's ratio for $[0/45/0/-45]_S$ laminate.

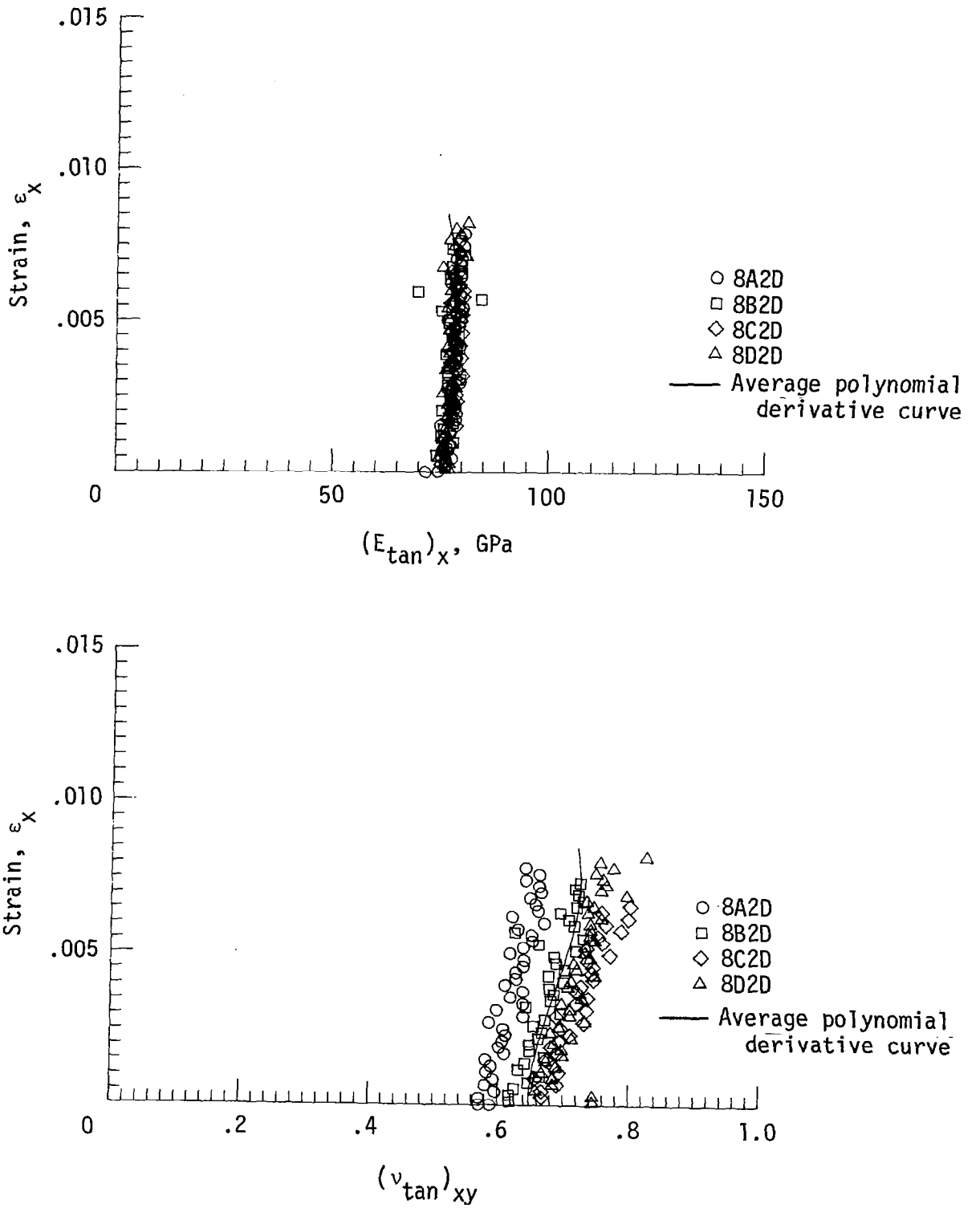

Figure 44. - Tangent modulus and Poisson's ratio for $[45/0/-45/0]_S$ laminate.

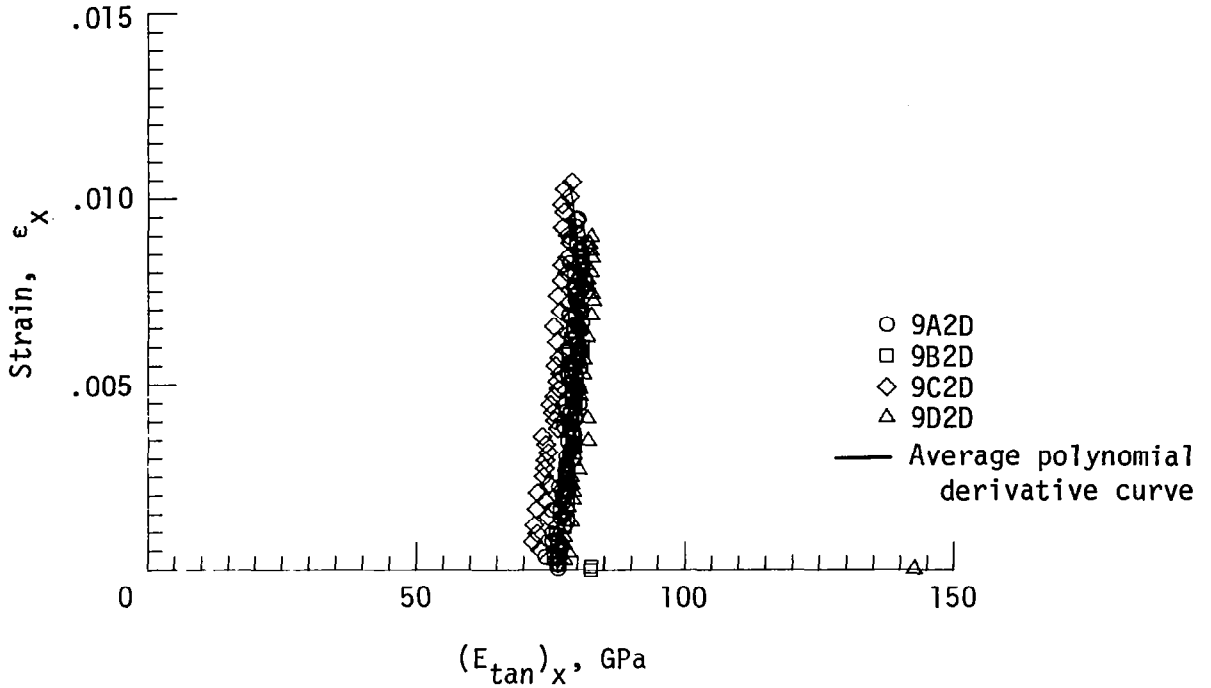

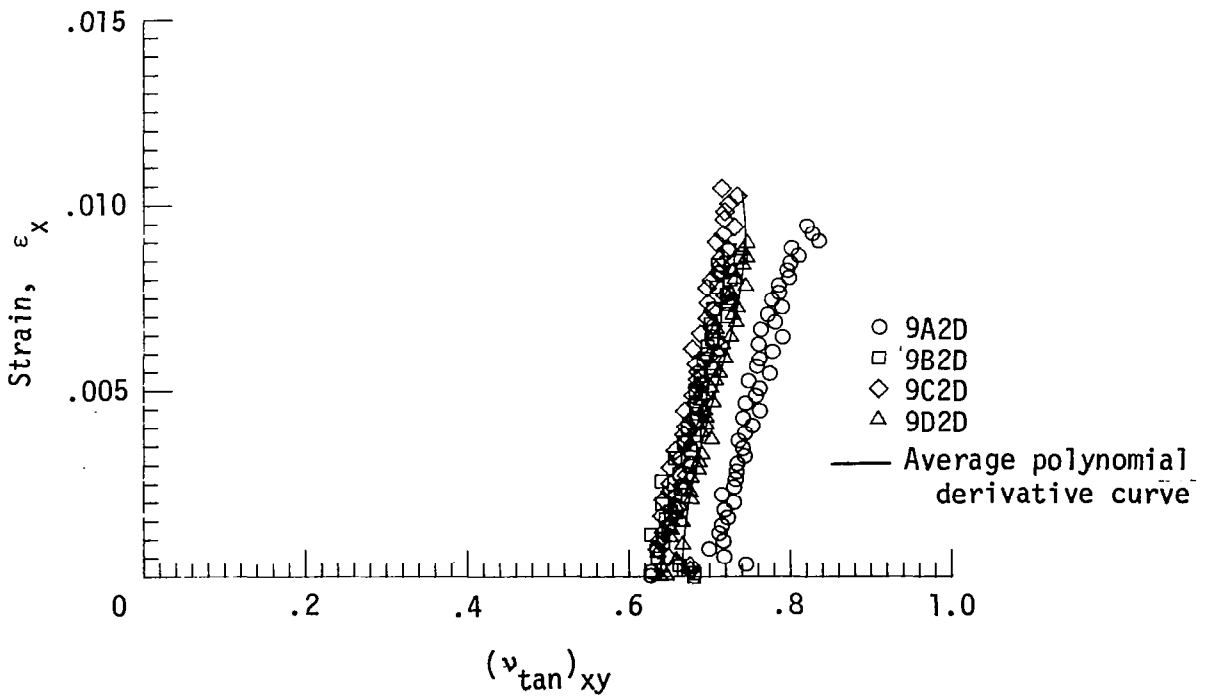

Figure 45. - Tangent modulus and Poisson's ratio for $[45/0/-45/0]_{2S}$ laminate.

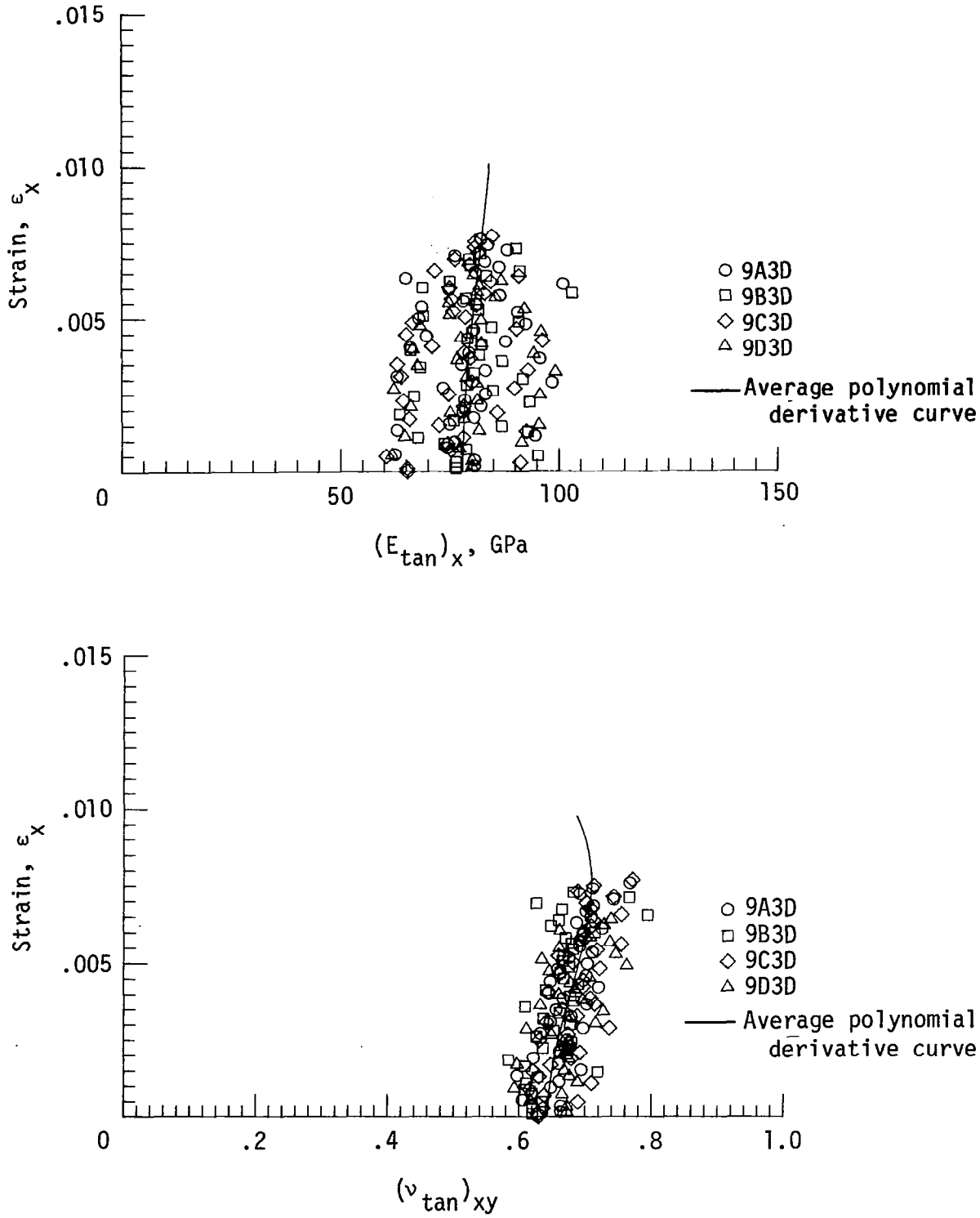

Figure 46. - Tangent modulus and Poisson's ratio for $[45/0/-45/0]_{2S}$ laminate tested with end tabs.

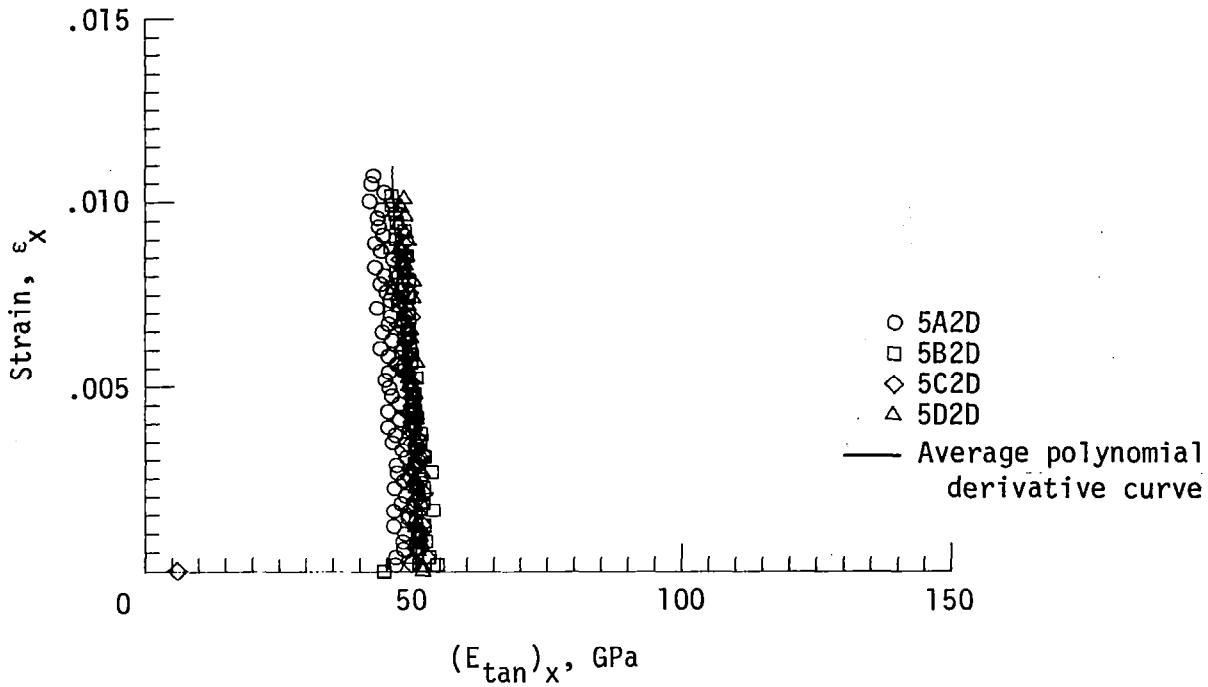

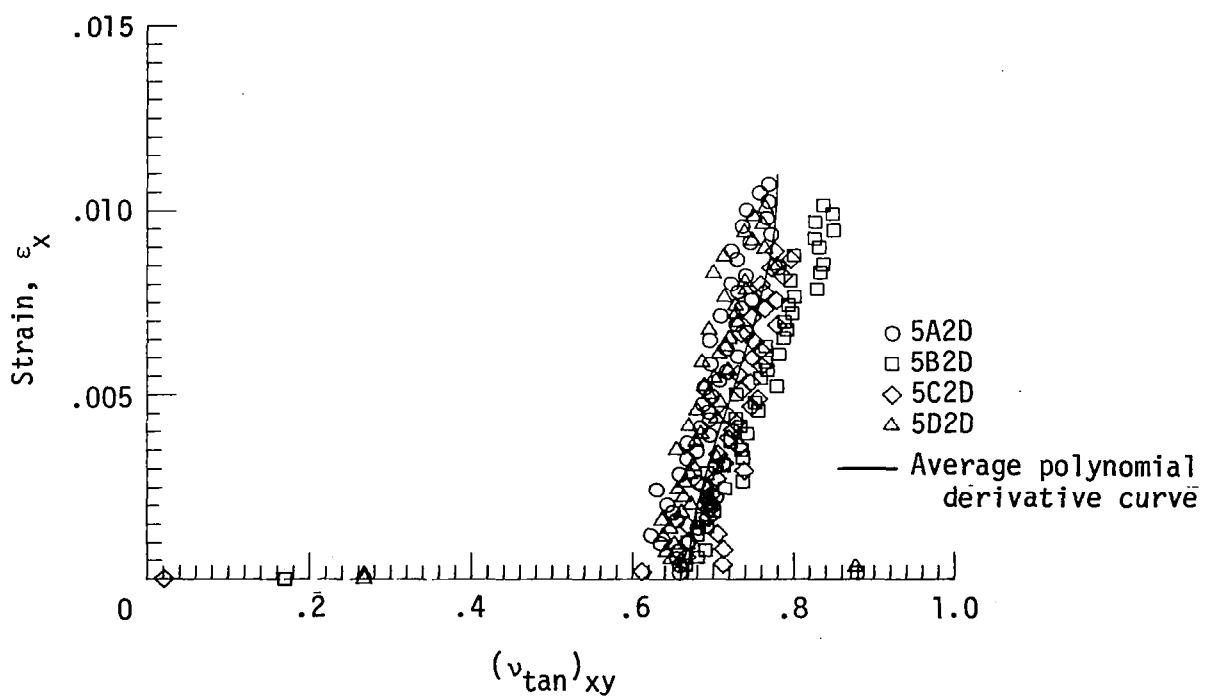

Figure 47. - Tangent modulus and Poisson's ratio for $[\pm 45/0/\pm 45/\overline{0}]_S$ and $[\pm 45/0/\overline{\mp 45}/0/\pm 45/0/\pm 45]_T$ laminates.

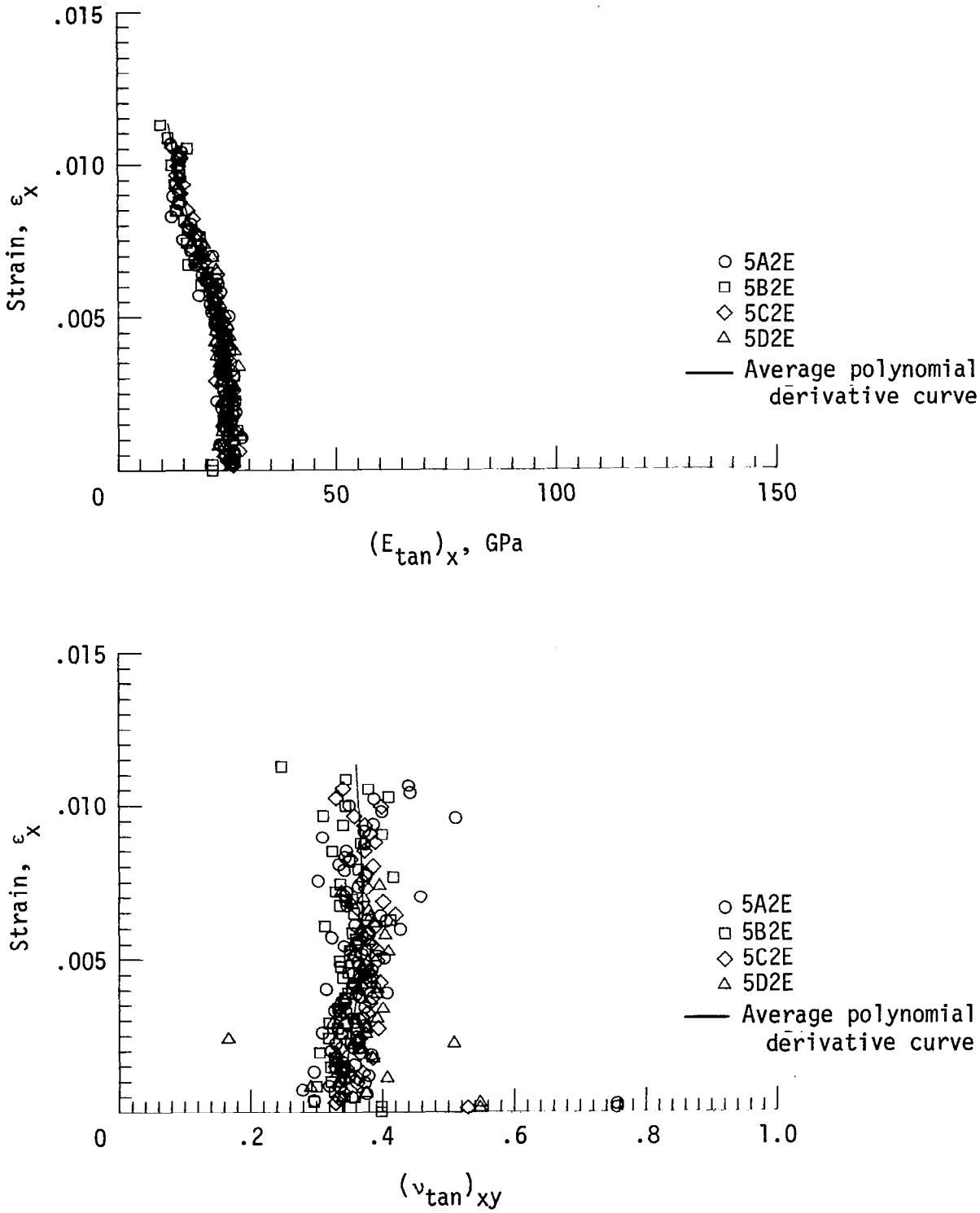

Figure 48. - Tangent modulus and Poisson's ratio for $[\pm 45/90/\pm 45/\overline{90}]_S$ and $[\pm 45/90/\mp 45/90/\pm 45/90/\pm 45]_T$ laminates.

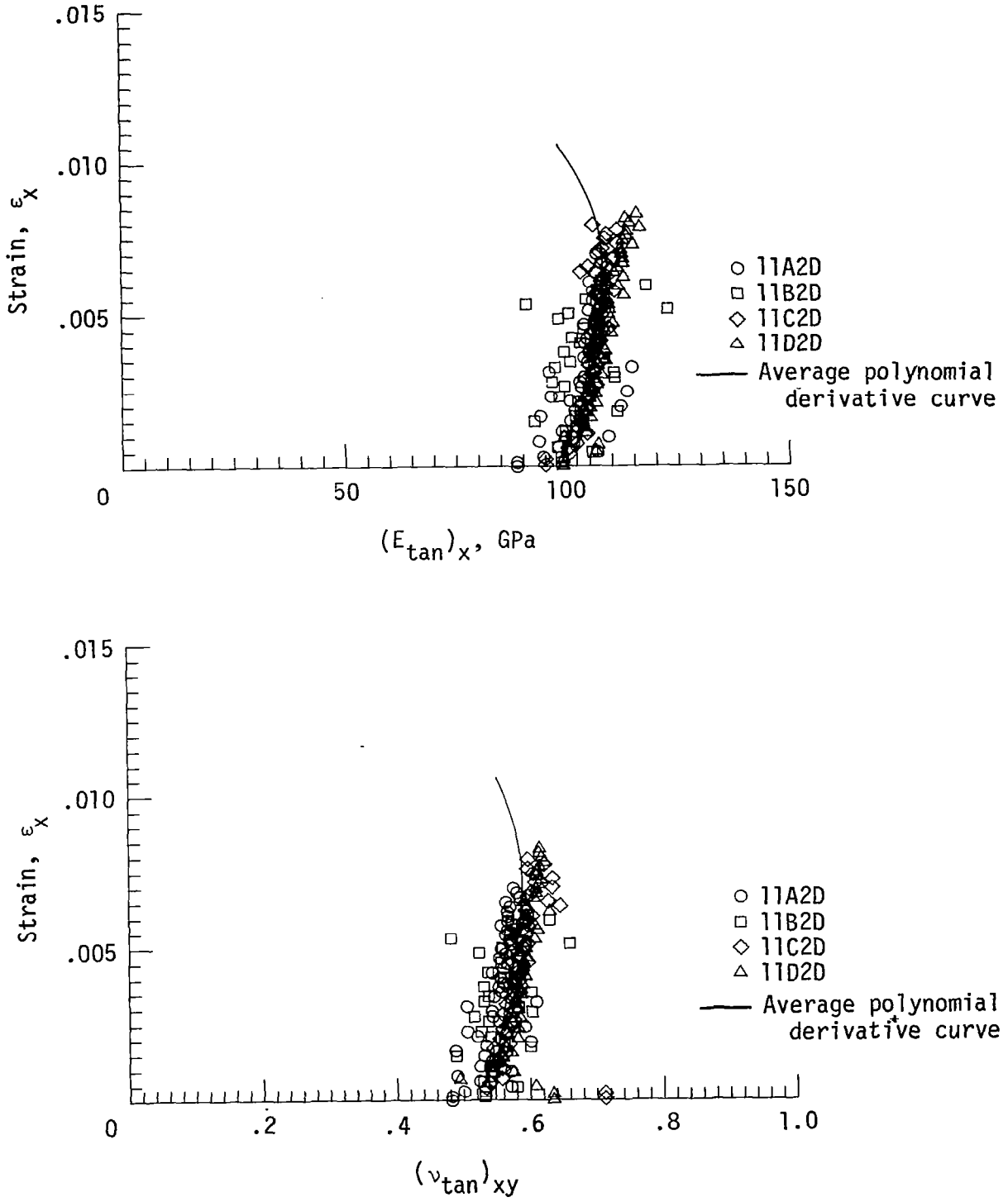

Figure 49. - Tangent modulus and Poisson's ratio for $[0_2/45/0_2/-45/0_2]_S$ laminate.

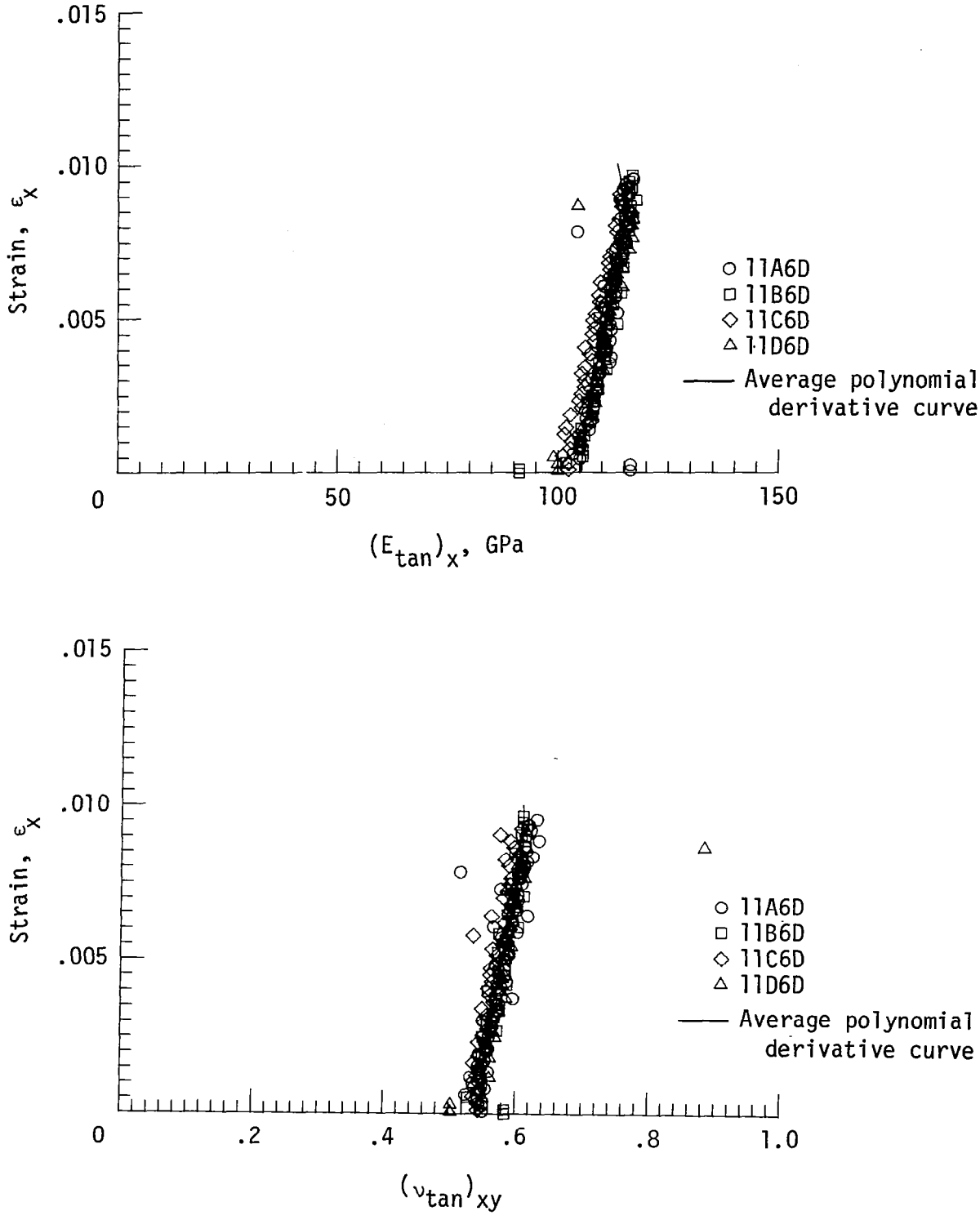

Figure 50. - Tangent modulus and Poisson's ratio for $[0_2/45/0_2/-45/0_2]_S$ laminate tested with end tabs.

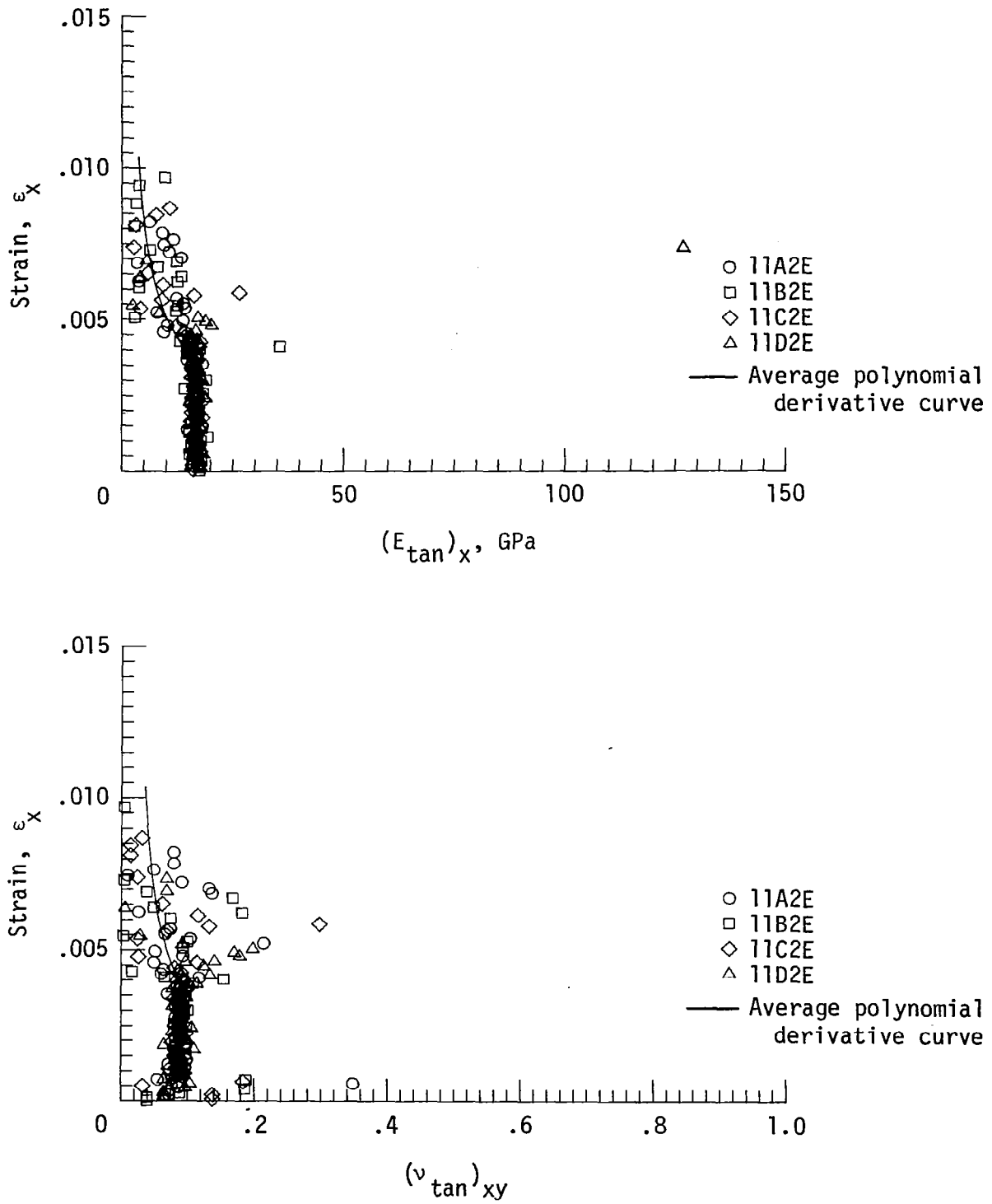

Figure 51. - Tangent modulus and Poisson's ratio for $[90_2/45/90_2/-45/90_2]_S$ laminate.

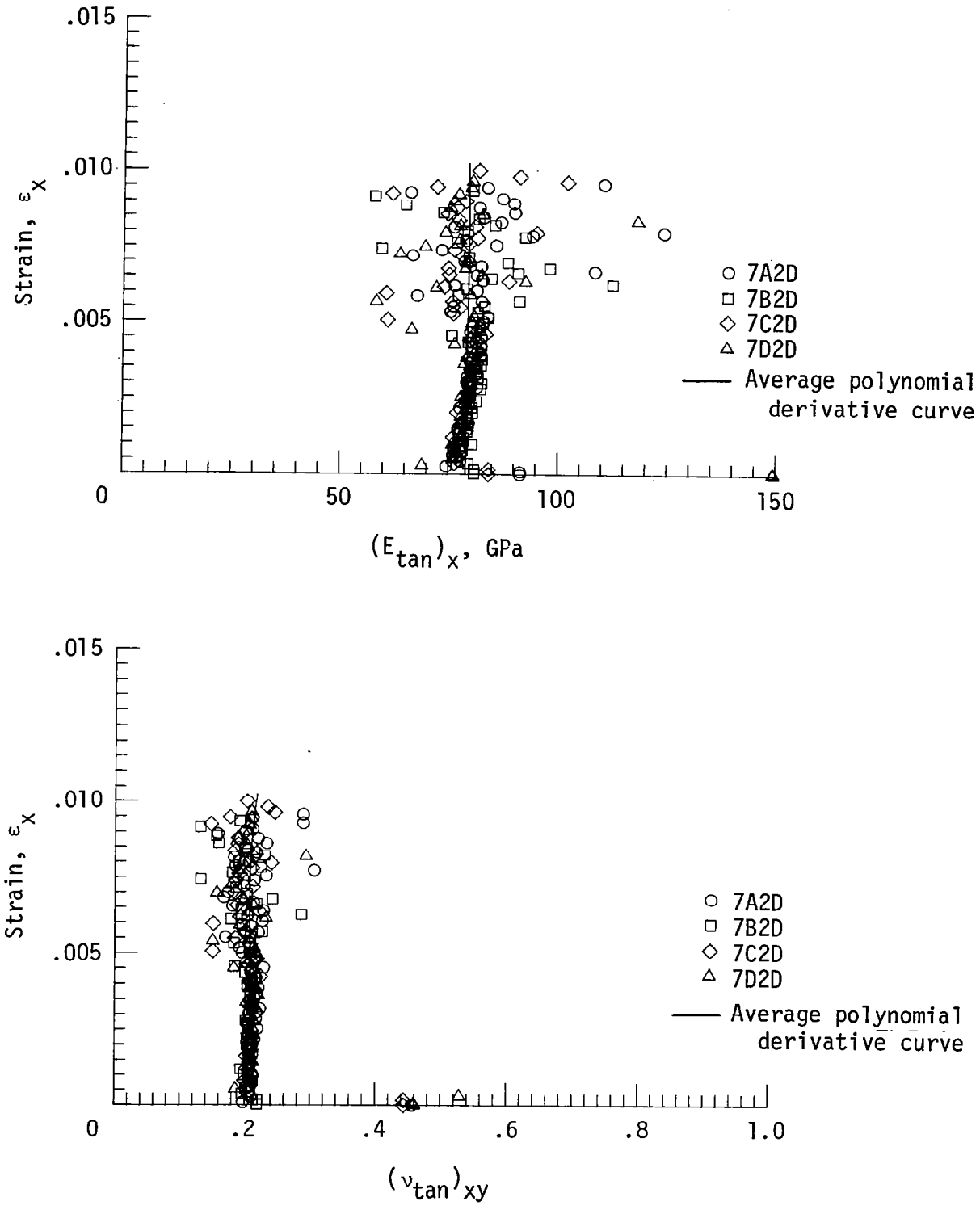

Figure 52. - Tangent modulus and Poisson's ratio for $[(90/0)_2/45/0/-45/0]_S$ laminate.

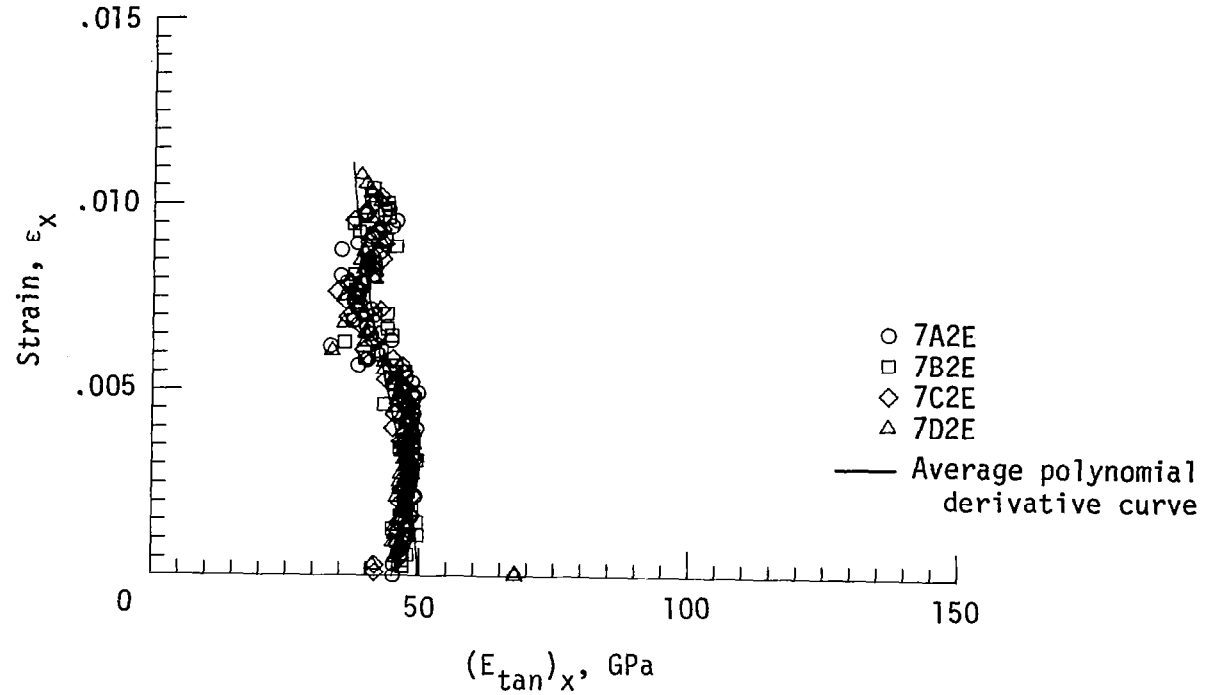

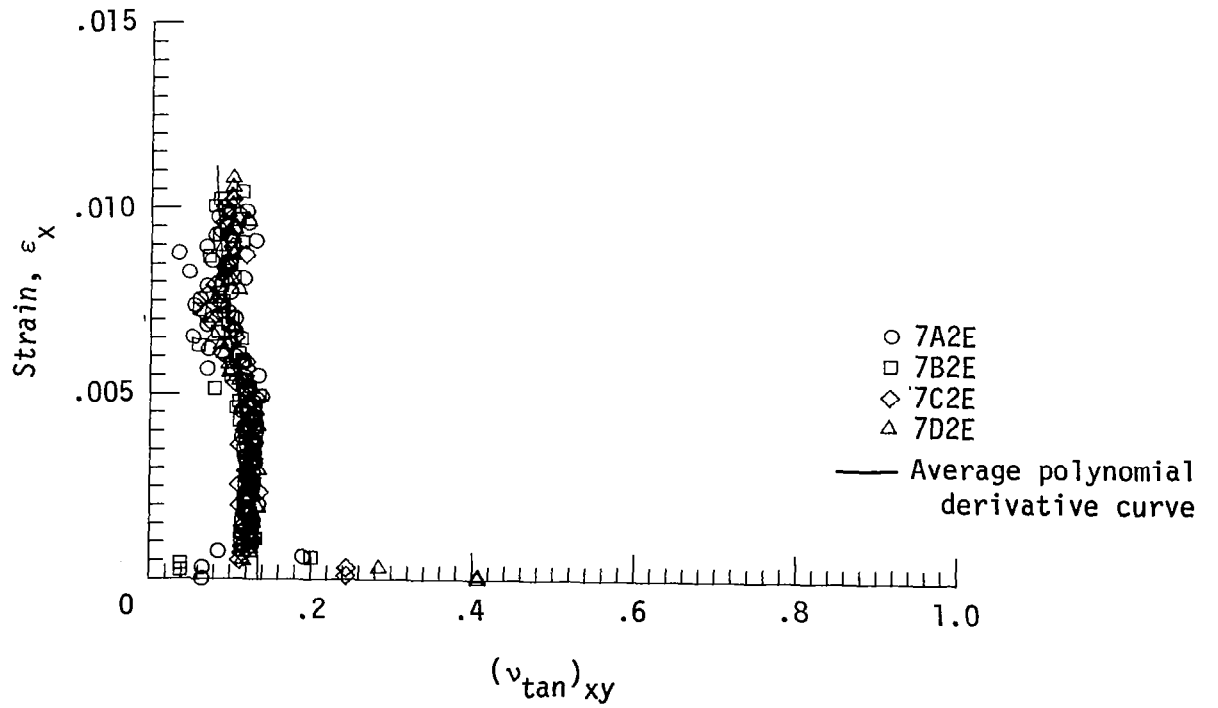

Figure 53. - Tangent modulus and Poisson's ratio for $[(0/90)_2/45/90/-45/90]_S$ laminate.

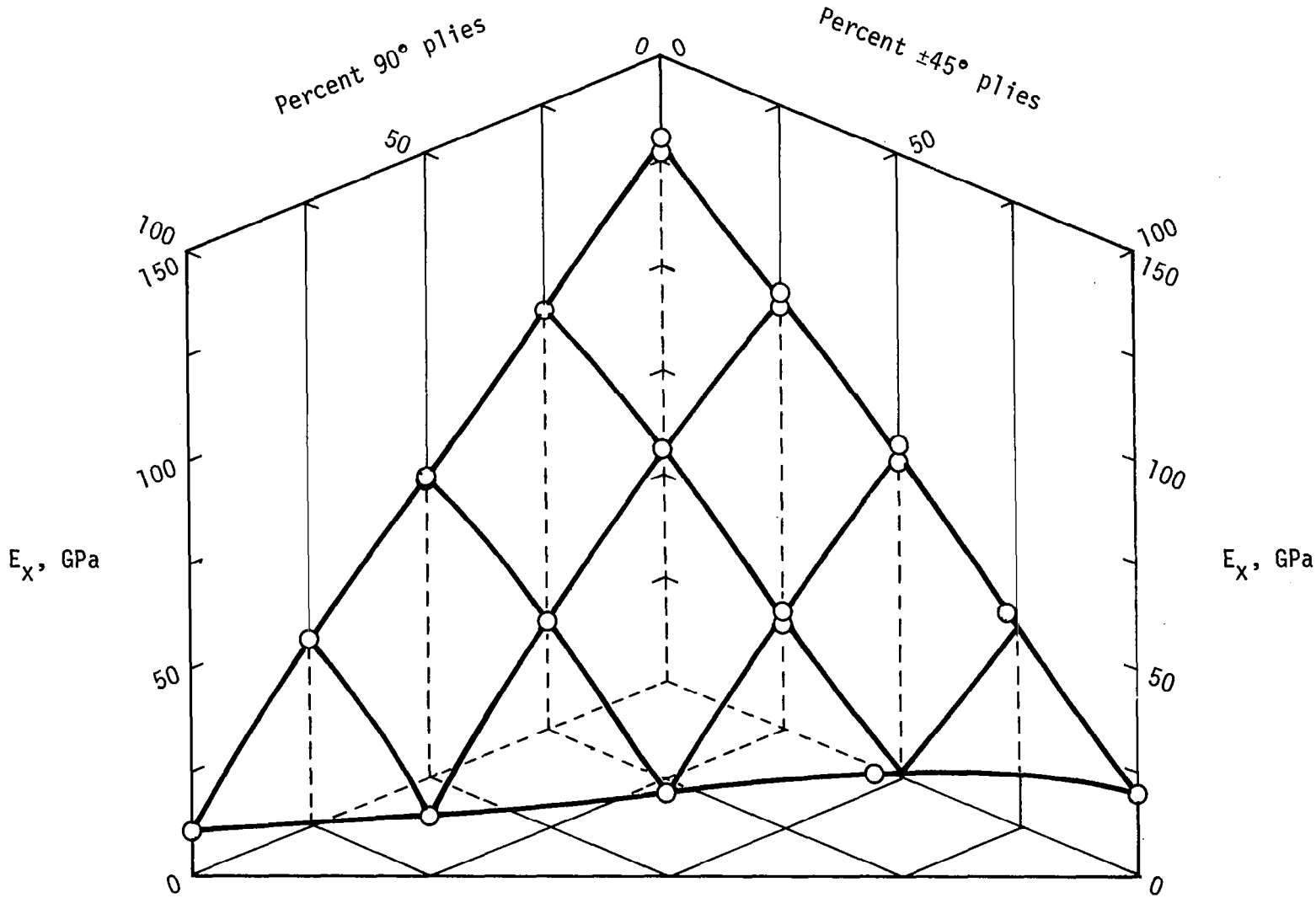

Figure 54. - Cordell plot of Young's modulus, E_x.

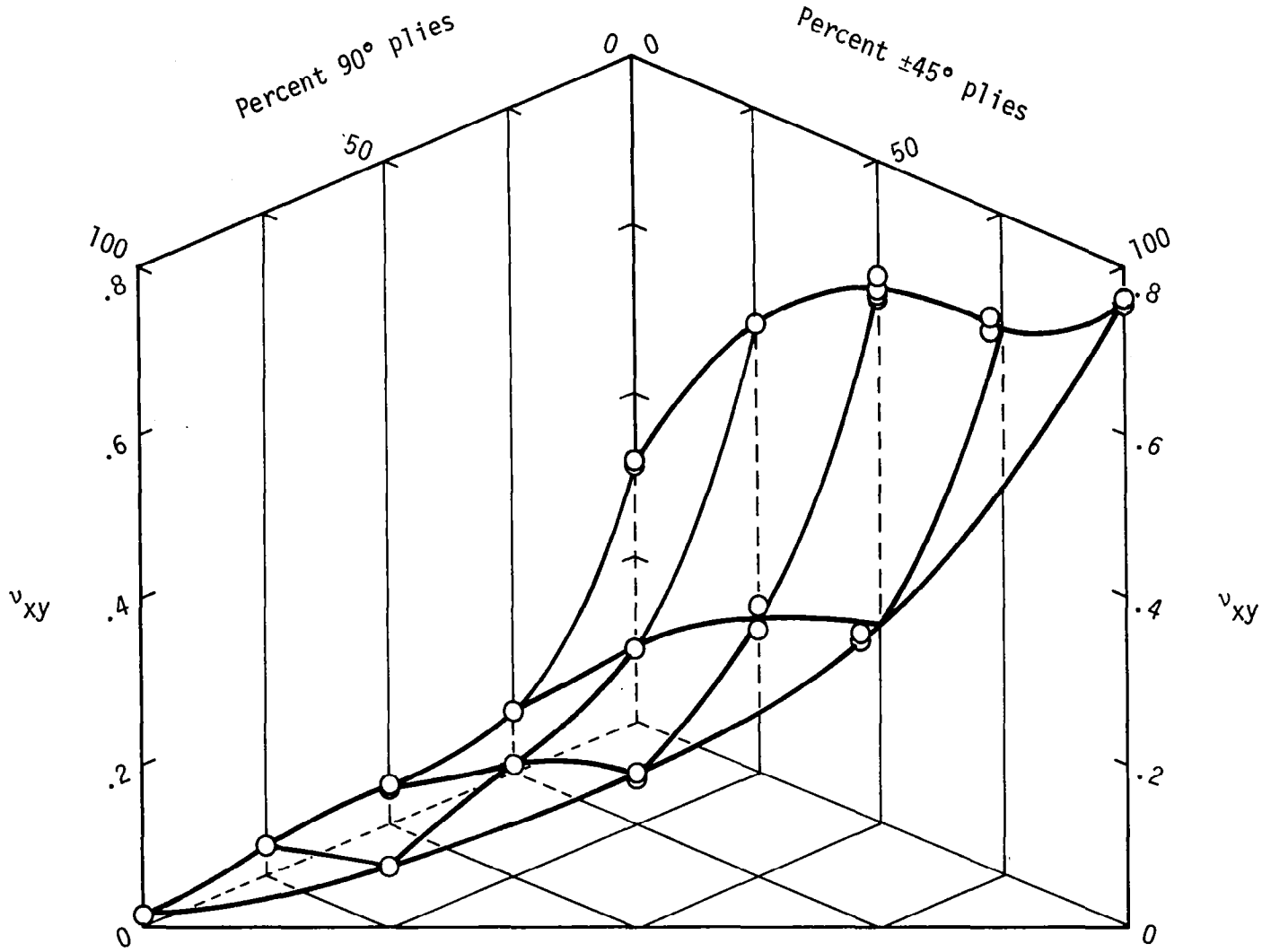

Figure 55. - Cordell plot of Poisson's ratio, ν_{xy}.

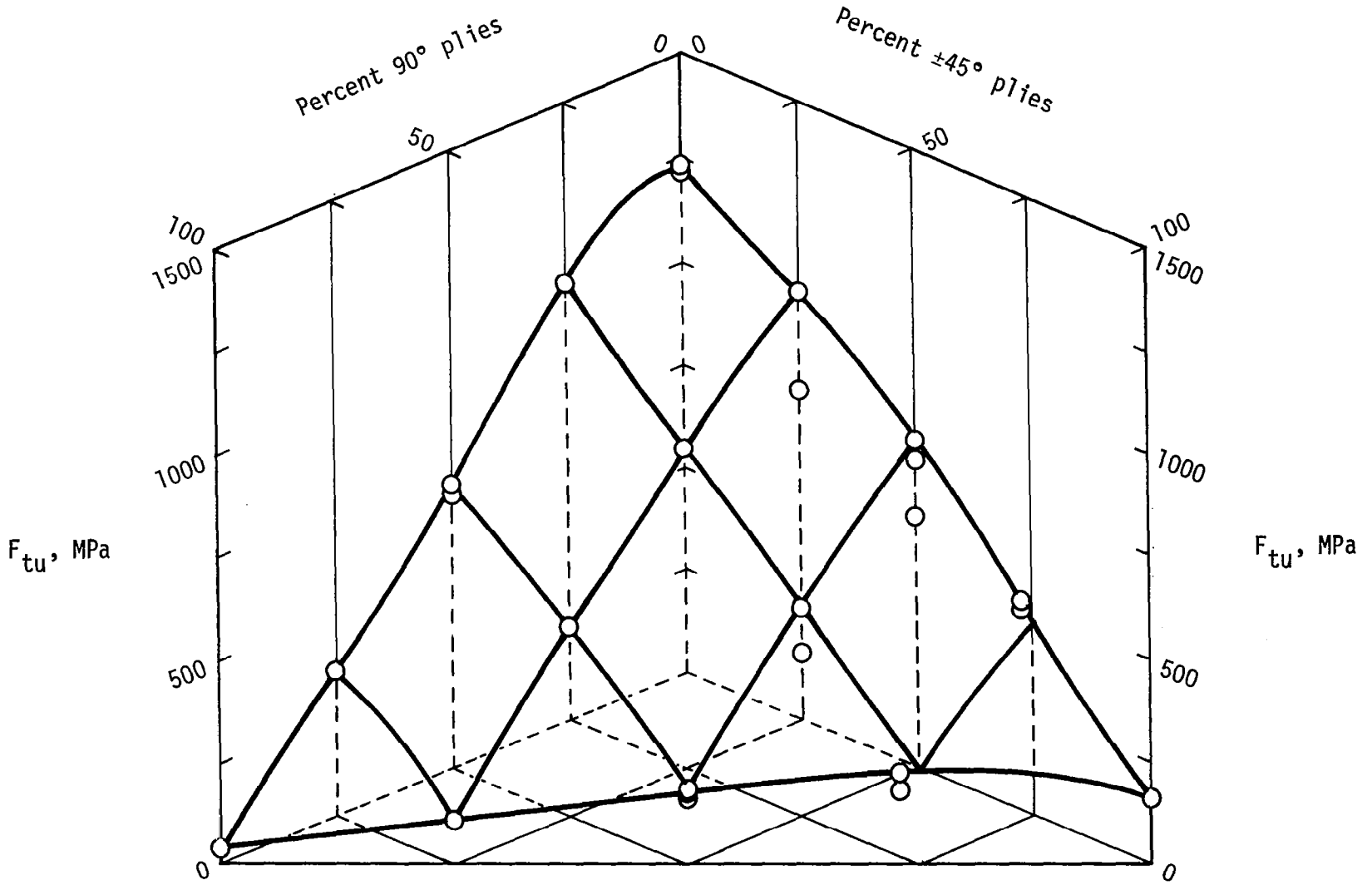

Figure 56. - Cordell plot of ultimate tensile strength, F_{tu}.